UNIVERSITY OF CALIFORNIA
RIVERSIDE

Eco-Approach and Departure Techniques for Connected Vehicles at Signalized Traffic Intersections

A Dissertation submitted in partial satisfaction
of the requirements for the degree of

Doctor of Philosophy

in

Electrical Engineering

by

Haitao Xia

June 2014

Dissertation Committee:
Dr. Matthew J. Barth, Chairperson
Dr. Yingbo Hua
Dr. Kanok Boriboonsomsin

The Dissertation of Haitao Xia is approved:

_____

_____

_____

Committee Chairperson

University of California, Riverside

Acknowledgements

First of all, I want to thank Dr. Matthew Barth for all the guidance and help all through the years of my Ph.D. program. I'm grateful that Dr. Barth accepted me as his Ph.D. student four years ago and let me work on the projects I'm really interested in. He provided me enough help by either directly advising or connecting me to internal/external resources to solve a lot of problems I've had on my various projects. He even worked with us and helped with various field tests. I also want to thank Dr. Barth for allowing me to attend a lot of conferences and workshops over the years, including every year's IEEE ITS conference, from which I was exposed to the research done by my peers and I gained perspective by talking to the people both inside and outside my research area. I really appreciate that he trusts me and lets me give a lot of presentations publicly. Another thing I'm really grateful for is that Dr. Barth never micromanaged us, but instead he gave us a lot of good ideas and let us play with them.

Another two people I really want to thank are Dr. Guoyuan Wu and Dr. Kanok Boriboonsomsin. Basically I learned how to write a research paper from Dr. Boriboonsomsin and he taught me some valuable lessons about research methodology. Dr. Wu offered me a lot of help and taught me a lot from his years of research experience. He's a very patient and helpful person. I'm very grateful that he would sacrifice his personal time from time to time to give me guidance and he spent a lot of time on other projects that he's not directly in charge of.

I also want to thank Mr. Michael Todd, Dr. George Scora and Mrs. Qiu Jin for their kind help in my various projects. I also learned a lot from their work and experience.

From working with BMW for the EAR project, I gained a lot of experience in field-testing. I want to thank Mr. Andreas Winckler, Mr. Friedrich Schweizer and Mr. Ravi Trivedi for their help in this project. It was full of challenge and fun working with them.

Lastly, I want to thank my parents for their unconditional support and love. I also want to thank my friends Ariel and Michael for giving me support and encouragement over the years. I'm very grateful to have them by my side.

ABSTRACT OF THE DISSERTATION

Eco-Approach and Departure Techniques for Connected Vehicles at Signalized Traffic Intersections

by

Haitao Xia

Doctor of Philosophy, Graduate Program in Electrical Engineering
University of California, Riverside, June 2014
Dr. Matthew Barth, Chairperson

Advanced "connected eco-driving" provides real-time advice to drivers based on real-time traffic and infrastructure conditions using communications technology as part of the connected vehicle concept. With connected eco-driving, even greater fuel and emission savings can be achieved without compromising traffic mobility. The concept of connected eco-driving takes advantage of real-time traffic sensing and infrastructure information, which can then be communicated to a vehicle with a goal of reducing fuel consumption and emissions. This dissertation focuses on connected eco-driving on arterial roadways with traffic control signals, referred to as "Eco-Approach and Departure" for signalized arterial roadways.

An initial dynamic Eco-Approach and Departure algorithm was initially developed for a single vehicle for fixed-timed signals, described in detail in Chapter 4. This algorithm shows individual vehicle fuel consumption and CO_2 reductions of around 10% - 15. The benefits have been proved by another research done by Li, etc. [11]. It was found that there are also significant indirect network-wide energy and emissions benefits

on the overall traffic [27], even at low penetration rates of the technology-equipped vehicles.

An additional amount of fuel is wasted on unnecessary acceleration/idling when the vehicle is departing the intersection. Therefore an enhanced eco-approach and departure algorithm [35] was developed that utilizes not only SPaT message but also the information of preceding equipped vehicles for better speed trajectory planning.

Lastly, the calibration criteria for microsimulation model itself were evaluated and a new set of processes to calibrate microscopic traffic model has been proposed.

Other connected eco-driving applications such as Eco-Speed Harmonization and General Eco-Driving Principles can also be coupled with the eco-approach and departure application to further improve fuel economy and reduce emissions. Another concept named Cooperative Adaptive Cruise Control was modeled in simulations (described in Chapter X) and can be coupled with the eco-approach and departure and other applications.

Keywords: Eco-driving, connected vehicle, Eco-Approach and Departure, DSRC, green wave, simulation calibration, micro-scale emission modeling

Contents

List of Figures

List of Tables

Chapter 1

Introduction

1.1 Eco Driving Concepts

Surface transportation has a significant impact on the environment. The transport sector in the United States accounts for 27% of greenhouse gas (GHG) emissions and 70% of the U.S. petroleum consumption. Light duty vehicles and heavy trucks consume the most fuel in the transport sector. Surface vehicles represent almost 80% of the transport sector GHG in the U.S. Fig.1.1 shows the energy consumption [4] and greenhouse gas emissions [5] by sector.

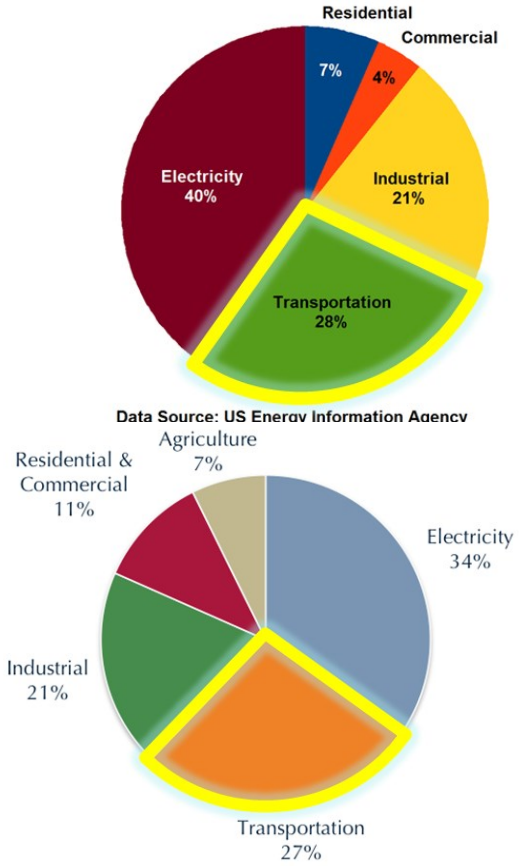

Fig.1.1. Energy consumption (left) and greenhouse gas emissions (right) by sector.

Policy makers are exploring a variety of strategies to reduce fuel consumption and carbon dioxide (CO_2) emissions from the transportation sector. In addition to vehicle technology improvements (e.g., new engines and drivetrains), alternative fuels, and VMT reduction methods, much can be gained through improved traffic system operations.

In recent years, there has been significant interest in developing Intelligent Transportation System (ITS) applications that are targeted towards energy savings and benefiting the environment. Many of these applications are highlighted in several major research programs such as Japan's Energy ITS research program [23], Europe's

ECOSTAND research program [24], and the U.S. Department of Transportation's AERIS Program (Applications for the Environment: Real-Time Information Synthesis, see [25]).

Out of all the different environmentally-beneficial ITS applications, those involving signalized intersections are relatively more promising in the near term, primarily because much of the supporting technology exists today that can be readily utilized, resulting in potentially significant benefits. These "eco-signal operations" applications can be generalized to include the use of connected vehicle technologies (i.e., vehicles that have communications capability) to decrease fuel consumption as well as GHG and criteria air pollutant emissions on roadways with traffic signals by reducing idling, reducing the number of stops, reducing unnecessary acceleration and deceleration events, and improving traffic flow at signalized intersections [26][27][30][31].

As one of the strategies to reduce fuel consumption and GHG emissions of motor vehicles from transportation sector, *eco-driving* has been gaining a lot of research interest in the United States as well as Asia and Europe recently, since it is one of the conservation programs that can be very cost effective [1]. The essence of eco-driving programs is to provide drivers with a variety of advice and feedback, and eventually modify a drivers' driving behavior in order to reduce fuel consumption and emissions while driving. The advice and feedback can be provided through various means including a website or brochure, class or training, or in-vehicle driving aids (e.g. eco-driving feedback systems on a vehicle's dashboard). Specific advice include items such as shifting to a higher gear as soon as possible, maintaining steady speeds, anticipating traffic flow, accelerating and decelerating smoothly, keeping the vehicle in good

maintenance, etc. Different eco-driving programs in Europe have been found to yield fuel economy improvements on the order of 5 to 15% [2]. This type of eco-driving is considered to be "static" in nature.

In contrast, more advanced *connected* eco-driving provides real-time advice to drivers based on real-time traffic light information and traffic congestion level for even greater and more consistent fuel and emission savings. The concept of connected eco-driving takes advantage of real-time traffic sensing and infrastructure information, which can then be communicated to a vehicle through wireless communication with a goal of reducing fuel consumption and emissions.

1.2 AERIS - Concept of Operations

In order to provide information to support and facilitate eco-friendly transportation choices for transportation system users and operators, the U.S. Department of Transportation (US-DOT) initialized a research program called AERIS (Applications for the Environment: Real-Time Information Synthesis). The AERIS Program developed several Concept of Operations (ConOps) documents for three high-priority operational scenarios – Eco-Signal Operations, Eco-Lanes, and Low Emissions Zones.

Eco-Lanes Operations are to dedicated freeway lanes – similar to HOV lanes – where they optimize dedicated freeway lanes for the environment to encourage use from vehicles operating in eco-friendly ways. One example is Variable Speed Limits (VSL) which is optimized for the environment based on data collected from vehicles. Another example is Connected Adaptive Cruise Control (CACC), where drivers may opt-in to

CACC and establish loosely-coupled “platoon” applications. The last example is Wireless Inductive/Resonance Charging infrastructure embedded in the roadway that allows electric vehicles to charge their batteries while the vehicle is moving [7].

Low Emissions Zones Operations geographically define areas that seek to incentivize “green transportation choices” or restrict specific categories of high-polluting vehicles from entering the zone to improve the air quality within the geographic area [ref]. Incentives may be based on the vehicle’s engine emissions standard or emissions data collected directly from the vehicle using V2I communications. Geo-fencing the boundaries of the Low Emissions Zones allow the possibility for these areas to be responsive to specific traffic and environmental conditions (e.g., pop-up for a severe non-attainment air quality day, special event, etc.) [8].

Eco-Signal Operations uses connected vehicle technologies to decrease fuel consumption and decrease GHG and criteria air pollutant emissions by reducing idling, the number of stops, unnecessary accelerations and decelerations as well as improving traffic flow at signalized intersections. The overall operational scenario features the specific applications such as: (1) Eco-Approach and Departure at Signalized Intersections, (2) Eco-Traffic Signal Timing, (3) Eco-Traffic Signal Priority, (4) Wireless Inductive/Resonance Charging, and (5) Connected Eco-Driving [6].

The Connected Eco-Driving application consists of three major components: applying general eco-driving principles, and eco-approach and departure at signalized intersections and eco-speed harmonization. When applied on a signalized corridor, each

component has its own effective range. Chapter 6 will discuss the connected eco-driving application in more detail.

As a vital part of the eco-signal operations and one of the major components of the connected eco-driving application, *Eco-Approach and Departure at Signalized Intersections* can significantly improve fuel economy and reduce emissions and it is easy to implement in real world. It operates dynamically with very low latency due to its simple and efficient algorithms. As described earlier, it can also be integrated as a component into a larger connected eco-driving concept, and be easily coupled with other applications to further improve vehicles' fuel economy, increase network capacity and reduce traffic congestion. The focus of my dissertation is primarily on this eco-approach and departure concept, where I have designed and developed a variety of techniques in this research area.

1.3 Contributions

There are several key contributions of my research. Much of my experimental work was done using high-fidelity microscale traffic simulation tools. As a critical component of the microsimulation analysis, calibration techniques are vital.

- One of my contributions has been developing an improved calibration methodology for micro-scale traffic simulation. Compared with traditional calibration methods that only take into account macroscopic traffic parameters, I have also integrated microscale simulation parameters in the calibration process, resulting in a better match to real-world data after applying this new method.

- My research has laid the fundamental groundwork for eco-approach and departure techniques that can be applied to vehicles travelling on arterial roadways. The fundamental algorithm is straightforward to implement and has low computation overhead, allowing for a vehicle to execute it in real-time. The fundamental algorithm has been evaluated on several vehicles (BMW, Nissan, Jeep) during a number of field studies as well being implemented in a variety of microscopic traffic simulation modeling scenarios. Both simulation and field tests showed 10% to 20% fuel saving and emissions reduction. Not only was it found that individually equipped vehicles benefit, it was also discovered that equipped vehicles have a positive effect on the un-equipped vehicles in terms of fuel saving.
- As an extension to the fundamental eco-approach and departure technique, my research further developed an enhanced dynamic eco-approach and departure algorithm. This enhanced version takes into account the traffic conditions downstream of the signalized intersection and provides trajectories that are more adaptive to different traffic congestion levels. An additional 10% of fuel savings and emissions reductions were achieved by applying this enhanced version, compared to the original version.
- The eco-approach and departure techniques were also integrated with other eco-driving applications (Eco-Speed Harmonization and General Eco-Driving Principles) and evaluated in simulation. An extensive sensitivity analysis was carried out, showing how these different applications perform individually and

how they interact with each other in different traffic scenarios. This research provides a good foundation for future field implementations.

1.4 Organization

The dissertation is organized in the following way. Related research about connected vehicles and signalization is provided in Chapter 2. Chapter 3 describes the new calibration techniques and criteria for microsimulation analysis. Chapter 4 describes in detail the eco-approach and departure (EAD) techniques, starting with the fundamental algorithm and transitioning to the enhanced version. Also in Chapter 4, an EAD technique for multiple intersections and actuated traffic signals are also discussed. The various field studies of the eco-approach and departure techniques are provided in Chapter 5. Other eco-driving applications that can be coupled with EAD are described in Chapter 6. Chapter 7 provides conclusions of all the different research components in this dissertation and sheds some light on the future paths on the various research topics.

Chapter 2

Background

2.1 Connected Vehicle

Connected vehicle research addresses a suite of technologies and applications that use wireless communications to provide connectivity among vehicles (V2V), among vehicles and roadside infrastructure (V2I) and among vehicles, infrastructure and mobile devices. Connected vehicles technology can be implemented by DSRC (Dedicated Short Range Communications) or cellular network (e.g. 4G/LTE). The data sent from vehicles include real-time location, speed, acceleration, emissions, fuel consumption and other vehicle diagnostic data. The data communicated to vehicles can be real-time traffic information, safety messages, traffic signal phase and timings, eco-speed limits, eco-routes, parking information, etc.[3]

DSRC is a Wi-Fi radio adapted for vehicle environment, and it is inexpensive to produce in quantity. The original FCC spectrum was allocated in 1999. Its messages are transmitted 10times/sec. The basic communication range is 300m. Basic safety message includes vehicle position, speed, heading, acceleration, size, brake system status, etc. Compared to cellular network, DSRC is more reliable, but it will be expensive to equip this technology on both vehicles and infrastructure. The most constraint of DSRC compared to cellular network is its limited communication range. DSRC is suitable for optimization driving behavior for one intersection at a time, while cellular network can apply to all the upcoming signals as far as the cellular network can cover.

Connected vehicles can also utilize other sensing technologies, such as radar and LIDAR. Radar was found to be able to operate in the greatest range of visibility and weather among all the active and non-active sensing technologies. As used in Google Self-Driving Car, 3D LIDAR is a robust all-in-one system. Since 3D LIDAR can not only detect relative speed, angle, and distance to obstacles as radar, it can also classify roadside obstacles by detecting their 3D features [76].

Connected vehicle technology can be used alone or coupled with other roadside infrastructures [77] in various research fields. It can be used in vehicle positioning [77], queue length estimation [77], signal control [80] and crash identification [79], etc.

2.2 Traffic Light Synchronization

Mobility is one of the most important ingredients when designing a traffic control strategy. Traffic lights are used to control traffic and give priorities to competing traffic flows on a road since city traffic often exceeds the capacity. It is shown in the study by Brockfeld et al. [9] that CA traffic model can be used to optimizing traffic lights for city traffic.

Mobility is not solely determined by traffic demand, but also by the characteristic of the traffic lights. The most important parameters of traffic lights include cycle time, split and offset. Cycle time is the period of time of a total traffic light cycle. Split is the fraction of green time to the cycle time. And offset is the offset time between two traffic lights at two neighboring intersections.

In a green wave strategy, signals on a signalized corridor switch in a form of progressive cascade so that a group of vehicles (aka. Platoon) on the mainline street can pass multiple intersections without having to stop. Note that mainline traffic will eventually be broken when signal priority is given to cross-street traffic. In some cases, the signal coordination is static, which means the offsets between neighbor intersections are fixed and may be calculated based on progression speed of the traffic and intersection spacing. Signal coordination can also be dynamic, in which case roadside sensor data may be used to measure real-time traffic flows, which in term, can be used to calculate the offsets among intersections.

2.3 Eco-Speed Control at Signalized Intersections

At the foundation of the eco-driving operations are wireless data communications between enabled vehicles and roadside infrastructure. For example, in the eco-approach application, a traffic signal broadcasts its signal phase and timing (SPaT, defined in SAE J2735 Message Sets [85]) and Geometric Intersection Description (GID or map) information to approaching vehicles. In-vehicle systems then use this information along with the vehicle's position and speed, to perform calculations and provide speed advice to the driver, allowing the driver to adapt the vehicle's speed to pass through the upcoming signal on green or to decelerate to a stop in the most eco-friendly manner. In essence, this eco-approach technology encourages "green" driving while approaching, passing through, and departing signalized intersections.

In order to improve safety and reduce congestion, University of Groningen proposed a prototype called Intelligent Speed Adapter (ISA) [81], which provides speed feedback and advices speed limits on roadways. It was found in this research that the speed variation of the vehicles with ISA devices is smaller than other vehicles, resulting in less fuel consumption. This means driving with less acceleration and deceleration and maintaining a constant speed can avoid unnecessary fuel usage.

There are a few different approaches to optimize energy efficiency through speed control at signalized intersections. A predictive cruise control system was proposed by Asadi and Vahidi [82] that used optimization to reduce idle time at the stop lights. This system calculates a set speed and keeps vehicles travelling around this set speed to achieve timely arrival at green light. Another research by Virginia Tech [75] adopts A-star algorithm to minimized fuel consumption of the upstream and downstream of an intersection. It calculates the optimal speed and acceleration recursively in each time step on a discretized model. The major limit of this approach is its computation time overhead, which makes it impossible to give real time speed recommendation in real world.

On the other hand, traffic signal control can be integrated with vehicle speed control to further improve traffic mobility and fuel efficiency. Malakorn and Park [80] investigated such a method by integrating intelligent traffic signal control with Cooperative Adaptive Cruise Control. The signal controller analyzed the arriving windows of all the approaching vehicles and determines the best arrival time for each vehicle. With a target arrival time, each vehicle simply accelerates or decelerates to a

speed and maintains the speed till passing the intersection. It showed both mobility benefits and environmental benefits.

This research applies dynamic eco-driving on connected vehicles in an arterial corridor with fixed-time traffic signal control, where signal phase and timing (SPaT) information of traffic lights is sent to the vehicles through wireless communication as they run through the corridor. The vehicles can then adjust their speeds while traveling through the corridor with the goal of minimizing fuel consumption and emissions. A dynamic eco-driving velocity planning methodology has been developed and is described in detail in the next chapter.

Chapter 3

Microscale Traffic Simulation Calibration

3.1 Background

The U.S. Environmental Protection Agency's Motor Vehicle Emission Simulator (MOVES) model is the regulatory emissions model for all states in the U.S. except for California. MOVES has been purposefully designed so that it can be used to support emission calculation at multi-scales, from macro (e.g., national emissions inventory development) to meso (e.g., regional transportation conformity analyses) to micro (e.g., project-level conformity and hot spot analyses) [56].

In order to analyze traffic network emissions quantitatively, practitioners often rely on traffic simulation models to generate traffic performance or vehicle activity data for use with the MOVES model. Thus, there has been recent interest in the interface between traffic simulation models and MOVES. To date, research efforts in this area have been focused on the post processing of traffic model outputs to prepare necessary vehicle data inputs for MOVES. In general, there are three approaches for linking traffic models with MOVES [57]:

A. Using Link Average Speeds

In this approach, a traffic simulation model will output the average speed for each roadway link in the network, which will be used directly as an input for MOVES (e.g., [58]). MOVES will then generate emission outputs corresponding to the default vehicle operating mode (OpMode) distribution that is based on typical driving cycles for that average speed. The default vehicle OpMode distributions are different for different roadway types in MOVES, therefore, the emission outputs for the same average speed but different roadway types will be different.

B. Using Link Driving Cycles

In this approach, fine-grained traffic models such as microscopic traffic simulation (or microsimulation) models will output the driving cycles (i.e., second-by-second speed profiles) of vehicles on roadway links. All or a subset of these driving cycles can then be entered into MOVES directly or can be aggregated into a set of representative driving cycles first before being entered into MOVES (e.g., [59]). MOVES will then calculate the vehicle OpMode distribution base on the supplied driving cycles and subsequently generate the corresponding emission outputs.

C. Using Link-Specific Vehicle Operating Mode Distribution

In this approach, the vehicle OpMode distribution needs to be created from the driving cycles of vehicles on roadway links first before being used as an input for

MOVES (e.g. [60]). MOVES will then generate emission outputs corresponding to the supplied vehicle OpMode distribution. Alternatively, look-up tables containing emission rates for each of the OpMode can be generated from MOVES and applied to the created vehicle OpMode distribution [61].

Of these three approaches, the first approach is the most straightforward and is commonly applicable as link average speed is a standard output of traffic models. However, it may not appropriate for the analysis where the vehicle OpMode distribution could be significantly different from the default ones in MOVES, such as when analyzing the impact of intelligent transportation system (ITS) projects that reduce vehicle stops and idling (e.g., traffic signal coordination). The second and third approaches have higher fidelity and are more appropriate for such analyses. However, they require the use of fine-grained traffic models such as microsimulation models that can generate second-by-second vehicle speed profiles as an output.

The advantages of microsimulation models include their ability to model the detailed movements of individual vehicles in the traffic stream, the ability to model queuing in oversaturated traffic conditions, the ability to model the influence of roadway geometry and ITS technology, etc. To date, microsimulation models have primarily been used for traffic operation studies and analyses (e.g., [62][63]). However, they have also been used for emissions evaluation of various traffic flow improvements and ITS implementations (e.g., [64][65]).

To properly use microsimulation models for any traffic studies and analyses, modelers must ensure that the simulation network is well calibrated so that it replicates

the real-world traffic condition. Several criteria have been suggested for use when calibrating a simulation network in microsimulation models. These criteria may be different depending on the type of network (i.e., freeway versus arterial) being simulated. As an example, Table 1.Table 3.1 lists the calibration criteria for freeway network suggested by the Wisconsin Department of Transportation (DOT) [66]. For arterial network, there are a variety of calibration criteria that have been used, but the common ones are based on link flow [67], link speed [68], and travel time [69].

Table 3.1. Freeway network calibration criteria suggested by Wisconsin DOT [69]

Criteria & Measures	Acceptability Targets
Hourly Flows: Modeled versus Observed	
Individual link flows	
Within 100 vph, for flow < 700 vph	> 85% of the cases
Within 15%, for 700 vph < flow < 2700 vph	> 85% of the cases
Within 400 vph, for flow > 2700 vph	> 85% of the cases
Sum of all link flows	Within 5% of the sum value
*GEH** statistic for individual link flows	
GEH < 5	> 85% of all cases
GEH statistic for sum of all link flows	*GEH* < 4
Travel Time: Modeled versus Observed	
Point-to-point travel times	
Within 15% or one minute, whichever is higher	> 85% of all cases
Visual Audits	
Individual link speeds	
Visually acceptable speed-flow relationship	To analyst's satisfaction
Bottlenecks	
Visually acceptable queuing	To analyst's satisfaction

*The GEH (Geoffrey E. Havers) statistic is computed as:

$$GEH = \sqrt{\frac{(q_m - q_0)^2}{(q_m + q_0)/2}}$$

where q_m is modeled hourly volume at a location and q_0 is observed hourly volume at a location.

It is well known that vehicle emissions are sensitive not only to speed, but also to acceleration. A vehicle cruising at 40 mph will release significantly lower emissions compared to the same vehicle driving in stop-and-go condition that still yield an average speed of 40 mph. Similarly, a traffic stream with an average speed of 40 mph could produce different levels of emissions depending on the driving patterns (i.e., trajectories) of the vehicles in the traffic stream. Therefore, a proper characterization of the vehicle driving patterns is very important for emissions modeling, especially at the micro scale.

As the current microsimulation calibration criteria are based only on macroscopic traffic parameters, it is of interest to examine whether these criteria are sufficient to make the simulated vehicle trajectories at the micro scale represent those in the real-world or not. Thus, the research described in this Chapter addresses two questions: 1) whether current calibration criteria based on macroscopic traffic parameters is adequate for micro-scale emissions modeling, and 2) if not, how do we improve the calibration of micro-scale emissions modeling.

Observed vehicle trajectories from the Next Generation Simulation (NGSIM) project [70] are used as a ground truth for comparison with simulated vehicle trajectories. In the NGSIM project, trajectories of all vehicles in the traffic stream at four sites in the U.S. were collected from video data using a customized software program that detects and tracks vehicles from video images The NGSIM dataset used in this study is from the site at Lankershim Boulevard near the interchange with US-101 (Hollywood Freeway) in

Los Angeles, California. Fig.3.1 shows the aerial imagery of this site. The road stretch is approximately 1,600 feet in length, with four signalized intersections and three to four through lanes in each direction along the main street where the speed limit is 35 mph. The traffic lights at intersections 1 and 2 are controlled by 2070 controllers [83], while the other 2 traffic lights are controlled by 170 controllers [84].

Video data of traffic at the site were recorded from 8:30 a.m. to 8:45 a.m. on June 16, 2005. Detailed vehicle trajectories were transcribed from the video data at a resolution of 10 frames per second. However, it was noted that the acceleration values provided in the NGSIM dataset may not be reliable [71]. Therefore, in this study only the speed values from the NGSIM dataset were used. They were first aggregated into a one-second interval before being used to calculate second-by-second acceleration values based on the central finite difference method (using polynomial of second degree) [72].

Fig.3.1. NGSIM site at Lankershim Blvd. in Los Angeles, CA

3.2 Methodology

The Paramics microsimulation software package was used to simulate the traffic at the study site. It is a suite of microsimulation tools that model behavior of individual vehicles and interaction between them stochastically. The inputs to Paramics include network geometrics, vehicle dynamics, traffic control settings, and demand information. The typical outputs include statistics at the network level (overall travel time, total travel distance, and average speed), on a link basis (traffic flow, queue length, delay, speed, and density), or at specific locations (instantaneous detector-type information). In addition, Paramics can also generate detailed vehicle trajectories as an output. For more information about Paramics, please refer to [73].

High-resolution satellite images from Google Map (Year 2005) were used as a background to guide the coding of the road geometry in the simulation network. However, the resolution of the images does not allow for proper determination of lane width as well as the exact locations of turning bays. More detailed road geometry settings were coded based on the drawings in the NGSIM report [74]. As part of the network coding, virtual loop detectors were also coded at the same locations as those in the real network.

It should be noted that the version of Paramics used in this study neither support the 2070 nor the 170 signal controllers. Therefore, fixed timing scheme was used to emulate the signal timings for each cycle by complying with the observations from the video data. The actual origin-destination (O-D) trip table was provided in the NGSIM report and was used as a starting point. The simulation time was set to 17 minutes, where

the first 2-minute period was used to load vehicles onto the network before collecting data. In order to reproduce the traffic environment based on NGSIM data, signal phase and timing and traffic demand were aggregated minute by minute for 17 minutes (2-min warm-up and 15-min data collection). Vehicles were categorized into 13 FHWA-defined classes based on vehicle lengths from NGSIM data. Therefore, within each minute, traffic demand was further divided into 13 OD matrices for the 13 vehicle types. The number of time steps was set to 5, which means that the vehicle positions were calculated 5 times per second.

For the simulation network calibration, link flow and travel time were used as the calibration criteria. This is partly because the observed values of these two traffic parameters are already available in the NGSIM report. Also, link flow and travel time are the required data inputs when conducting project-level emission analyses with MOVES based on the first approach discussed earlier. In the calibration of link flow, the 15-minute simulation period was broken down into three 5-minute data aggregation periods. The link flows for all the road segments in each 5-minute period was collected and compared with the observed values. Note that the link flows were collected at the stop line on the approaching link of each intersection. Travel times were collected for vehicles travelling from southernmost to northernmost and northernmost to southernmost of the network. Tweaked parameters during the calibration process include mean target headway time, mean reaction time, mean acceleration/deceleration profiles, speed memory and simulation time step, among which, the first two parameters were tuned in link level.

All the parameters aforementioned can be directly modified in Paramics except mean acceleration/deceleration profiles. In Paramics, vehicles' acceleration/deceleration rates are defined by maximum rates, and each acceleration/deceleration rate corresponds with a speed bin. In order to calibrate vehicles' acceleration/deceleration behaviors, we need to have an assumption that

$$\frac{target\ maximum\ acc/dec}{baseline\ maximum\ acc/dec} = \frac{target\ mean\ acc/dec}{baseline\ mean\ acc/dec} = \rho$$

Where baseline maximum acc/dec is the maximum acc/dec rate we used in one simulation run; baseline mean acc/dec is the mean acc/dec rate we aggregated from the output of the simulation run; target mean acc/dec is the ground-truth mean acc/dec rate from NGSIM data; target maximum acc/dec is the calibrated acc/dec rate we set in Paramics. Note that a few iterations are needed to match the acceleration/deceleration profiles to real-world data as closely as possible.

In order to avoid getting dramatic shapes of the acceleration/deceleration profiles which may be caused by the randomness of both the NGSIM data and simulations, we decided at first to keep the general shapes of the maximum acceleration/deceleration profiles by only multiplying the whole profiles with a global mean factor ρ_G calculated by

$$\rho_G = \frac{\sum \rho_i}{n}$$

Where ρ_i is the factor ρ calculated at each time step for each vehicle in simulations, and n is the total time steps of all the vehicles in simulations. Since the whole maximum

acc/dec profiles are multiplied by only one factor ρ_G, it can be guaranteed that the acc/dec behaviors are realistic as long as the default acc/dec profiles defined in Paramics is valid.

Further fine-tuning of the maximum acceleration/deceleration profiles were accomplished by applying ρ on specific speed bins instead of applying a global ρ_G on all the speed bins. These specific speed bins are considered heavily related to the discrepancies in the VSP distributions, which will be discussed in the next section.

Table 3.2 and Table 3.3 show the calibration results of link flows and travel times, respectively. According to Table 3.2, the link flow data matches all the criteria in Table 3.1. According to Table 3.3, the percentage errors of travel time are within +/-4%.

Table 3.2. Calibration results of link flow

Intersection	*NB*			*SB*			*WB*			*EB*		
	NGSIM	**Sim**	**GEH**	**NGSIM**	**Sim**	**GEH**	**NGSIM**	**Sim**	**GEH**	**NGSIM**	**Sim**	**GEH**
1	536	544	0.34	1352	1348	0.11	904	872	1.07	-	-	-
2	1512	1352	4.23	1964	1864	2.29	208	160	3.54	248	264	1.00
3	892	1148	8.02	2116	1980	3.01	56	56	0.00	32	12	4.26
4	1160	1112	1.42	2164	2028	2.97	36	20	3.02	36	36	0.00

Table 3.3. Calibration results of travel time

	NB	*SB*	*Ave.*
NGSIM	80.97	56.65	66.60
Sim.	77.87	58.34	65.98
STD	3.53	2.69	2.86
% Err.	-3.83%	2.98%	-0.93%

As microsimulation models are stochastic in nature, a different random seed number will cause the simulation results to be different. Thus, multiple numbers of

simulation runs should be made. The minimum number of runs required can be calculated using the following equation:

$$N = (t_{\alpha/2} \cdot \frac{\delta}{\mu\varepsilon})^2$$

where μ and δ are the mean and standard deviation of the estimated emissions based on the already conducted runs; ε is the allowable error specified as a fraction of the mean μ; $t_{\alpha/2}$ is the critical value of the t distribution at the significance level α. In this study, this calculation was performed for every run. After each link, if N was greater than the current number of runs, an additional run was made and N was recalculated. In our simulation, the significance level was set to 0.05. The allowable error was chosen to be 5%. This process was repeated until N was smaller than or equal to the current number of runs. The final number of runs was 5 for this simulation study.

3.3 Results and Discussion

Fig.3.2 shows the comparison of the VSP distributions between observed and simulated. The distribution of the simulated one was developed from the vehicle trajectories from all the five runs. Fig.3.2 and Table 3.4 both present the p-values from the Kolmogorov-Smirnov (KS) tests between the observed and simulated VSP distributions. According to the test results before calibration, the two VSP distributions are significantly different from each other at 5% alpha level, since the p-value of VSP distribution is 0.0327, which is less than 0.05, so the null hypothesis is not rejected and the VSP distributions generated from simulation is significantly different from the VSP

distributions from NGSIM. After calibration, the null hypothesis is rejected since the p-value 0.1976 is higher than 0.05.

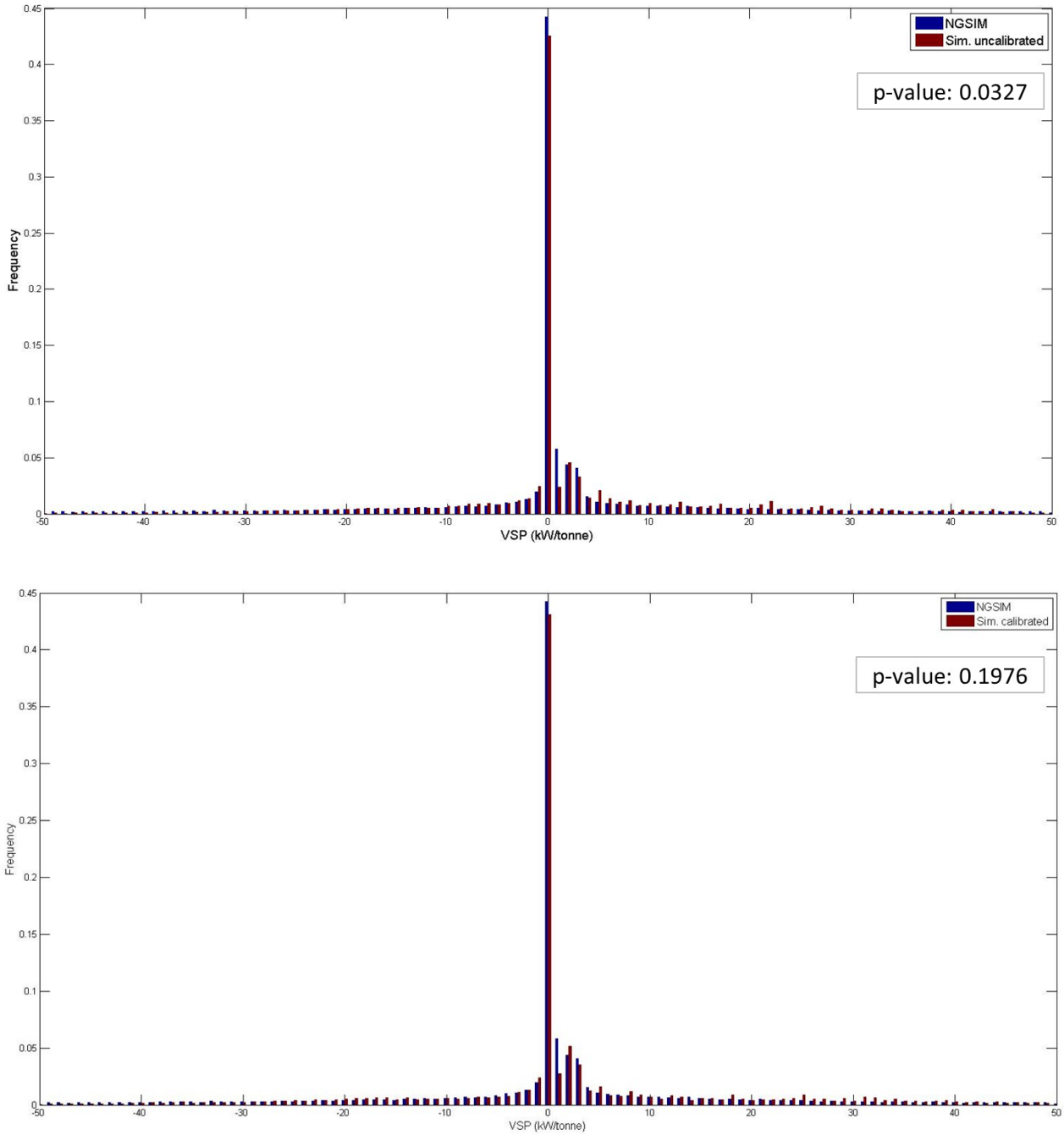

Fig.3.2. VSP distributions of simulated and measured vehicle trajectories.

Table 3.4. p-values from KS tests of observed vs. simulated VSP distributions.

	NGSIM	*Run_1*	*Run_2*	*Run_3*	*Run_4*	*Run_5*	*CMB*
NGSIM	\	\	\	\	\	\	\
Run_1	0.1976	\	\	\	\	\	\
Run_2	0. 1976	0.9926	\	\	\	\	\
Run_3	0. 1976	0.9995	0.9926	\	\	\	\
Run_4	0. 1976	0.9995	0.9627	0.9926	\	\	\
Run_5	0. 1976	0.4496	0.7992	0.4496	0.6828	\	\
CMB	0. 1976	0.9926	1.0000	0.9926	0.9926	0.7992	\

*A combined data sample from all 5 simulation runs

Table 3.5 shows the emission results based on the vehicle OpMode distributions and the corresponding MOVES emission rates. It can be seen that after calibration, the errors of CO, NO_x and PM2.5 rates have seen significant reductions while there is no dramatic change for energy rate and CO_2 rate. Since these greenhouse gases are closely related to vehicles' behaviors, such as acceleration/deceleration and idling, a better matching of these data between simulations and NGSIM shows that micro-scale calibration can make simulation better at capturing microscopic behaviors in real world.

Table 3.5. Emission results

(a) Before calibration on acceleration profile

Absolute Values						
	Energy(kJ/mi)	**CO_2(g/mi)**	**CO(g/mi)**	**HC(g/mi)**	**NO_x(g/mi)**	**PM2.5(g/mi)**
NGSIM	9154.89	659.81	15.13	0.53	2.40	0.14
Run1	10012.01	720.09	11.83	0.51	1.88	0.08
Run2	10004.50	719.40	11.76	0.51	1.80	0.08
Run3	10297.44	740.99	12.06	0.54	2.11	0.09
Ave.	10104.65	726.82	11.88	0.52	1.93	0.08
Error						
	Energy(kJ/mi)	**CO_2(g/mi)**	**CO(g/mi)**	**HC(g/mi)**	**NO_x(g/mi)**	**PM2.5(g/mi)**
Run1	9.36%	9.14%	-21.83%	-3.20%	-21.76%	-44.56%
Run2	9.28%	9.03%	-22.32%	-3.74%	-25.18%	-46.79%
Run3	12.48%	12.30%	-20.29%	1.26%	-12.15%	-37.82%
Ave.	10.37%	10.16%	-21.48%	-1.89%	-19.70%	-43.06%

(b) After calibration on acceleration profile

Absolute Values						
	Energy(kJ/mi)	**CO_2(g/mi)**	**CO(g/mi)**	**HC(g/mi)**	**NO_x(g/mi)**	**PM2.5(g/mi)**
NGSIM	9154.89	659.81	15.13	0.53	2.40	0.14
Run1	10088.36	725.59	15.74	0.55	1.95	0.12
Run2	10083.18	725.15	15.39	0.54	1.92	0.12
Run3	10116.57	727.75	15.67	0.55	2.03	0.12
Ave.	10096.04	726.16	15.60	0.55	1.96	0.12
Error						
	Energy(kJ/mi)	**CO_2(g/mi)**	**CO(g/mi)**	**HC(g/mi)**	**NO_x(g/mi)**	**PM2.5(g/mi)**
Run1	10.20%	9.97%	4.02%	2.87%	-18.86%	-15.52%
Run2	10.14%	9.90%	1.68%	2.49%	-20.34%	-18.67%
Run3	10.50%	10.30%	3.53%	3.47%	-15.71%	-15.08%
Ave.	10.28%	10.06%	3.08%	2.95%	-18.30%	-16.42%

3.4 Summary

The U.S. EPA MOVES model is the regulatory emissions model for all states in the U.S. except for California. MOVES has been purposefully designed so that it can be used to support emission calculation at multi-scales, from macro (e.g., national emissions inventory development) to meso (e.g., regional transportation conformity analyses) to micro (e.g., project-level conformity and hot spot analyses).

For quantitative project-level analyses, practitioners will have to rely on traffic models to generate traffic performance or vehicle activity data for the "build" scenario for use with the MOVES model. As the current state-of-the-practice calibration criteria for micro-simulation models are based only on macroscopic traffic parameters, it was of interest to examine whether these criteria are sufficient to make the simulated vehicle trajectories at the micro scale represent those in the real-world or not. The research described in this chapter investigated this issue using an NGSIM dataset as a ground truth. It was found that the microsimulation calibration criteria based on macroscopic traffic parameters alone are not adequate to represent vehicle trajectories at the micro scale.

After carefully calibration on the microscopic parameters including mean target headway time, mean reaction time, mean acceleration/deceleration profiles, speed memory and simulation time step, it was found that after micro-scale calibration, not only the macroscopic criteria were met, the VSP distribution from simulation has much better match to that from NGSIM data, which means after micro-scale calibration, the simulation can capture real-world driving behaviors more accurately. The emission

results further prove that micro-scale calibration can make simulation better at capturing microscopic behaviors in real world.

Chapter 4

Fundamental Eco-Approach and Departure Technique

4.1 Dimension of Analysis

Eco-Approach and Departure (EAD) was originally designed to address the problem that how a vehicle can pass a signalized intersection with the minimal fuel consumption and emissions. The first version of EAD was analyzed in extensive simulations and field tests, both of which showed around 13% benefits of fuel saving and emission reduction.

In order to analyze EAD on vehicles in traffic, extensive network simulations were conducted, including sensitivity analyses on traffic demand, penetration rate of technology-equipped vehicles, communication range, communication delay, signal settings and vehicle year model, etc. During these network simulations, an enhanced algorithm was developed to address the issue that EAD trajectory planning of one vehicle may be affected by the time delay caused by its proceeding vehicles that haven't passed the next intersection.

As majority of the signalized intersections in the US are actuated by pedestrian calls and/or vehicle calls, it's critical to develop a more advanced EAD algorithm to work for actuated signal control. The first version of EAD algorithm for actuated signals was developed for a single vehicle scenario. This first version targets the arrival time for a

guaranteed green window initially, and then adjusts the arrival time as any early green phase or green phase extension is triggered when one vehicle is travelling through an actuated intersection.

In the future, a more sophisticated algorithm will be designed to extend the target green window into the early green phase and green extension by predicting the onset of green phase based on historical signal data.

On the other hand, after we calculated an optimal speed trajectory, we need the vehicle to follow the recommended speed trajectory. During our field tests on different vehicles at different locations, we designed an intuitive onboard human machine interface (HMI) to give driver speed recommendation. However, in some cases, we found it's hard for driver to follow closely to the recommended speed trajectory, especially when there is traffic around. In the future, we can take advantage of Adaptive Cruise Control (ACC) technology to assist vehicle to follow the recommend speed more accurately.

4.2 Algorithm Description

The relationship between fuel consumption/emissions and vehicle velocity has been studied extensively at a microscopic, physical level [10]. In general, when considering fuel and emissions normalized by distance traveled, the fuel-speed function takes on a generalized parabolic shape as shown in Fig.4.1. At lower speeds, vehicles are spending a greater time on the roads and therefore have a high fuel/distance value. At higher speeds, the engine needs to work harder to overcome aerodynamic resistance, therefore the emissions are higher. In between these extremes, the fuel consumption and

emissions are minimized, generally around 35 mph, depending on the vehicle type. As a result, in order to minimize overall fuel consumption and emissions while traveling down the road, it is best to maintain a steady-state velocity at these mid-range speeds.

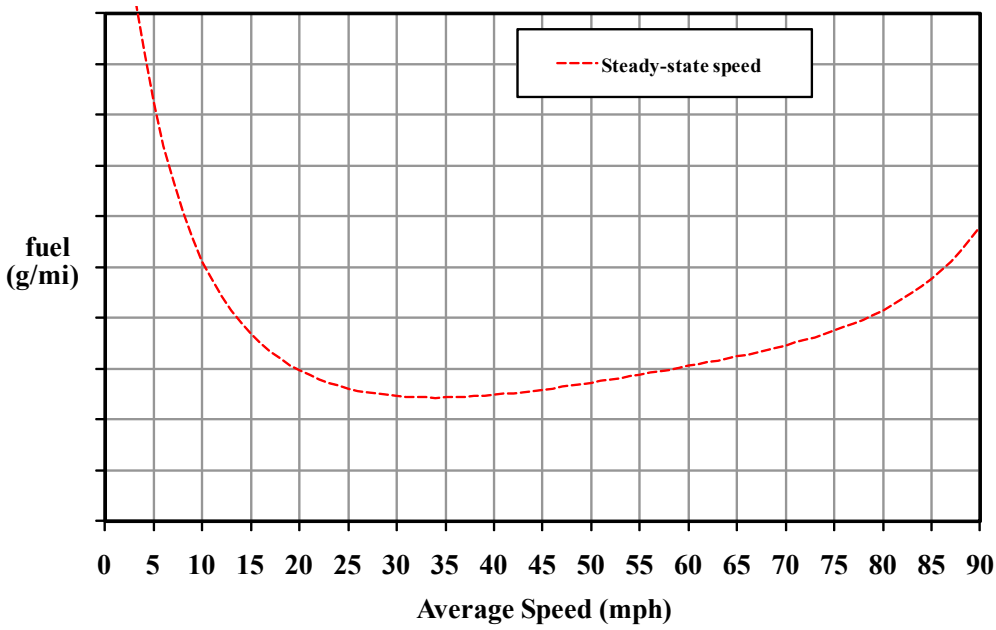

Fig.4.1. Fuel consumption versus average cruise speed generalized functional relationship [10]

Let's now consider the scenario of a single traffic light and its corresponding space-time diagram as shown in Fig.4.2. In this figure, the traffic light changes its phase with time, as shown with the green, yellow, and red lines. For illustrative purposes, four different vehicle velocity trajectories are shown with the same initial velocity of $v_i(t)$ starting from the same point $d(t)$. Let's consider that at time t, signal phase and time information is received by the vehicle. We then consider the four cases:

Case 1: vehicle cruises through the intersection with constant speed;

Case 2: vehicle speeds up to pass the intersection and then gets back to initial speed after the intersection;

Case 3: vehicle slows down and stop at the intersection;

Case 4: vehicle slows down and passes the intersection with a mid-range speed, and then speeds up to its initial speed.

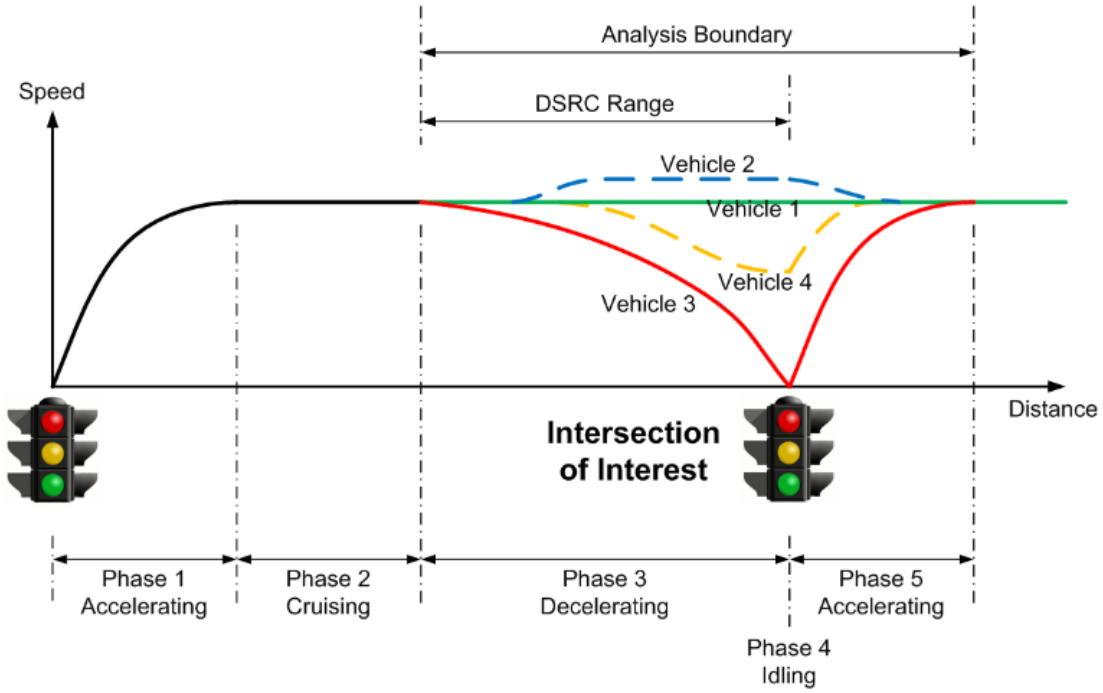

Fig.4.2. Time-space diagram representing different vehicle trajectories approaching an intersection

Even though these different trajectories cover the same distance, their fuel consumption and emissions vary greatly. Vehicle 1 uses the least fuel since it doesn't need to accelerate. Vehicle 2 consumes more fuel than vehicle 1 since there is a slight acceleration and deceleration before and after the intersection. Vehicle 3 uses the most

fuel since it decelerates to a full stop and then accelerates from stop to its initial speed. Finally, vehicle 4's fuel consumption is comparable to vehicle 2 since both vehicles have a slight speed up and slow down during their trips.

Therefore, as a vehicle travels down a signalized corridor, it is better to speed up or slowdown in advance if maintaining current speed can't make itself pass the intersection within green phase. As it approaches a signal, it is possible to dynamically adjust its velocity to minimize fuel consumption and emissions. The overall functional requirements of the vehicle are to: 1) try and maintain a steady state speed around the speed limit; 2) maintain safe headway distance to vehicles in front; 2) never cross the intersection on red; 3) avoid if possible idling at the intersection; (4) if idling is inevitable, then try to minimize the idling time at the traffic signals. An overall vehicle planning algorithm that takes all of these into account has been designed and is described in greater detail in the next section.

The overall block diagram of the arterial velocity planning algorithm is shown in Fig.4.3 [32]. The control logic for the velocity planner requires several input parameters:

v_{limit}: the local speed limit;

d_s: safe headway distance;

t_H: safe headway time;

v_p: the velocity of the proceeding vehicle;

v_{max}: the maximum speed based on car following logic and local speed limit;

v_c: the current vehicle velocity;

d_0: the distance from the vehicle to the intersection;

t_{signal}: the possible green time window for vehicle to pass the intersection;

t_{r1}: the time until the signal changes to red;

t_{g1}: the time until the signal changes to green;

t_{r2}: the time till the signal changes to red the second time;

v_{target}: the target velocity window for vehicle to pass the next intersection in green phase;

v_l, v_h: the target minimum and maximum speed of v_{target}.

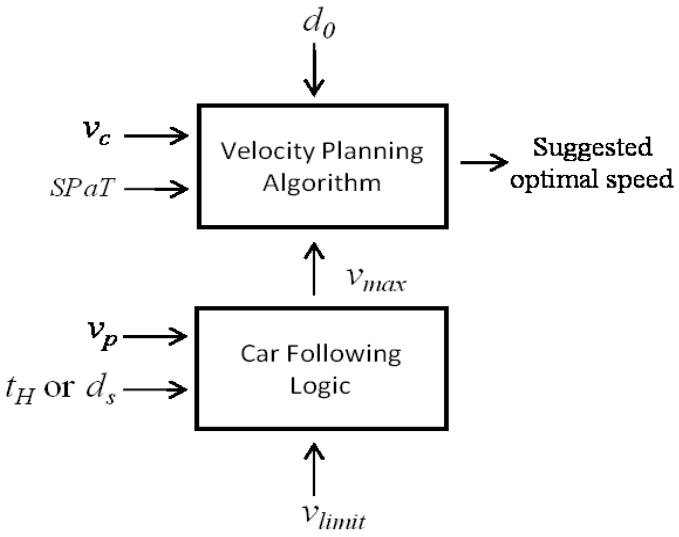

Fig.4.3. Block Diagram of the Arterial Velocity Planning Algorithm

The control logic for the optimal velocity tries to minimize one vehicle's acceleration and deceleration before the next intersection so the vehicle can pass the intersection with a target speed that is closest to its initial speed. Therefore, after passing the intersection, the vehicle can get back to its initial speed with the minimal fuel usage. The vehicle speed trajectory is designed as a piecewise sinusoidal profile, where the

acceleration and deceleration are optimized to achieve the target speed in the shortest amount of time, while ensuring the driving comfort by limiting the jerk (second derivative of speed). In order to avoid idling, the vehicle should reach the intersection during the green phase of the signal. Depending on the current phase of the signal, the travel time to the intersection is given as:

$$t \in \begin{cases} [0, t_r) \cup [t_g, t_{r1}) & if\ signal = green \\ [t_g, t_r) & if\ signal = red \end{cases}$$

Fig.4.4 then represents the target velocity selection algorithm. The acceleration and deceleration trajectory planning are as follows.

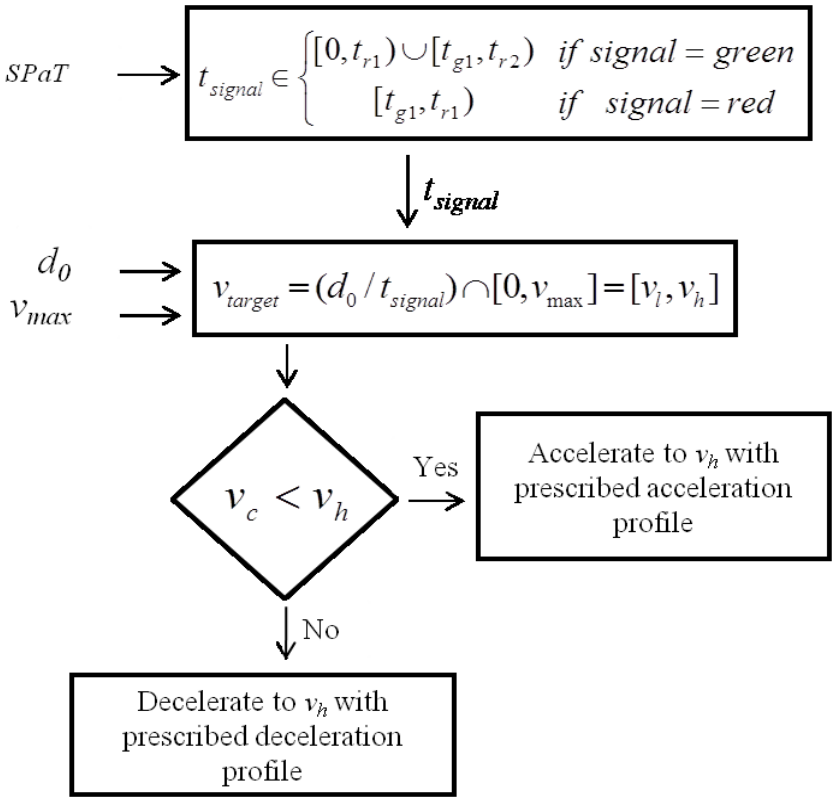

Fig.4.4. Control logic for optimal velocity determination

In order to stay within the targeted range of velocity, or to achieve a velocity so the vehicle can reach the intersection at a specific time, the vehicle will need the ability to accelerate or decelerate at specific times, as indicated in Fig.4.4. There are an infinite number of ways to accelerate or decelerate from one speed to another speed; several trajectory planning algorithms have been suggested in the literature including constant acceleration/deceleration rates, linear-acceleration/deceleration rates, and constant power rates. In our design, we wanted to choose an acceleration/deceleration profile that minimizes fuel consumption/emissions and is still comfortable to the passengers (i.e., has low jerk) as shown in Fig.4.5 (acceleration) and Fig.4.6 (deceleration).

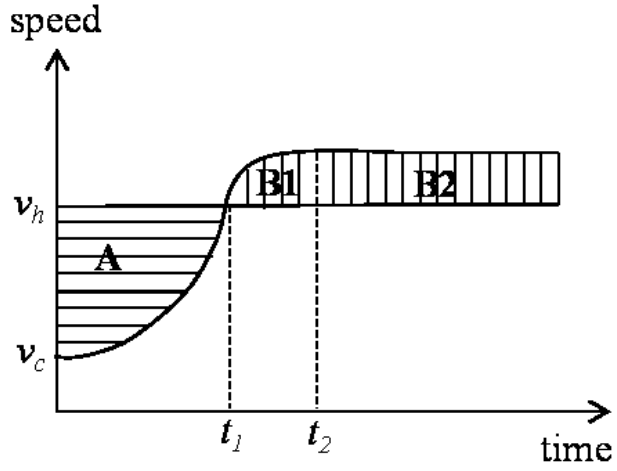

Fig.4.5. Acceleration profile for reaching a specific location at a specific time

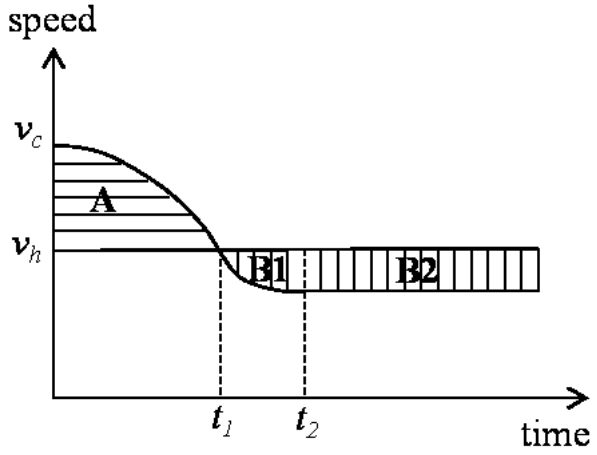

Fig.4.6. Deceleration profile for reaching a specific location at a specific time

In order to ensure a smooth trajectory, we have chosen a family of velocity profiles with a trigonometric increase in velocity given by:

$$\begin{cases} v_h - v_d\, cos(mt) & t \in [0, \frac{\pi}{2m}) \\ v_h - v_d \frac{m}{n} cos\, n\left(t - \frac{\pi}{2m} + \frac{\pi}{2n}\right) & t \in \left[\frac{\pi}{2m}, (\frac{\pi}{2n} + \frac{\pi}{2m})\right) \\ v_h + v_d \frac{m}{n} & t \in \left[\left(\frac{\pi}{2n} + \frac{\pi}{2m}\right), \frac{d_0}{v_h}\right] \end{cases}$$

where d_0 is the target distance, v_h is the upper bound of the target speed, and v_d is defined such that $v_d = v_h - v_c$. The three regions in above equation are divided by $\pi/2s$ and $(\pi/2a + \pi/2s)$, which are t_1 and t_2 in Fig.4.5 and Fig.4.6 respectively. The parameters m and n define the family of velocity profiles. Different values of (m, n) correspond to different velocity profiles. Parameter m controls the rate of change of acceleration/deceleration in region A and parameter n controls the rate of change of acceleration/deceleration in region B of in Fig.4.5 and Fig.4.6 Given a value of m, the

choice of n will depend on the requirement that the vehicle has to reach the next intersection at a specific time. It's assumed that if the vehicle travels at this constant target speed v_h, it will reach the next intersection within green phase in the shortest time. Since the vehicle's initial speed may not be exactly equal to v_h, in order to reach the next intersection in the same shortest time, the area (means traveled distance in a velocity-time diagram) of A has to be equal to the area of B1 and B2 in Fig.4.5 and Fig.4.6. With this constraint, we can write:

$$\int_0^{\frac{\pi}{2m}} (v_h - v_d\, cos(mt))dt - \int_0^{\frac{\pi}{2m}} v_h dt$$

$$+ \int_{\frac{\pi}{2m}}^{\frac{\pi}{2m}+\frac{\pi}{2n}} \left(v_h - v_d m \frac{cos\, n\left(t - \frac{\pi}{2m} + \frac{\pi}{2n}\right)}{n} \right) dt \;=\; \int_{\frac{\pi}{2m}}^{\frac{d}{v_h}} v_h dt - \int_{\frac{\pi}{2m}+\frac{\pi}{2n}}^{\frac{d}{v_h}} \left(v_h + v_d \frac{m}{n} \right) dt$$

Solving the above equation gives the following equation relating m and n:

$$n^2 - m\left(Tm - \frac{\pi}{2}\right)n - m^2\left(1 - \frac{\pi}{2}\right) = 0$$

The above equation is quadratic in n, for a value of m. The above equation has real roots only if $m \geq 3.08/T$ or $0 \leq m \leq 0.06/T$. For a value of m, n can take the positive value:

$$n = \frac{1}{2}\left(m\left(Tm - \frac{\pi}{2}\right) + \sqrt{m^2\left(\frac{\pi}{2} - Tm\right)^2 - 4m^2\left(\frac{\pi}{2} - 1\right)} \right)$$

where $T = \frac{d}{v_h}$, i.e., the time required to reach the target distance. The larger the value of m, the sharper the acceleration will be. The limit of m will be dictated by the power of the vehicle, safety, and the ride pleasure (i.e., constrained jerk). When combined with the total integrated tractive power of the trajectory, it can be seen that to minimize fuel consumption for the total acceleration maneuver, we should choose m as large as possible. This is counter-intuitive to the standard eco-driving advice that says that we should always accelerate slowly. When given a time and distance constraint, the best trajectory will accelerate quickly, reach a target velocity, and then remain at a constant velocity for a long period of time until the position is reached.

The maximum jerk can be calculated by

$$jerk_{max} = -v_d mn$$

By taking into consideration the ride comfort, previous research results by K. S. Yi, and J. T. Chung [12] has shown that a driver can tolerate up to a maximum acceleration of 2.5m/s^2 with a gradually increasing jerk profile. Therefore we choose a constraint on the maximum *m* value given by:

$$|jerk_{max}| = v_d mn \leq 10 \; and \; |a_{max}| \leq 2.5 m/s^2$$

After vehicle passes the next intersection, it needs to get back to its initial speed. The same sinusoidal profile was used as the departure speed trajectory. Since there is no time constraint in designing the departure trajectory, we used a symmetric profile where m = n. Since it's a symmetric profile, we have

$$v_h = (v_0 - v_c)/2$$

where v_0 is vehicle's initial speed.

4.3 Single Vehicle Simulation

Using the Eco-Approach and Departure algorithm for arterial roadways described in the previous section, we have applied this to a hypothetical 11-signalized intersection corridor. For the corridor, the link lengths between intersections was set to 600m, the speed limit was set to 40 mph. Each intersection is equipped with a fixed-time traffic light. Three phases were set up for each signal. The effective green time was set to 20s, with the cycle length of 50s. There was no time offset among the signals. Driver's mean reaction time and mean headway time are both set to 1 second.

The simulation was performed for a typical light-duty vehicle defined in CMEM, with a weight of 0.79 metric tons, and has more than 100k miles traveled. The road grade of all the links in the simulated corridor is assumed to be zero. The fuel consumption and emissions were determined for this single vehicle type using the well-validated Comprehensive Modal Emissions Model (CMEM, see previous studies by M. Barth, D. Schulz, K. Boriboonsomsin [13][14][15][16][17][18]).

Due to the stochastic nature of the micro-simulation, multiple runs were made using different seed numbers. The required number of runs is determined by the same method we discussed in section 3.2. In our simulation, the significance level was set to 0.05. The allowable error was chosen to be 1.5%.

For each simulation run, we also created the vehicle velocity profile for a baseline case (i.e. for vehicles that do not have the eco-driving velocity planning algorithm) for

comparison purposes. For this baseline comparison, we assumed that the typical driving behavior along a signalized corridor is where the drivers attempts to cruise at or around the speed limit until they are visually aware of the traffic signal ahead. If the signal is green, the driver simply maintains the cruise speed while crossing the intersection. If the signal is red, the driver slows down, stops, and then waits until the light turns green. Once the signal turns green, the driver accelerates back to the speed limit on the link. This driving behavior is applied at every intersection in the baseline case.

For comparison purposes, the energy and emissions for the baseline case (i.e. for vehicles that do not have the eco-driving speed planning algorithm) are also calculated for the same type of vehicle. Table 4.1 shows the energy and emissions comparison results between the vehicles equipped with and without such velocity planning for the vehicles. The results for both cases are given in terms of the average value and the standard deviation. According to Table 4.1, equipped vehicles consumed about 12.48% less fuel and produced 13.22% less CO2 emission. Furthermore, the difference of travel time per mile (TTPM) on average is relatively small, approximately 0.73% faster for the equipped vehicles as compared to the unequipped vehicles.

Table 4.1. Single Vehicle Energy, Emissions and TTPM Comparisons

	Unequipped		Equipped		Improvement
	Avg.	*S.D.*	*Avg.*	*S.D.*	
Fuel (g/mi)	167.87	1.97	146.91	2.56	12.48%
CO_2 (g/mi)	439.60	3.57	381.49	3.72	13.22%
TTPM (sec/mi)	122.08	1.43	121.18	1.23	0.73%

4.4 Network-Wide Simulation

4.4.1 Single-lane Network Simulations

One of the key questions is whether this dynamic eco-driving technology would also provide energy and emission benefits to the overall traffic and not just those vehicles equipped with the technology alone. This would be due to the influence of the technology-equipped vehicles may have on the driving profiles of the unequipped vehicles. In this section, we examine these indirect network-wide benefits for different levels of congestion and different market penetration rates of the technology.

Similar to the analysis in the previous section, we have evaluated Eco-Approach and Departure for a hypothetical 11-signalized intersection corridor, using the Paramics traffic micro-simulation environment. The energy and emissions from each individual vehicle in the simulation were determined through a CMEM plug-in module to Paramics. Multiple simulation runs were performed for different levels of congestion and different technology penetration rates.

For the experimental corridor, the link lengths are set to 600m, with only one lane in each direction. The road grade is set to be zero for all links. For simplicity, we only simulated one-way traffic on the corridor through all the intersections without any turning movements. Each intersection is equipped with a fixed-time traffic light. Three phases were set up for each signal. The effective green time was set to 20s, with the cycle length of 50s. There was no time offset among the signals. The speed limit was set to 18 m/s for the entire corridor, and the SPaT information was set to be available 300m prior to the intersection, roughly corresponding to the typical range of a DSRC transceiver. Again, driver's reaction time is set to be 1 second.

Similarly, the simulation was performed for a typical light-duty vehicle. For simplicity, there is only one vehicle category used in our simulation for all vehicles. Taking into account the limited power of the vehicle, driving safety, and ride pleasure, the maximum acceleration was set to 2.5 m/s2, and the maximum jerk was set to 10 m/s3.

Once a technology-equipped vehicle enters the DSRC range (300 m), we replace its default velocity profile with one based on the dynamic eco-driving velocity planning algorithm. The standard car-following logic is still used to guarantee the vehicle's safe headway distance.

Different levels of traffic volume were applied to the network, ranging from 100 to 600 vehicles/hour/link to represent different levels of congestion. A traffic volume greater than 600 vehicles/hour/link created extensive queuing in this network setup. In addition, different penetration rates of the technology-equipped vehicles were set ranging from 5% to 100%.

During the simulation, fuel consumption and CO_2 emissions are calculated for all the simulated vehicles over space and time. Each simulation run is performed for two hours where the first hour is a warm-up period allowing traffic to build up in the model. Similarly to single vehicle simulation, multiple runs were made for each scenario using different seed numbers. The allowable error was also chosen to be 1%.

Since at the same penetration rate and under the same congestion level, fuel saving (%) is very close to emission reduction (%) in value, so they have similar trends when varying penetration rate and congestion level. Therefore, here we only examine fuel saving in different scenarios.

Fig.4.7 shows the fuel saving at different penetration rates of technology-equipped vehicles ranging from 5% to 100% and for different amount of traffic volume from 100 to 600 vehicles/hour/link. It is observed that the level of congestion does not significantly affect the fuel savings until the technology penetration rate reaches 50%. In general, more fuel savings can be achieved at higher penetration rates.

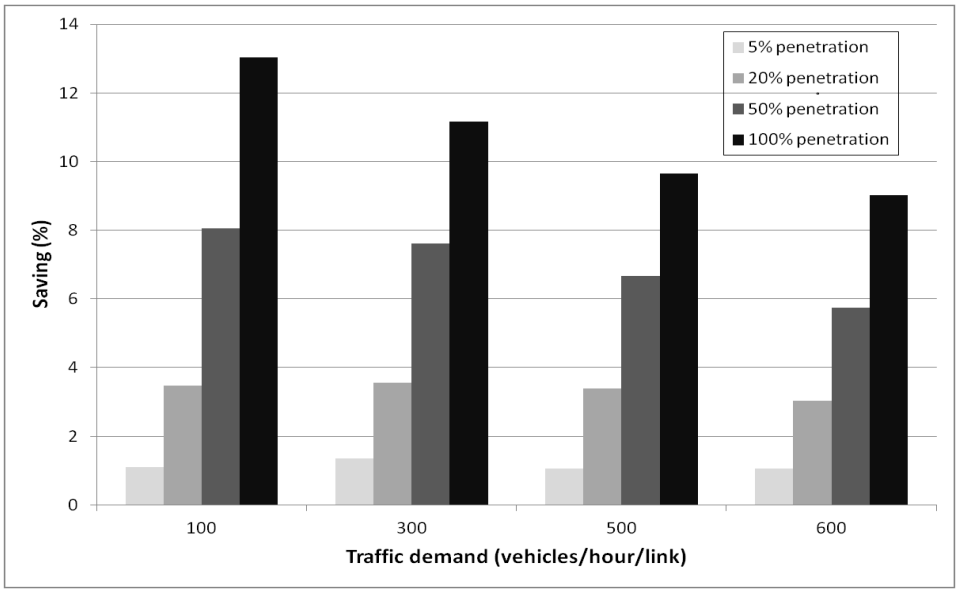

Fig.4.7. Fuel savings at different penetration rates under different congestion levels

In addition, even under low or moderate penetration rate, positive indirect network benefits can be achieved due to the behavior adaptation of un-equipped vehicles to the equipped ones. For example, a vehicle that is not equipped with the application may follow a vehicle equipped with the application and travel in a very eco-friendly way (i.e., less unnecessary acceleration/deceleration).

Fig.4.8 illustrates the energy benefits from this indirect effect of technology-equipped vehicles on their following unequipped vehicles. The solid lines are the energy savings of the whole network, and the dashed lines are the energy savings from the technology-equipped vehicles only. It is clear from Fig.4.8 that the technology-equipped vehicles have a positive effect on their following unequipped vehicles in terms of fuel savings. This positive effect is due to the technology-equipped vehicles forcing their following unequipped vehicles to have similar velocity trajectories to themselves. As a

result, the following unequipped vehicles also achieve less fuel consumption and emissions.

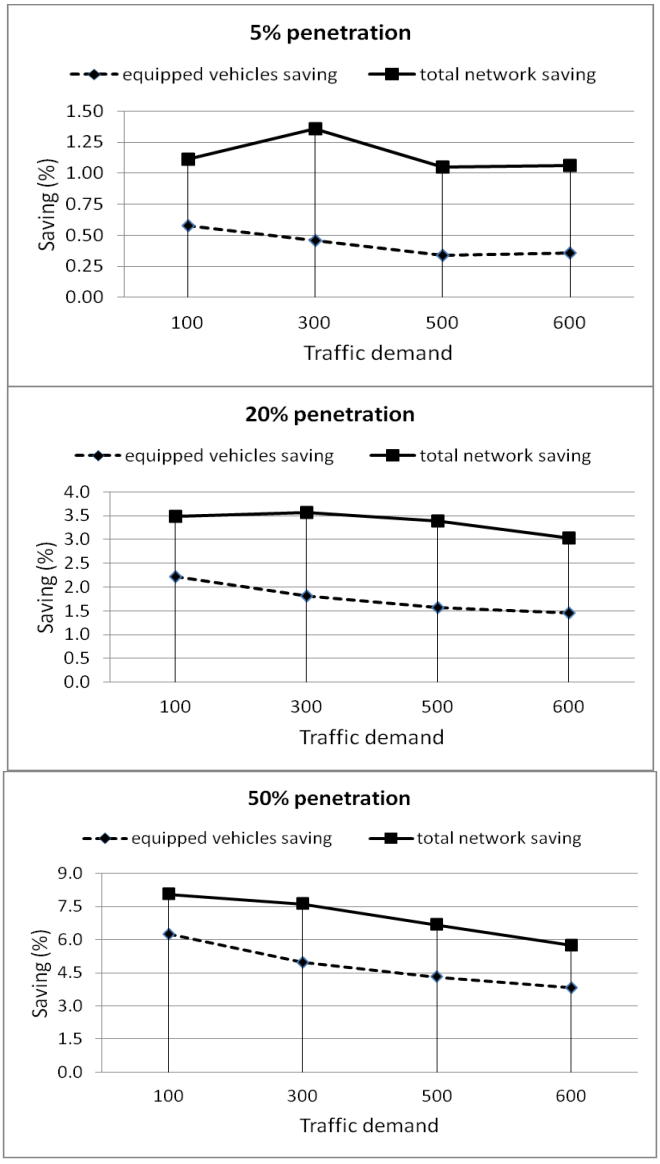

Fig.4.8. Energy benefits from indirect network effect at different penetration rate

It is noteworthy that the total fuel savings roughly double that only from equipped vehicles at low penetration rate (5% and 20%). It's also found that at some levels of congestion, at 5% penetration, this positive effect even triples the fuel savings. More detailed data at 20% penetration rate can be found in Table 4.2. The implication is that even with a low penetration of the vehicles equipped with the dynamic eco-driving technology, the overall fuel savings and emission reductions for the entire traffic network are still significant, due to the indirect effect of technology-equipped vehicles on other unequipped vehicles that provides energy/emission benefits to the unequipped vehicles in addition to the technology-equipped vehicles themselves.

Table 4.2. Indirect Fuel and Emission Benefits at 20% Penetration

Volume	Total saving		Connected vehicles		Indirect network benefit	
	Fuel	CO_2	Fuel	CO_2	Fuel	CO_2
100	3.48	3.24	2.22	2.40	157%	135%
300	3.56	3.42	1.82	1.87	196%	183%
500	3.39	3.07	1.57	1.60	216%	192%
600	3.02	2.76	1.45	1.49	208%	185%

4.4.2 Multiple-lane and Multiple Cycle Lengths Analysis

In order to examine our algorithm in multiple-lane network, we extended our previous network from one lane to three lanes per direction. We also varied the signal cycle length from 60s to 90s, with the percentage of green phase kept the same as 40% of the total cycle length. The other network parameters, such as number of intersections, link lengths and speed limit etc., stay the same. The same vehicle type was used in simulations. Similarly to previous simulation setup, multiple runs were made for each scenario using different seed numbers. And the allowable error was also kept down below 1%.

Fig.4.9, Fig.4.10 and Fig.4.11 show fuel savings for different cycle lengths and green phase durations. Comparing Fig.4.9, Fig.4.10 and Fig.4.11 with Fig.4.7, we found that as the cycle length was extended from 50s to 60s, 90s and 120s, generally less fuel was saved. This may be due to that as both cycle length and green phase duration were

extended, vehicles now have more chances to travel through intersections without having to slow down or stop, in which case there is no huge difference in fuel consumption between equipped and unequipped vehicles.

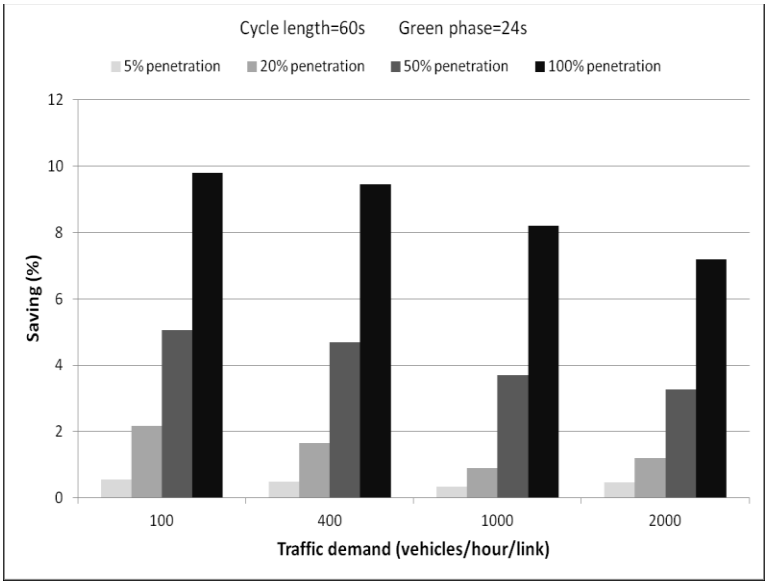

Fig.4.9. Fuel savings when cycle length is 60s with 24s of green phase

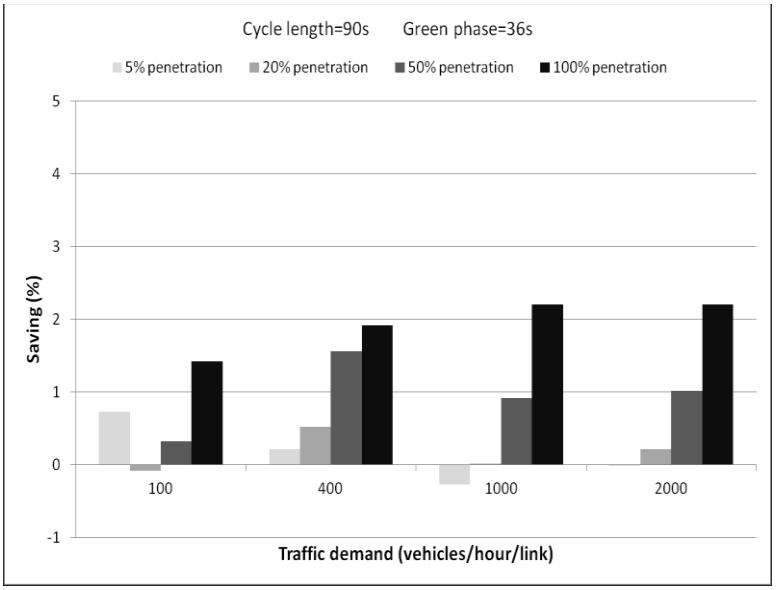

Fig.4.10. Fuel savings when cycle length is 90s with 36s of green phase

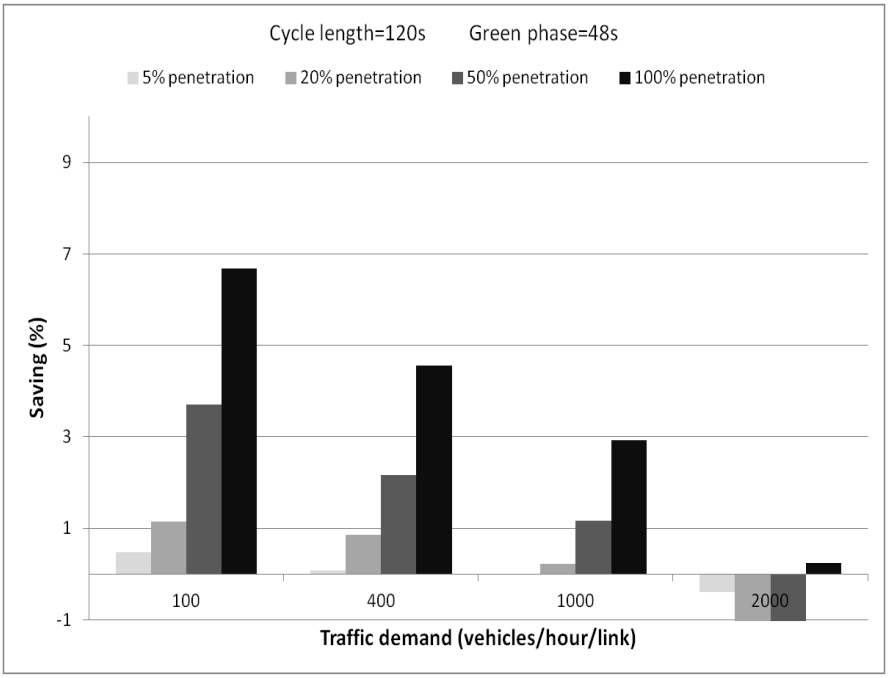

Fig.4.11. Fuel savings when cycle length is 120s with 48s of green phase

It's also noted that, as cycle length was increased from 90s to 120s, more fuel savings were achieved at low and medium congestion levels (100, 400, 100 vehicles/hour/link). Based on our observation during the simulations when the cycle length set to be 90s, we found that at low and medium congestion levels, most vehicles passed the first intersection without slowing down and then came to a full-stop at the second intersection, and so on. This indicates that most vehicles in this scenario either passed the intersection at full speed or applied full-stops at the intersections. In above two cases, equipped vehicles and unequipped vehicles have similar driving patterns. Therefore, less fuel savings were obtained in this scenario, as shown in Fig.4.10.

Fig.4.11 shows some negative savings at the highest congestion level (2000 vehicles/hour/link), at low and medium penetration rates (5%, 20% and 50%). Since we

extended the number of lanes per direction from one to three, vehicles now have more flexibility to change lanes. Especially under high congested condition, when a vehicle finds its proceeding technology-equipped vehicle slows down, this vehicle may have to slow down first to keep safe headway distance from its proceeding vehicle, and then it may change lane and accelerate back to its previous speed if adjacent lane is relatively free. This kind of behavior can increase unequipped vehicles' fuel consumptions. Moreover, indirect network energy/emission benefit from car-following logic is also reduced due to the lane-changing behaviors. However these effects don't have significant impact on the total fuel consumption of the network (around 1% increase). When penetration rate reaches 100%, since there is no unequipped vehicles contributing to these effects, fuel savings are always positive at all congestion levels, as shown in Fig.4.9, Fig.4.10 and Fig.4.11.

4.4.3 Summary

Fuel consumption and emissions are directly related to the acceleration/deceleration patterns of the vehicles traveling on the arterial and the idling at traffic signals. Unlike freeways, traffic on the signalized corridors suffers from inherent acceleration/deceleration maneuvers at the traffic signals and idling when they are waiting for the lights to change. By taking advantage of the recent developments in communication between vehicles and road infrastructure, it is possible to obtain the signal phase and timing information. Using this real-time signal information, we have

developed a dynamic eco-approach and departure algorithm that attempts to guide a vehicle through an arterial corridor using a minimum amount of fuel.

Based on this research, there are several key findings that are counter-intuitive when compared to typical eco-driving advices. When traveling on a roadway where there are specific points where traffic is controlled (traffic lights), specific constraints emerge in time and space; as a result, it has been found that hard accelerations that quickly get a vehicle up to a target speed and then have a steady cruise to reach a specific location at a specific time are less fuel consuming compared to a velocity profile that takes a longer period of time of acceleration to reach the same point of time and space. Similarly, it is beneficial to decelerate quickly, and then hold a steady state cruise speed when reaching a traffic signal just as it is turning green. At that point, it takes less energy to accelerate back up to typical speed traversing the corridor, compared to starting from a stop.

Results of our algorithms show approximately 12% fuel economy improvement and 13% emission reductions in individual vehicles over a standard baseline case without the velocity planning.

In addition to these individual vehicle benefits, a set of experiments were also carried out to determine if there is a network-wide energy/emissions savings from having a low penetration rate of dynamic eco-driving technology equipped vehicles in the traffic stream. It is concluded that there is indeed additional network-wide fuel savings and emission reductions, due to the fact that unequipped vehicles are forced to follow the trajectories of the dynamic eco-driving vehicles in front, based on the car following logic. In the experiments, the maximum fuel saving and emission reduction occur during low

congestion condition (corresponding to traffic volume of 100 vehicles/hour/link). Even at low technology penetration rates, significant fuel savings and emission reductions were still achieved. Under these low-penetration conditions, the total traffic energy/emission savings typically double what is saved from the technology-equipped vehicles alone (e.g., total 3.39% savings compared to 1.57% savings from equipped vehicles at the penetration rate of 20%).

We also tested our algorithm in a multiple-lane network with different signal cycle lengths. As both the cycle lengths and green phase duration increase, vehicles have more chances to pass intersections without stop or slowing down. Also since vehicles have more flexibility to change lanes, indirect network energy/emission benefit from car-following logic is weakened. Therefore, fuel savings are not as high as in previous simulations.

4.5 Enhanced Algorithm

4.5.1 Algorithm Description

In previous section, we developed a fundamental eco-approach and departure system, which can provide a driver recommendation on the speed trajectories to ensure that the vehicle approaches and departs a signalized intersection with as little fuel consumption and pollutant emissions as possible. Such systems rely on the infrastructure to vehicle (I2V) communication (e.g., through cellular network or dedicated short-range communication) to access the approaching signal phase and timing (SPaT) information sent from RSE (Road-Side Equipment) to the connected vehicle. OBE (On-Board

Equipment) in the connected vehicle process this information to provide speed advice to the driver of the vehicle, enabling the driver to alter the vehicle's speed to pass through the next traffic signal on green or to decelerate to a stop in the most eco-friendly manner without compromising the intersection delay. However, the design of the subject vehicle's speed trajectory is optimized on single vehicle and does not consider the traffic conditions ahead. Therefore, the actual speed profile may not be able to follow the design target due to car-following constraints, i.e., always keeping safe distance in-between vehicles. As a result, an additional amount of fuel is wasted on unnecessary acceleration/idling. Our previous studies also showed that as traffic gets more congested, the system-wide relative benefits from the developed dynamic eco-approach algorithm decreases. A potential reason is that the equipped vehicle has no access to the queue information (e.g., queue length) in front of it when approaching the intersection. The longer the queue is, the more unexpected acceleration/deceleration or idling maneuvers that are not considered in the planned speed trajectories would be. As a result, much less benefits can be gained to reduce fuel consumption and pollutant emissions during levels of high congestion.

Therefore we proposed an enhanced eco-approach system which utilizes not only SPaT message but also the information of preceding equipped vehicles for better speed trajectory planning. Then, we use microscopic traffic simulation tool(s) to evaluate the performance of the enhanced system. In order to better predict traffic conditions, queue information can be collected at each intersection and formatted as intersection delay t_{int_delay}, which can be utilized by each approaching vehicle to plan its optimal speed

trajectory based on the estimated intersection delay caused by the queue. The design logic of the optimal speed trajectory is shown in Fig.4.12.

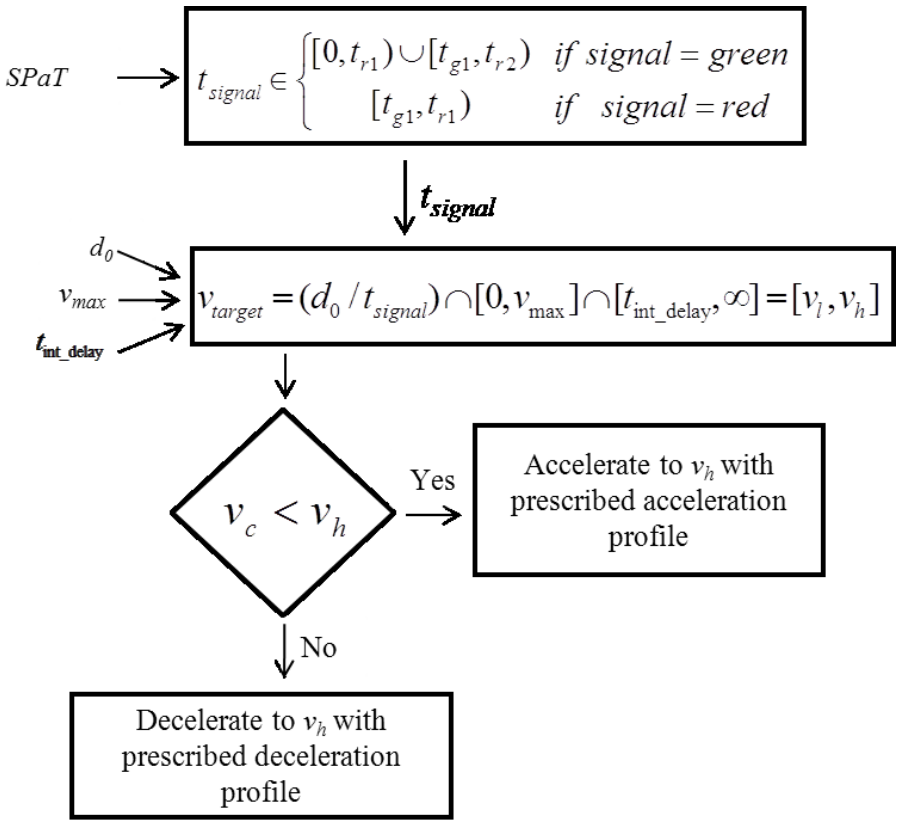

Fig.4.12. Design logic of the optimal speed trajectory

v_{limit} is the speed limit, ds is safe headway distance, t_H is safe headway time, v_p is the speed of the proceeding vehicle, and v_{max} is the maximum speed restrained by the car following model. Further, v_c is the current speed, d_0 is the distance to intersection, t_{signal} is the time window for vehicle to pass the intersection within green phase, t_{r1} is the time till the next red phase, and t_{g1} is the time till the next green phase, and t_{r2} is the

time till the next next red phase. v_{target} is the target velocity window. v_l, and v_h are the lower and higher bounds of v_{target}.

First, we assume each vehicle takes up a constant time slot t_{slot} when it passes through an intersection. It is found that 2 seconds is a reasonable approximation for this time slot. To implement this mechanism, every incoming vehicle will schedule a 2-second time slot from the earliest green phase of the intersection. In the meantime, each intersection keeps track of the total time slots that have been occupied by all the approaching vehicles within communication range, so as to provide the next coming vehicle with the earliest arrival time. The estimated intersection delay t_{delay} is calculated by

$$t_{delay} = nt_{slot}$$

where *n* is the total number of approaching vehicles within the communication range. Once current green phase is filled up, the intersection will start to guide vehicle into the next green phase, and so on. In case if a vehicle cannot make it to the next earliest arrival time even by travelling at speed limit, the vehicle will choose the earliest feasible time that it is capable of reaching. As a result, vehicles will travel through intersections one group after another like platoons.

On the other hand, on a signalized corridor, especially when the link lengths between intersections are relatively large, closely packed platoons of vehicles from previous intersection tend to dissolve over time [19]. Our platoon-based eco-approach method can address this issue by not only keeping vehicles moving in platoons, but also minimizing the total fuel consumption and emissions. Fig.4.13 shows the formation of

this platoon-like movement in a time-distance diagram. The grey lines represent green phases, while the dark black lines are red phases.

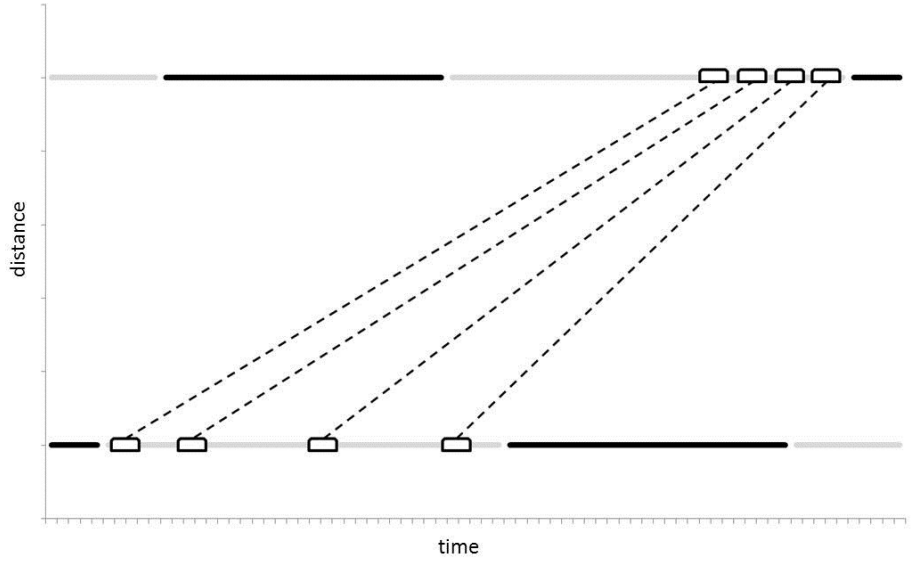

Fig.4.13. Illustration of enhanced eco-approach application in a time-distance diagram

4.5.2 Simulation Analyses

We applied the enhanced eco-approach algorithm on a hypothetical corridor with three fixed-time signalized intersections. The lengths of the links between neighboring intersections are set to 500 meters. The speed limit was set to 50 mph. The effective green time for the pass-through phase is 30 seconds, with the total cycle length set to 60 seconds. In order to evaluate the improvement in terms of fuel consumption and emissions, there is only one lane in each direction, and there is only mainline traffic fed into the simulations (no cross traffic, and no turning movements). Communication range was assumed to be infinite (e.g., through 4G/LTE) in this simulation. Sensitivity analyses on traffic demand, penetration rate, communication range and communication delay were

conducted on a multiple-lane network with cross traffic and turning traffic, and they will be discussed later in this session.

The simulation was performed for a typical light-duty vehicle. The road grade of all the links in the simulated corridor is assumed to be zero. The fuel consumption and emissions were determined for this single vehicle type using the well-validated CMEM model.

Multiple runs were made for each testing scenario using different seed numbers, due to the stochastic nature of the micro-simulation. The seed number is the starting number for the RNG (random number generator) used by Paramics. To initialize a simulation run, a random number is generated based on a uniform random distribution to determine the time gap between consecutive vehicle releases. The minimum number of runs to ensure an error bound (ε) is determined the same way in Chapter 3.2. This calculation is performed for both CO2 emissions and fuel consumption. The higher calculated N of these two is the required number of simulation runs. Once the number of conducted runs is no less than the required number of runs, the simulation for that scenario is finished. Otherwise, one more run is made and the required number of runs is updated accordingly. In our simulation, the significance level was set to 0.05. The allowable error was set to 2%.

For comparison purpose, simulations were performed on baseline case (i.e. for vehicles that do not have the eco-approach strategy) for each scenario. For this baseline comparison, we assumed that the typical driving behavior along a signalized corridor is where the drivers attempts to cruise at or around the speed limit until they are visually

aware of the traffic signal ahead. If the signal is green, the driver simply maintains the cruise speed while crossing the intersection. If the signal is red, the driver slows down, stops, and then waits until the light turns green. Once the signal turns green, the driver accelerates back to the speed limit on the link. This driving behavior is applied at every intersection in the baseline case.

Fig.4.14(a) shows the fuel savings when vehicles don't have the information of intersection delays. Generally, as the penetration of connected vehicles gets higher, more fuel savings were achieved by implementing our eco-approach algorithm. The exception occurs in the relatively congested condition (600 vehs/lane/hr), where a higher penetration of connected vehicles doesn't achieve the most fuel savings, thanks to the increased lengths of queues at the intersections and more interruption from surrounding traffic, both of which prevent the eco-approach algorithm from making effective trajectory planning. As is shown in Fig.4.14(a), at the lower traffic demands (100 and 300 vehicles/lane/hour), the maximum fuel saving occurs at 100% penetration rate. At 600 vehs/lane/hr, the maximum fuel saving shifts to the penetration rate of 80%. The maximum fuel saving across all scenarios simulated occurred is approximately 31%, which occurs at 100% penetration rate when traffic demand is 300 vehs/lane/hr. Maximum fuel saving of 31% was achieved at 300 vehs/lane/hr.

In comparison, Fig.4.14(b) is the fuel savings when vehicles have the information of intersection delays. Compared with Fig.4.14(a), an overall increment on fuel savings is found at all congestion levels and penetrations of connected vehicles. More importantly, there is significant improvement in highly congested condition (600 vehs/lane/hr), with

the highest fuel saving reaching up to 38%, compared to the 27% when not considering the intersection delays.

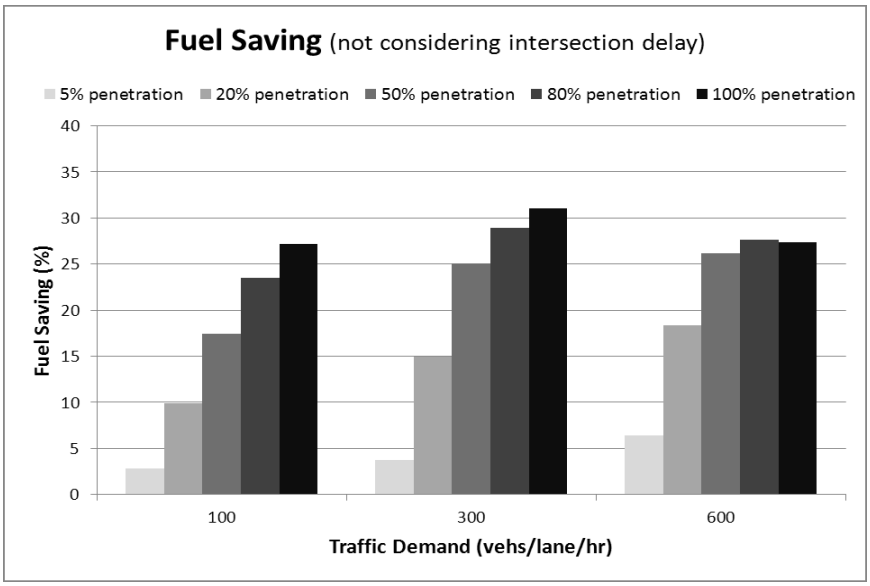

(a) Without consideration of intersection delay

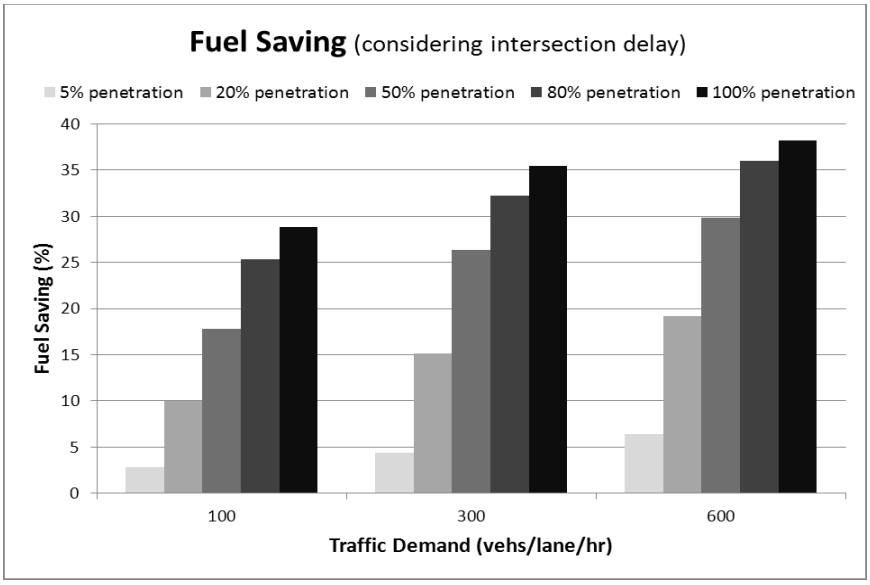

(b) With consideration of intersection delay

Fig.4.14. Fuel savings across different traffic demands and penetration

4.5.3 Sensitivity Analyses

Previous generic experimentation evaluated how much more fuel savings can be achieved by applying platoon control on top of the eco-approach strategy. In order to generalize our experiment, both cross traffic and turning traffic were added into the simulations. Also, two lanes were assigned for the through traffic, and one lane was added for left-turn only traffic, on both mainline and cross street. Right-turn was also permitted. Fig.4.15 shows the intersection layout and the traffic flows.

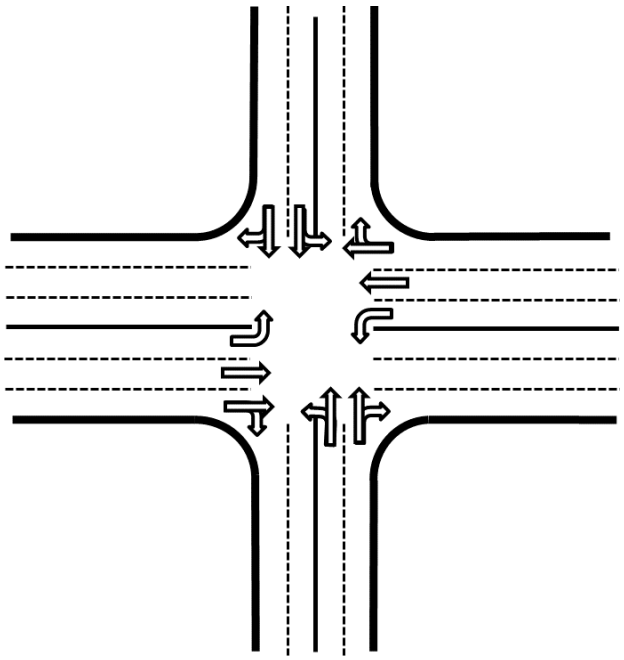

Fig.4.15. Intersection layout and traffic flows

1) Congestion Level

Fig.4.16 shows the fuel consumption for baseline and the enhanced eco-approach. In the simulations of eco-approach, all vehicles are connected to their upcoming intersections, and the communication range is assumed to be infinite. It can be

seen that under all levels of traffic demand, the enhanced eco-approach strategy significantly lowered fuel consumption. It was also found that as the traffic demand gets higher, there are slightly more fuel saving, since there were longer queues formed, thus more fuel consumption in the baseline scenario.

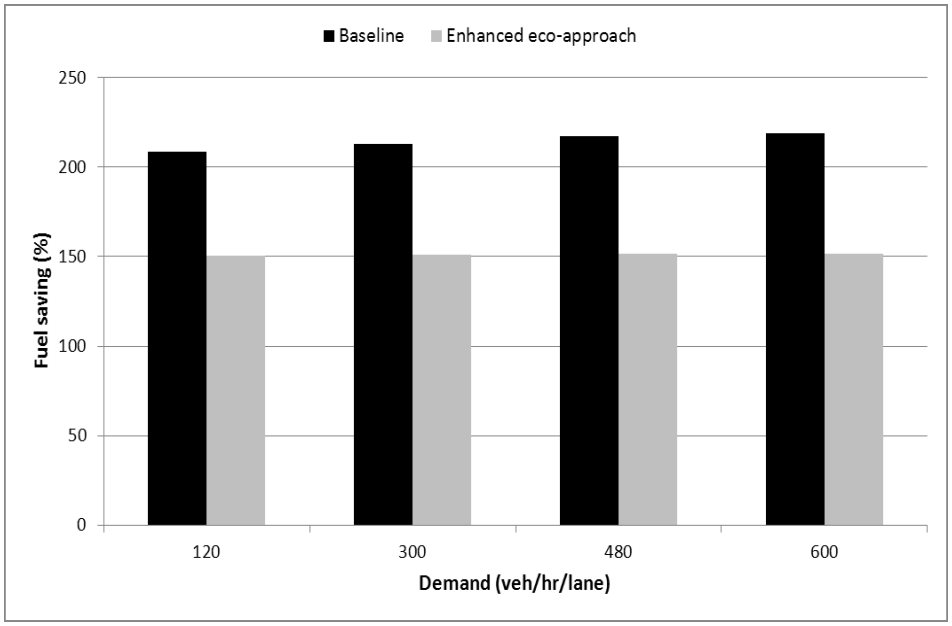

Fig.4.16. Fuel economy under different traffic demands

2) Penetration Rate

Fig.4.17 shows how fuel saving changes with traffic demand at different penetration rates of connected vehicles which are applied with the enhanced eco-approach strategy. It is apparent that more congested traffic leads to more fuel saving at different penetration rates of connected vehicles. It was also found that even low penetration (20%) of connected vehicles can achieve significant amount of fuel saving (7% - 11%) by applying the enhanced eco-approach strategy. At 100% penetration rate, more than 30% of fuel saving can be achieved.

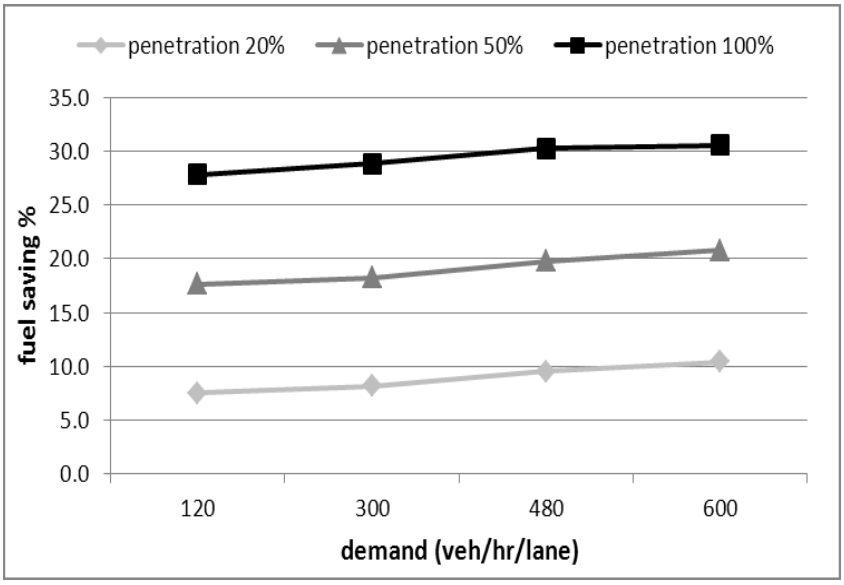

Fig.4.17. Fuel savings across different traffic demands and penetration

3) Communication Range

In previous simulations, the communication range is assumed to be infinite. Since the link lengths in this network are identically 600 meters long, the connected vehicles start receiving SPaT messages at 600 meters from the next intersections. Results in Fig.4.18 show how fuel saving achieved by this enhanced eco-approach can be affected by communication range. It's found that fuel savings drastically go down as communication range decreases. Since as the communication distance gets shorter, there's less room left for vehicles to plan their trajectories.

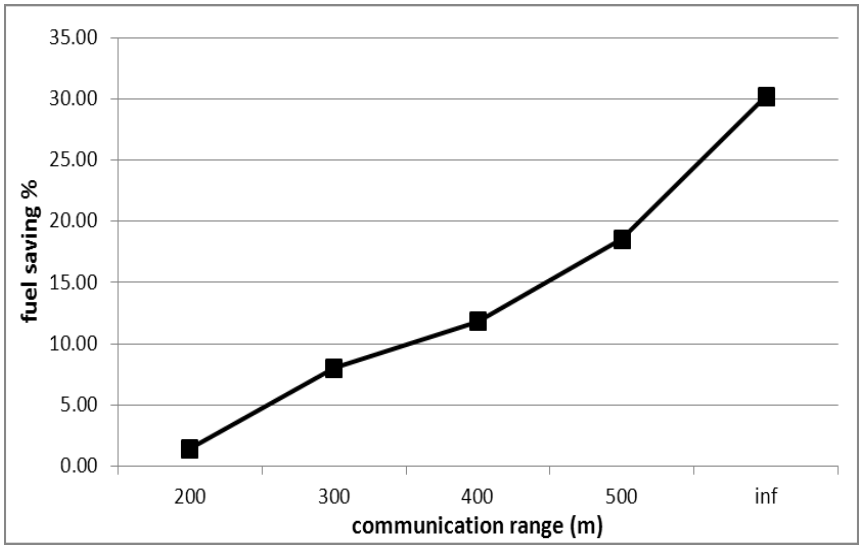

Fig.4.18. Fuel savings under different communication ranges

4) Communication Delay

In the real world, due to a variety of software and hardware issues, communication delay is inevitable. Based on extensive modeling, it has been found that the enhanced eco-approach strategy wasn't largely affected by the communication delay, as shown in Fig.4.19. Even when the signal is delayed for 10 seconds, fuel saving only decreases around 15%. When delay is under 2 seconds, there is no noticeable decrease of fuel saving.

Therefore, this strategy is very sensitive to communication range, but not very much affected by communication delay. In this regard, 4G/LTE network may be the ideal candidate for realizing this strategy.

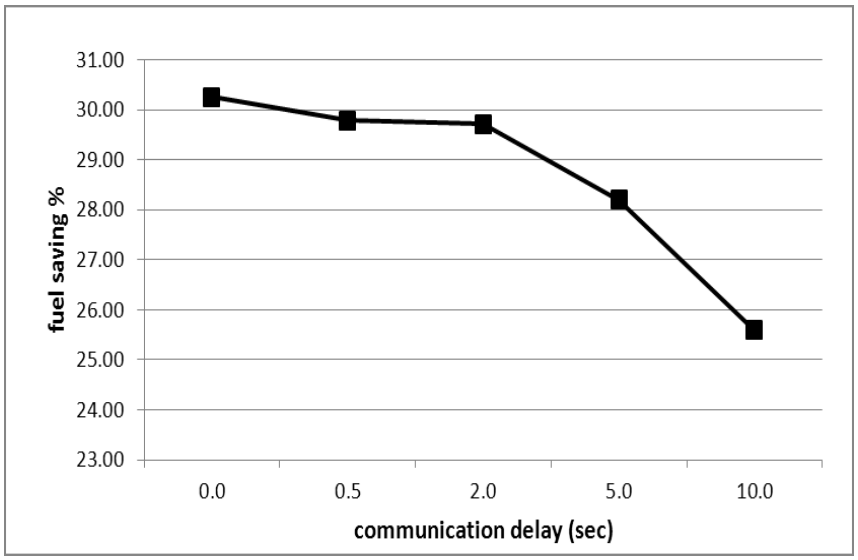

Fig.4.19. Fuel savings under different communication delays

4.5.4 Summary

In this section, we proposed an enhanced eco-approach application which considers not only the phase and timing of the signal but also the estimated intersection delay in front of the subject vehicle. The comparative study in a simulation environment exhibits that the proposed application outperforms its predecessor, which does not account for the estimated intersection delay, especially when traffic gets more congested. Simulation results also show that the network-wide fuel saving benefits of the proposed application are not sensitive to the congestion level, but to the penetration rate, communication range, and communication delay.

4.6 Eco-Approach and Departure for Multiple Intersections

The initial Eco-Approach and Departure only takes the signal phase and timing information of the next intersection, without considering the subsequent signalized

intersections if there is any. This research is to improve the algorithm by taking into account the signal phase and timing information from multiple consecutive intersections on a signalized corridor. Besides that, the opportunity of switching to a time saving behavior has to be provided. The main goal is to find an optimal speed trajectory that prefers leading the car through green phases while optimizing a weighted cost function of fuel consumption and time saving for the whole route. Furthermore, several weak and strong constraints that have to be considered have to be worked out and analyzed. This section only provides an initial approach on an algorithm that can be used for multiple fixed-time signalized intersections.

The overall architecture for multiple intersections is illustrated in Fig.4.20. Constraints, data of traffic lights, the car and the environment will be updated every time step to interact with the algorithm. The output will be a future speed profile including a recommendation for the velocity, acceleration, speed mode and gear. The amount of future fuel consumption shall be considered directly in the calculation of the future speed trajectory. Furthermore, the system shall use all possible speed modes to enable continuous speed profiles. The algorithm shall be created in a flexible way to allow dynamic and changing constraints. Besides that, an appropriate test track must provide traffic light data and data of the environment like the geographical positions of the upcoming traffic lights along the route.

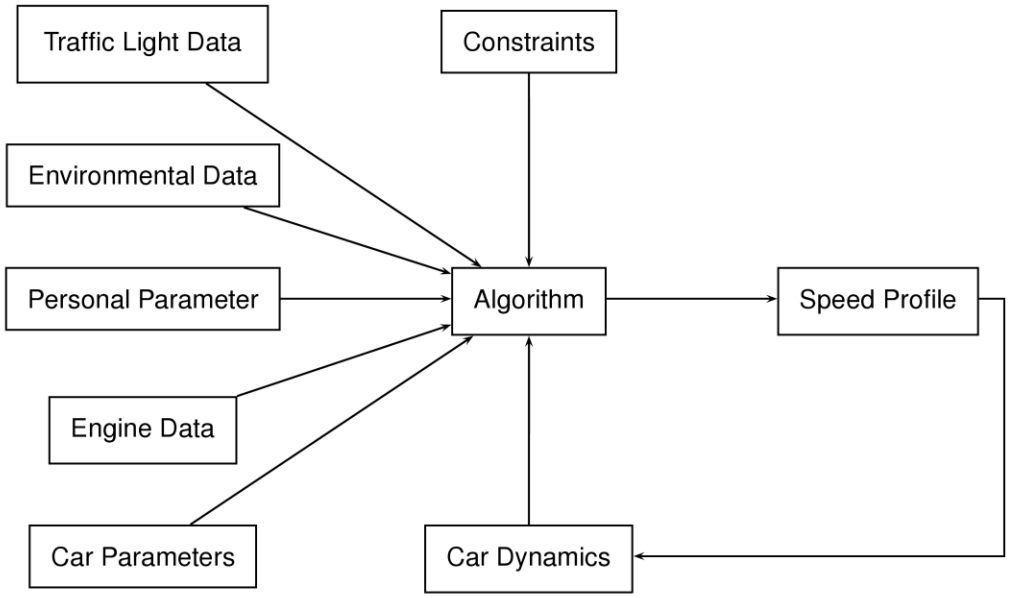

Fig.4.20. Architecture of the Smart Cruising Algorithm [20]

All possible speed modes have to be identified in a first step and very detailed fuel consumption maps have to be created. A very detailed calculation of fuel consumption and the dynamics of the vehicle have to be combined with the goal to enable a real-time system and to reduce computation time. This shall be achieved by a very detailed offline calculation for every speed mode. Consequently, online computation time is saved by using the created look-up tables at runtime.

In order to get a very exact fuel consumption calculation for various essential speed modes like acceleration, constant speed, sailing, shearing, braking, standstill and a mixture of these, it is essential to create a very detailed nonlinear model that describes the dynamics of the vehicle and the consumed fuel in these speed modes exactly.

In order to find an appropriate principle that solves the stated problem under the stated constraints, the goal is formulated in an abstract way to find similarities between

this problem and one that is thoroughly analyzed in optimization literature. The goal is to find an optimal trajectory through several stages (traffic signals) with some weighting possibilities (fuel consumption and time) that takes several different constraints (i.e. speed regulations, etc.) into account.

According to the formulated problem, a principle has to be found that compute the optimal solution. The algorithm has to make decisions considering the influence of these decisions for the future speed, arrival time and position of the vehicle. Since a certain number of stages are given due to the traffic lights, the principle has to handle a discrete problem, finding a continuous solution. The space for finding the optimal solution is not infinite, due to the realistic scenario and constraints. Furthermore, direct influence on the weighted fuel consumption and travel time is necessary. Based on the characteristics of this formulated problem, *dynamic programming* was chosen as the means to optimize the trajectory planning.

Dynamic Programming deals with situations where decisions are made in stages. The objective is to minimize a certain cost, i.e., a mathematical expression of what is considered an undesirable outcome. A key aspect of such situations is that decisions cannot be viewed in isolation since one must balance the desire for low present cost with the undesirability of high future costs. The dynamic programming technique captures this tradeoff. The basic model has two principle features, an underlying discrete-time dynamic system and a cost function that is additive over time.

Dynamic Programming is a multi-step optimization scheme which requires discrete steps for each iteration. The discretization in space (the longitudinal coordinate

of the car) is set to the positions of the upcoming traffic lights. The position of the car at the time the calculation is started is chosen as the origin. No positions between the traffic lights are considered. Reducing computation time is one reason for that, the second reason is the advantage of enabling natural continuous speed profiles between the traffic lights without many switches in speed mode.

For the discretization in time, only the green phases are considered. The number of time steps in every green phase decides the accuracy of the final result as well as the computation time needed. A reasonable tradeoff has to be found in order to decide about the value of this variable. Furthermore, discretization points that do not meet the constraints are eliminated in order to save computation time.

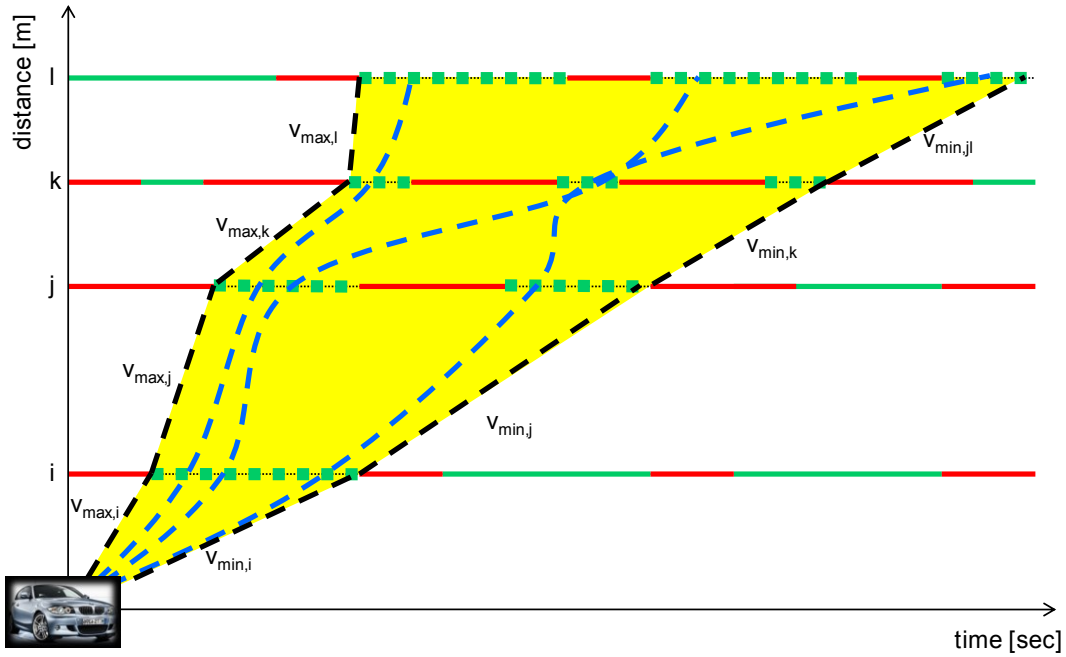

Fig.4.21. Problem description in time and space depicting discretization points

During the Dynamic Programming process, fuel consumption and vehicle dynamics for every iteration step are calculated. Figuring out the required speed mode for

every step is essential. The following section explains the way of choosing the optimal speed mode for a known distance d, a known time difference t for travelling this distance as well as a known initial velocity v_0. Based on this decision, the fuel consumption associated with the action performed is calculated. The possible speed modes include acceleration, constant speed, sailing, shearing, braking and a mixture of the stated ones.

Shearing denotes deceleration by the friction between engine and drive train while vehicle's kinetic energy is used to turn the engine. In this case the engine is still on and the fuel consumption for shearing is zero. Sailing in contrast refers to the state when the drive train is decoupled from the engine, which leads to a smaller deceleration than shearing. In this mode, the engine is still running, thus it has a constant fuel consumption rate which depends on the velocity.

Detailed analyses were conducted in order to find the optimal combinations of these modes in terms of fuel consumption and overall energy conservation. Fig.4.22 illustrates the decision process for an example with $v_0 = 70\ \frac{\text{km}}{\text{h}}$ and $t = 40$ s. Depending on the distance to travel d, the best mode can be extracted from the diagram. The three boundaries between the different modes are depicted as blue dashed lines and represent the trajectories when driving with constant speed as well as sailing and shearing.

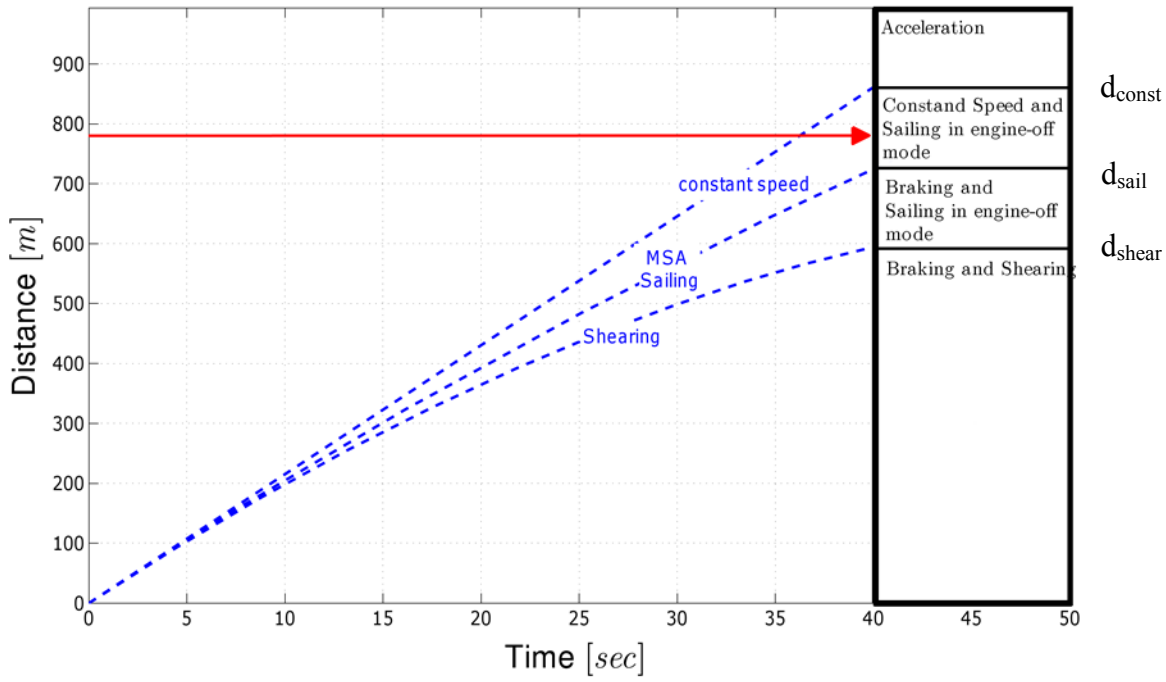

Fig.4.22. Speed mode decision logic

With these considerations, the optimal speed mode depending on d is chosen by the following logic:

1. $d > d_{const}$: In this case acceleration is required. The lowest constant acceleration possible is calculated and the speed mode is set to acceleration.
2. $d = d_{const}$: Here the final state can be ideally reached by holding the constant speed.
3. $d_{const} > d > d_{sail}$: If the car would pass too much distance with constant speed while it would pass a too short distance by sailing only, a mixture between constant speed and sailing is the solution. The most fuel efficient and energy-conserving combination is to maintain constant speed to a calculated intermediate point, followed by sailing.

4. $d = d_{sail}$: In this case the final state can be ideally reached by sailing only.
5. $d_{sail} > d > d_{shear}$: If the deceleration by only sailing is not high enough, a combination of sailing and braking after that will be used similar to case 3.
6. $d = d_{shear}$: Here the final state can be ideally reached by shearing only.
7. $d < d_{shear}$: If even the deceleration of shearing is not high enough, the optimal combination of shearing and subsequent braking is set as the resulting speed mode.

For each of the mixed modes, a sub-function is designed that solves the nonlinear optimization process of combining the essential speed modes in an optimal way that satisfies the input parameters v_0, t and d. As a result, these sub-functions yield the final velocity v_f, the absolute fuel consumption for the whole process fc and, if applicable, the position of an intermediate point in space-time (t_m, d_m) as well as the associated velocity v_m at this point. The essential speed modes can then be seen as special cases of these superimposed functions. The results of the functions are again tabulated in order to enable real-time feasibility of the online algorithm.

4.7 EAD for Actuated Signals

After extensive discussion about eco-approach and departure algorithm for fixed-time signals, it is worth exploring alternative solutions for actuated signals, since actuated signals are more widely implemented in real world and potential solutions for actuated signals can give us more flexibility to accommodate changes of signal timings.

Stevanovic, A. [21][22] evaluated a speed advisory system called GLOSA on both fixed-time and actuated signal timings. As expected, the results show speed advisory works better on fixed-time signal timings. On the contrary, the algorithm for actuated signal timings posed negative impact on the fuel consumption. In this chapter, a modified algorithm for actuated signals is discussed.

4.7.1 Algorithm Overview

The new algorithm divides the problem into three separate problems. These three problems result in different steps of the algorithm. In each step the results of the previous step are used to solve current problem (see Fig.4.23).

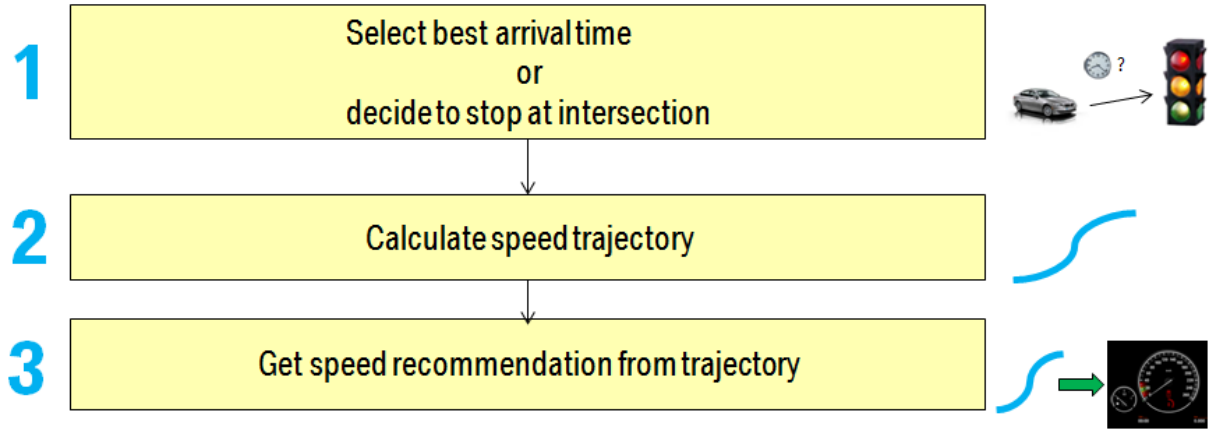

Fig.4.23. Algorithm overview

The first problem is to determine, if it is possible to arrive at the next intersection at green under given constraints: The driver must not travel above speed limit and the acceleration must not exceed a feasible maximum acceleration/deceleration threshold. Additionally the driver has to travel at least with an appropriate minimum speed. For the case, that it is possible to arrive at the next intersection at green, the time when it best to arrive at the intersection is calculated in this step.

The second problem is to determine a speed trajectory that allows the driver to arrive at exactly that point of time that was calculated in the first step.

Given a speed trajectory, the last problem consists of presenting the driver a speed recommendation that allows to the driver to follow the speed trajectory that was planned in the second step.

Fig.4.24 gives an overview of how the different steps are connected. Each step is described in detail.

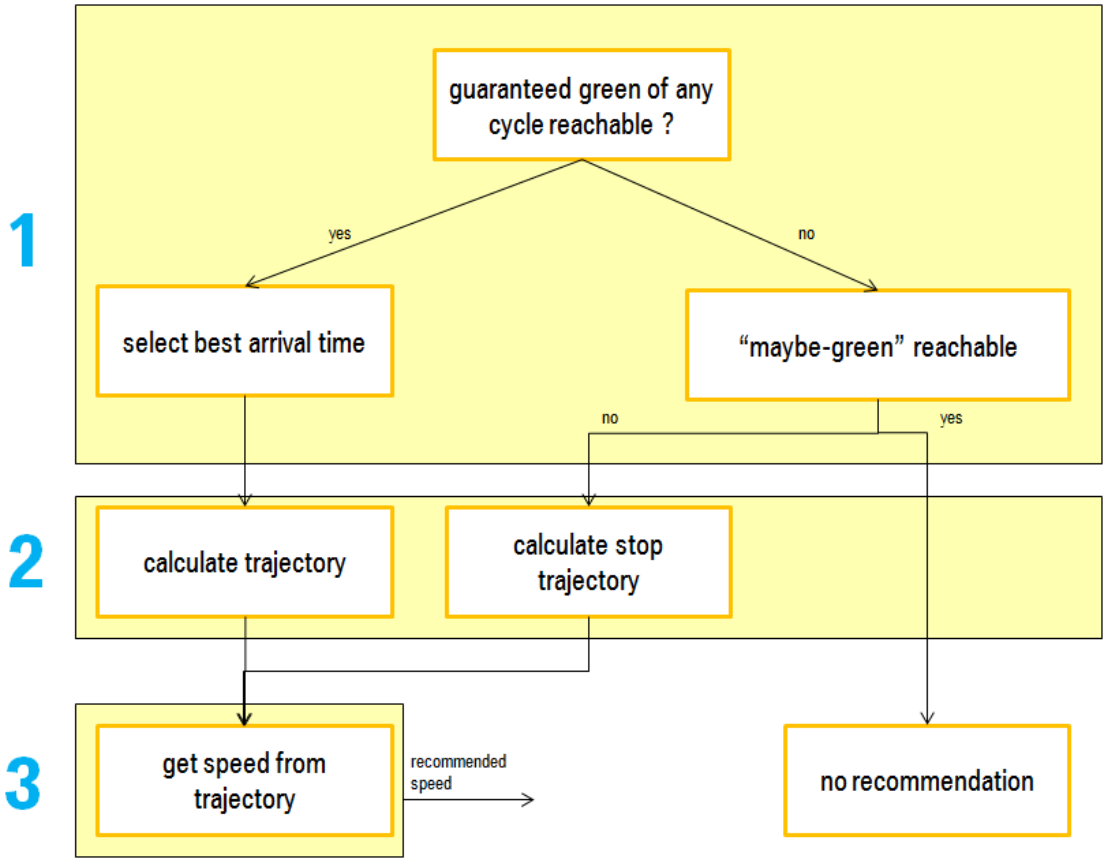

Fig.4.24. Detailed algorithm overview

First we determine a time interval within that it is possible for the vehicle to arrive at the next intersection and on the other hand the status of the traffic signal is green at the same time. So after the first sub step, the result is a time interval where it makes sense to arrive at the intersection. If there is no such interval the driver will have to stop at the intersection. To calculate this interval we first calculate some auxiliary values: The earliest arrival time t_{arr_min} and the latest arrival time t_{arr_max}. These times describe the earliest and the latest possible moment of an arrival at the intersection, given constraints like maximum/minimum speed, maximum acceleration/deceleration. The interval $[t_{arr\_min}, t_{arr\_max}]$ is now intersected with all guaranteed green intervals of the next traffic signal. The remaining part $[t_{min}, t_{max}]$ of $[t_{arr\_min}, t_{arr\_max}]$ is the desired interval (arrival possible and green status). Since we want to give a reliable recommendation, we don't use the maybe green interval, but the guaranteed green interval. Fig.4.25 depicts one possible situation and the according result. The red lines mark the speed trajectories that were used to determine the earliest and latest arrival time. The black line marks the trajectory for the case that the speed of the driver stays on the current level. The part of the guaranteed green that is possible to arrive is our desired interval (marked blue).

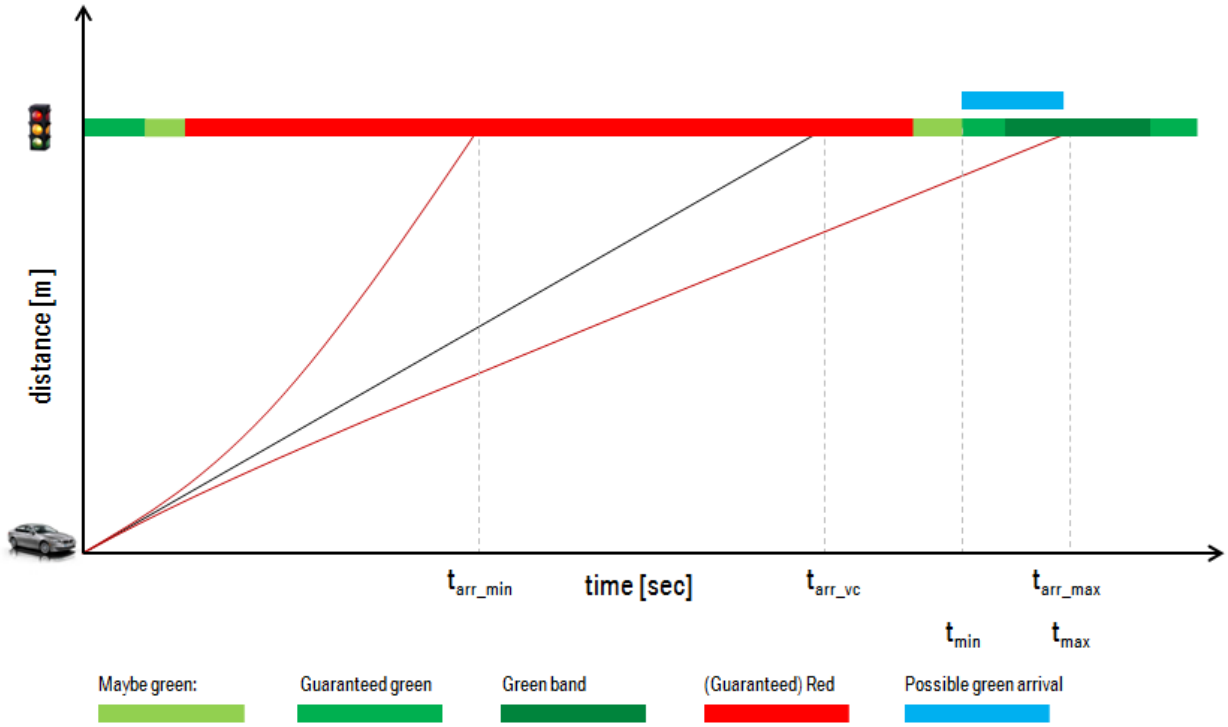

Fig.4.25. Determining the desired possible green arrival interval

If several guaranteed green intervals intersect with $[t_{arr\_min}, t_{arr\_max}]$, the first guaranteed green that intersects with $[t_{arr\_min}, t_{arr\_max}]$ is selected (see Fig.4.26). This assures that the driver can arrive at the destination as early as possible.

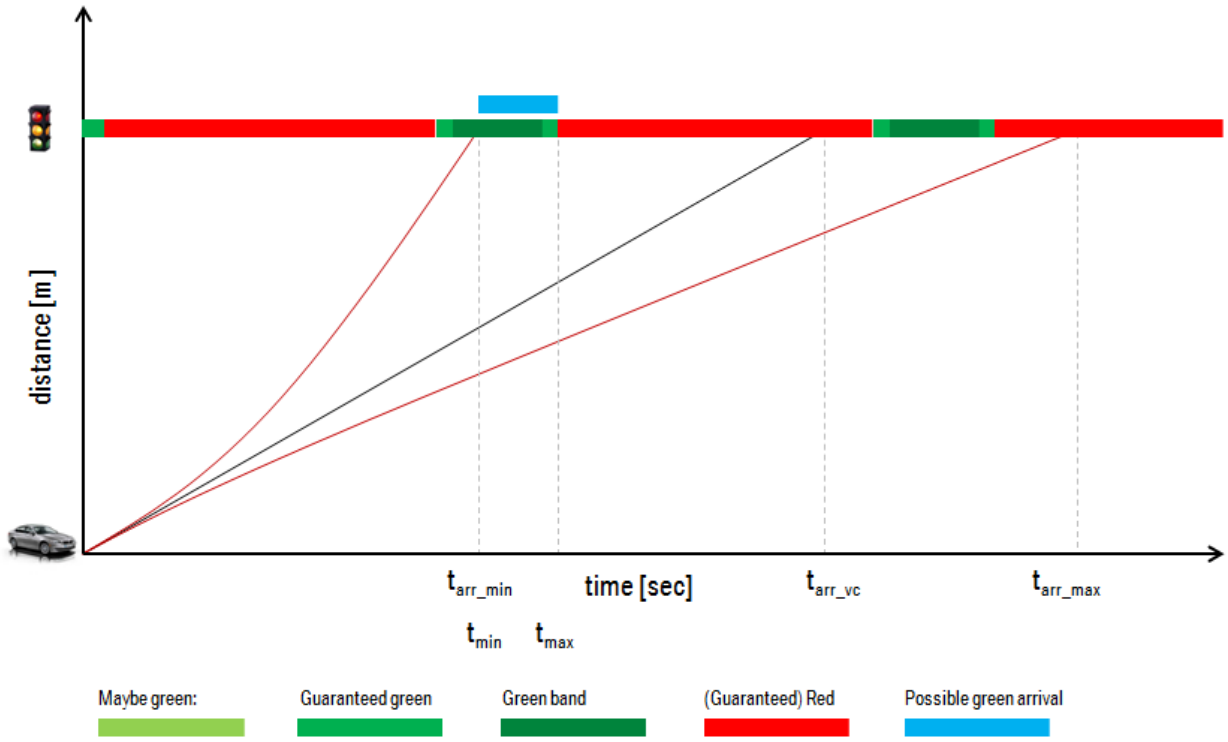

Fig.4.26. Several guaranteed greens reachable

For the current cycle, there is possibly a green window before guaranteed green called “Early green”, which describes a situation where the main arterial signal starts green earlier than the guaranteed green due to less service requests on non-coordinated phases (i.e. somewhere in the maybe green interval just before the start of guaranteed green). As soon as an “Early green” is observed, the remaining time of the maybe green before the start of guaranteed green is now guaranteed to be green, too. So the desired arrival zone can be extended like shown in Fig.4.27.

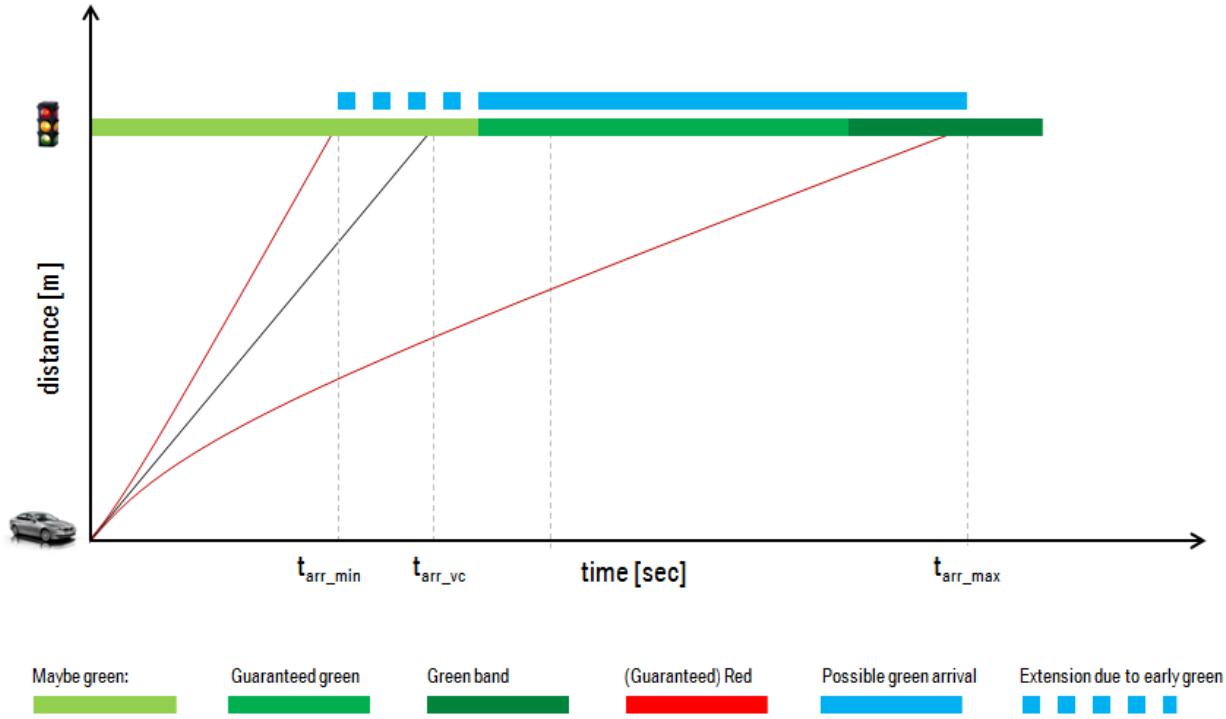

Fig.4.27. Early green including the maybe green

Fig.4.28 and Fig.4.29 show examples, where it is not possible to reach any guaranteed green. In these cases, it's not possible to give a speed recommendation with that the driver can arrive at the intersection at green for sure. But for some cases like in Fig.4.28, it is possible to arrive in the maybe green interval. Then, the algorithm gives no recommendation as there is a chance to arrive at green, but it is not sure. If it's even not possible to arrive at maybe green, it's inevitable to stop at the intersection (see Fig.4.29).

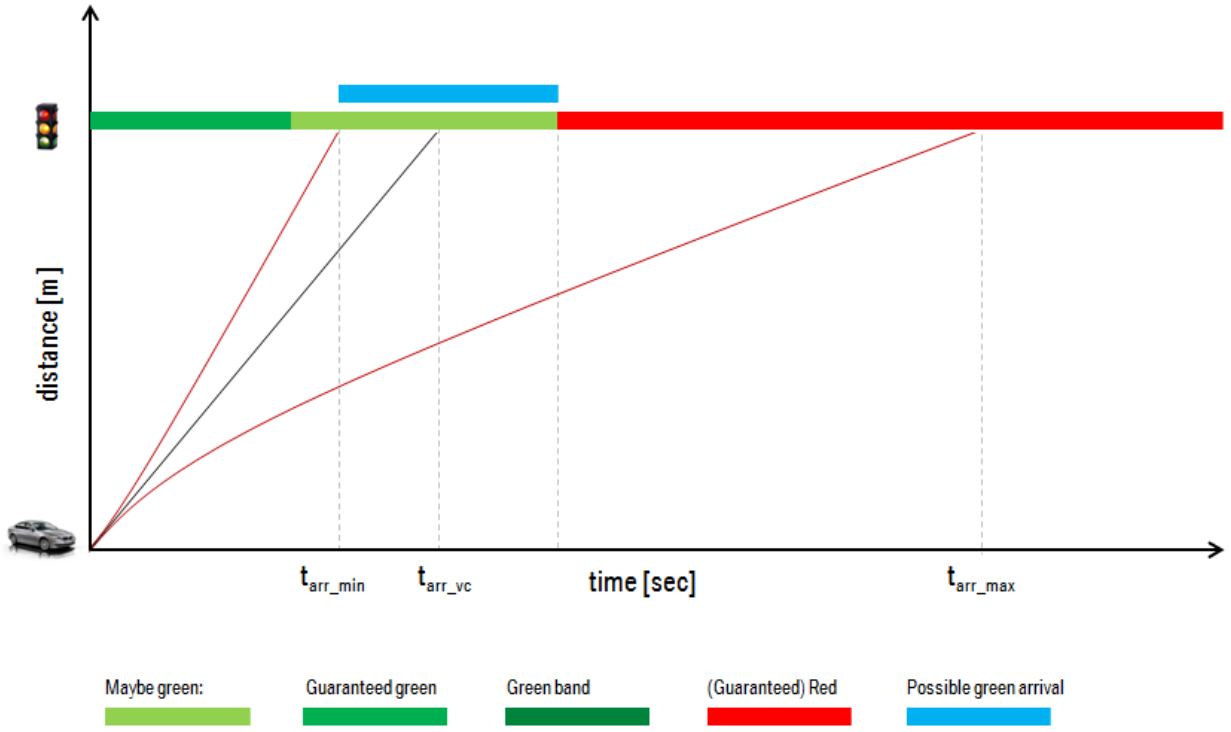

Fig.4.28. No guaranteed green reachable, but maybe green: no recommendation

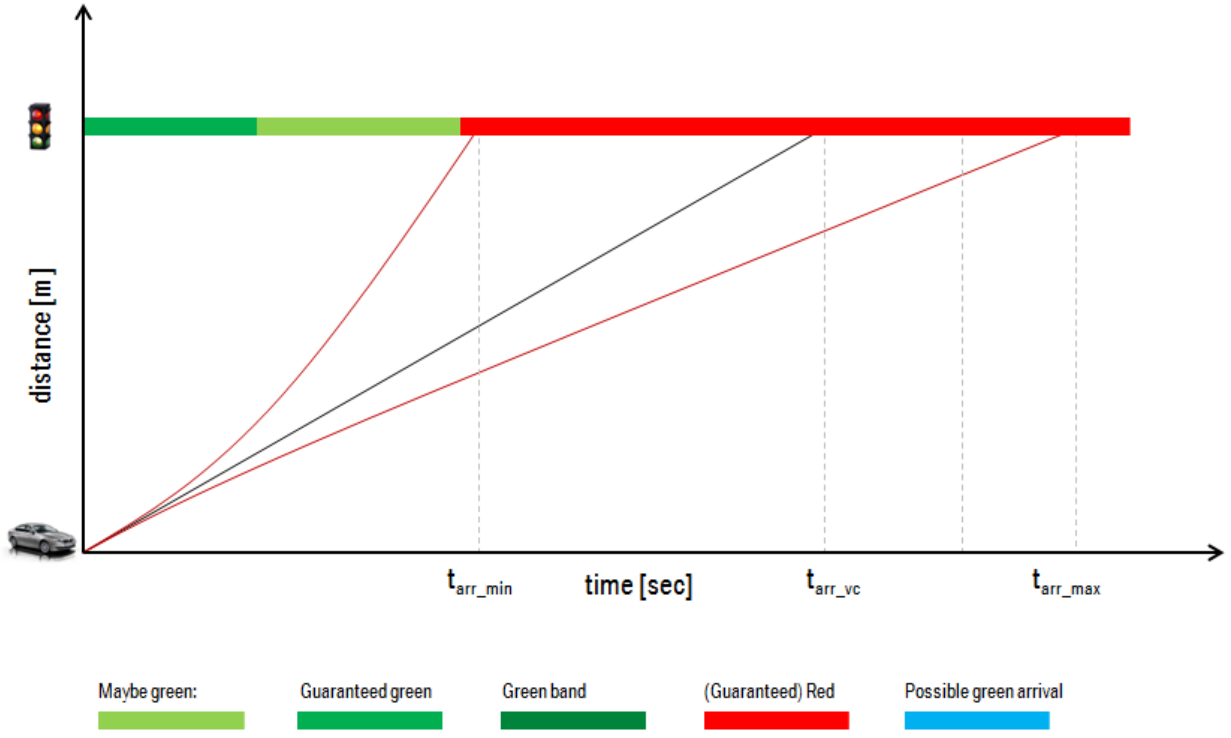

Fig.4.29. No green reachable: stopping inevitable

After having found an interval (marked blue in the previous images) where it makes sense to arrive at the next intersection the next sub step is to determine where it is best to arrive in this interval.

The best arrival time depends on the current velocity of the car as well as on the position of the green band relative to the desired arrival interval. To find the best arrival time we use 3 basic strategies. The strategy depends on the arrival without any recommendation (i.e. just maintaining the current speed):

1. Arrival before arrival interval: decelerate to start of arrival interval
2. Arrival in arrival interval, before green band: maintain speed
3. Arrival in or after green band: try to get to start of green band

The first strategy is somehow obvious. If the driver would continue driving at the current speed, he would arrive at red. Using the strategy he just arrives in the earliest moment where the signal is guaranteed green (see Fig.4.30).

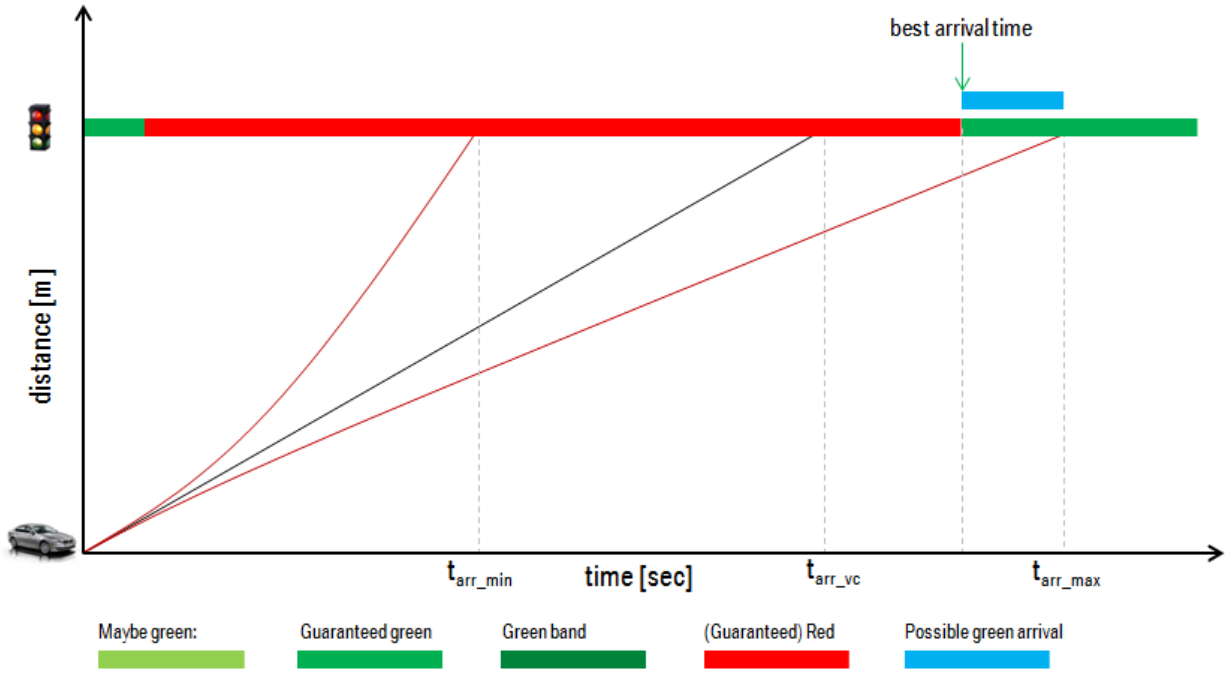

Fig.4.30. Arrival before arrival interval: decelerate to start of arrival interval

Maintaining speed in the second strategy (see Fig.4.31) is reasonable, as acceleration would make the driver get away from the green band and deceleration would confuse the driver as he is recommended to slow down although the he maybe already sees a green light. If it's really necessary to slow down to get into the guaranteed green of the next further downstream traffic signal that can also be done after passing the upcoming traffic signal.

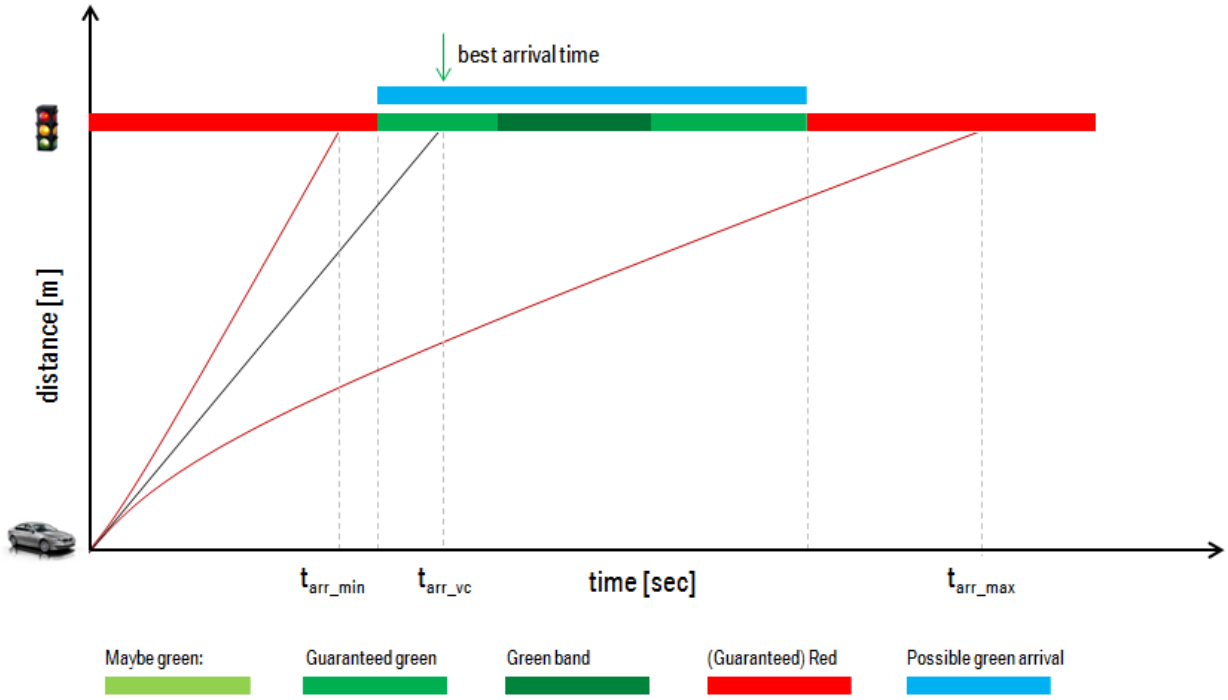

Fig.4.31. Arrival in arrival interval, before green band: maintain speed

The last strategy tries to let the driver arrive as close as possible to the start of the green band (see Fig.4.32). The start of the green band is optimal as it offers a maximal safety margin for unexpected delays (e.g. car in front). In cases that it's not possible to get to the start of green band due to speed limit and acceleration constraints, the best arrival time is selected as the earliest possible arrival time.

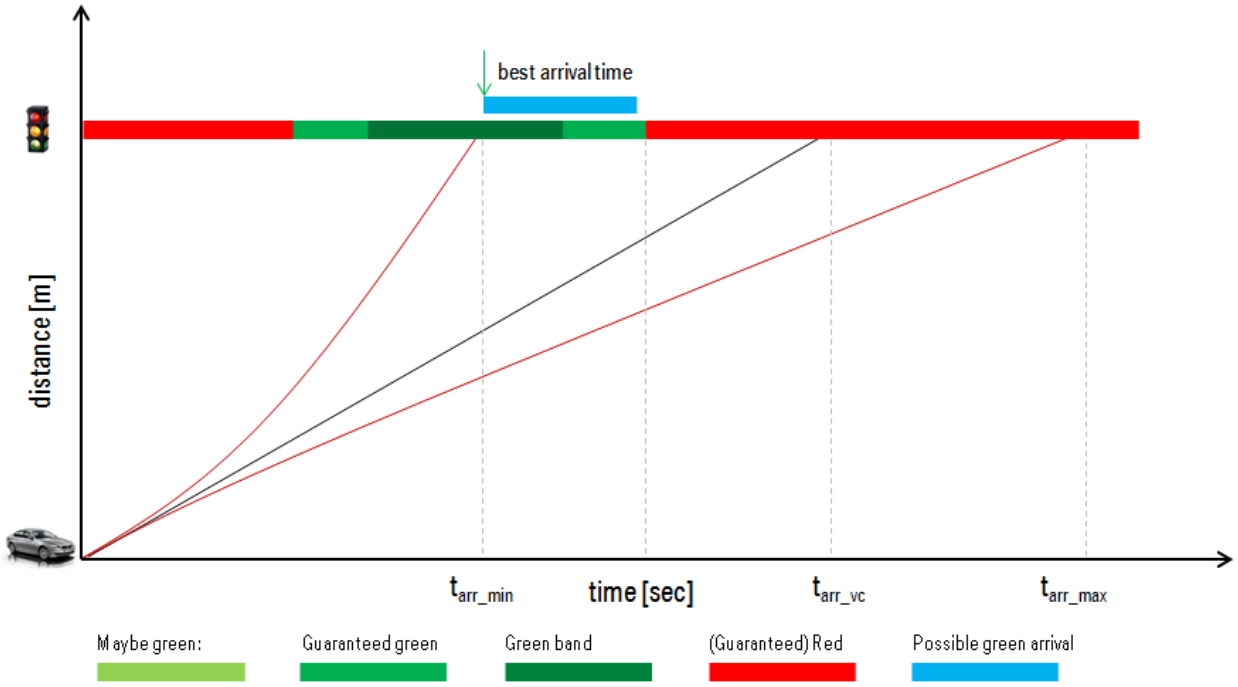

Fig.4.32. Arrival in or after green band: try to get to start of green band

To formalize these basic strategies in a way that is easy to implement them in an algorithm, many different cases of how arrival time t_{arr_vc} is positioned relative to possible green arrival interval and the green band are analyzed (see Fig.4.33). Based on these cases a decision tree was created (see Fig.4.34). Using this decision tree the best arrival time can be easily determined by the arrival time, the range of the arrival time $[t_{min}, t_{max}]$ and the start time of the green band t_{band_st}.

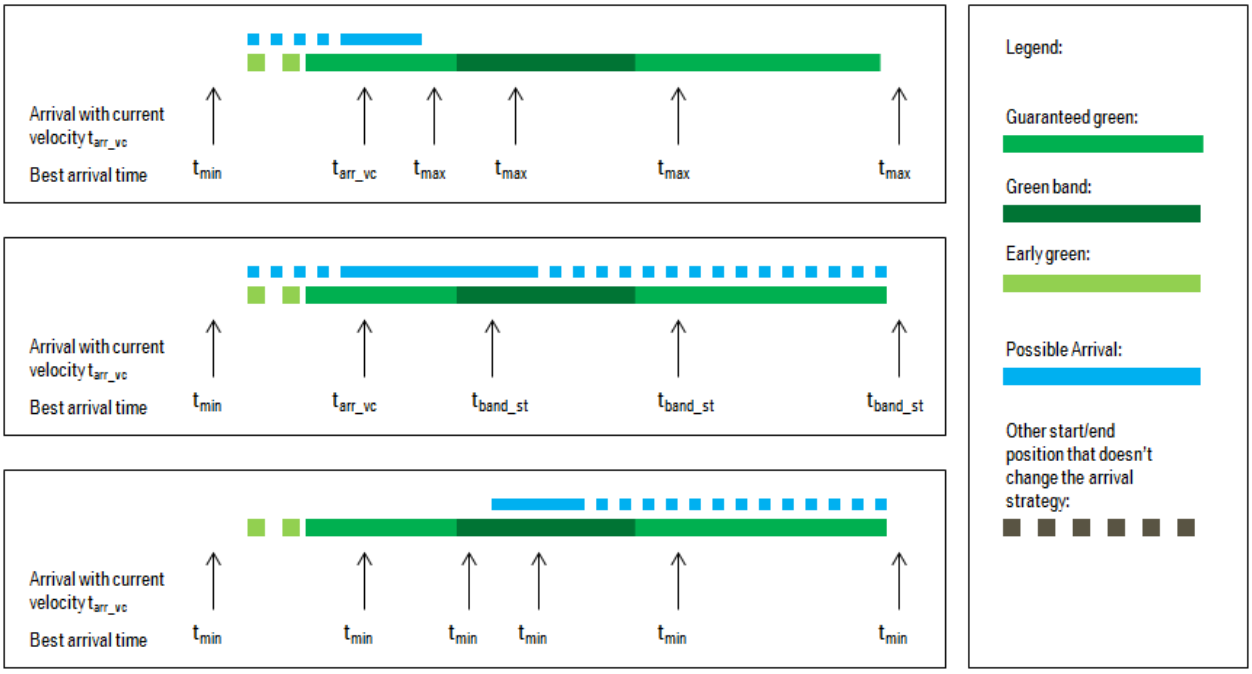

Fig.4.33. Best arrival time for different arrival scenarios

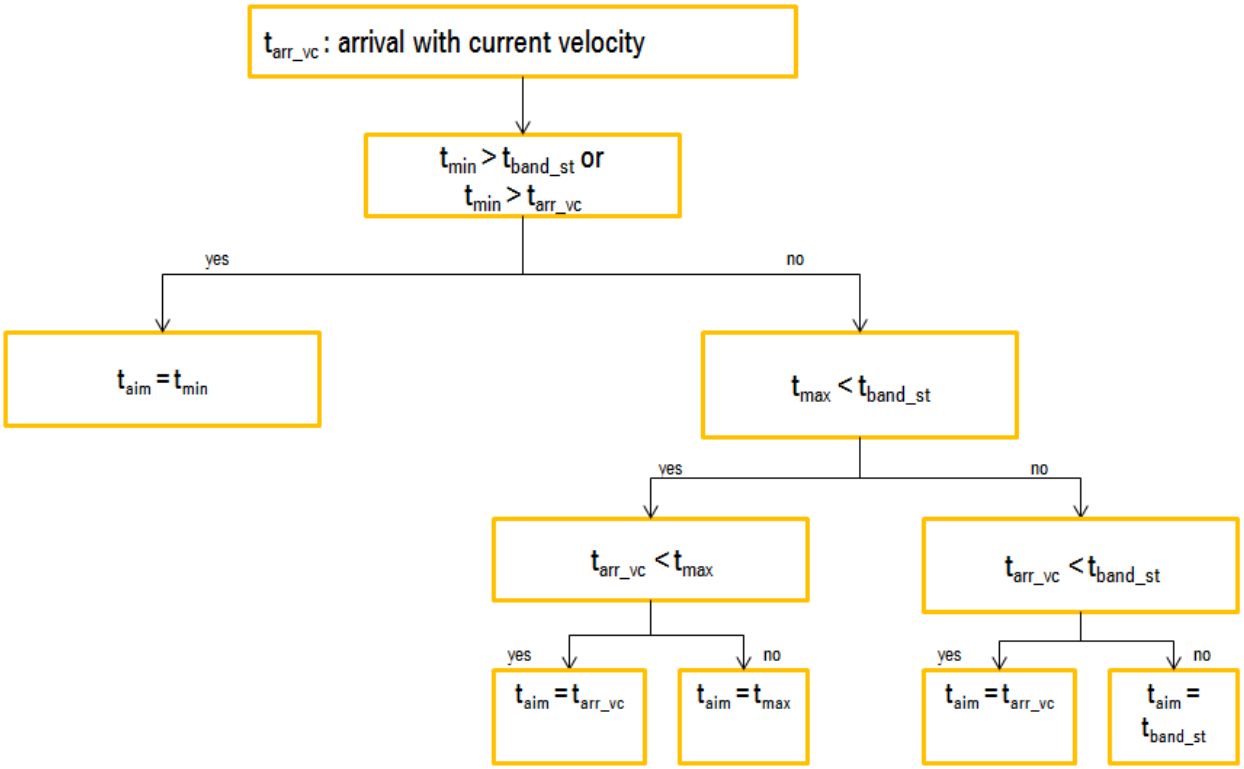

Fig.4.34. Decision tree used for determining the best arrival time

To sum up, there can be three different outcomes after the first step:

1. The optimal time to arrive at the next intersection
2. The decision to give no recommendation
3. The decision to calculate a stop trajectory in the next step

After the first step, either the optimal time to arrive at the next intersection is known or it is inevitable to stop. Additionally there is the case that no recommendation is given, but then there is no need for calculating a speed trajectory. Once the target arrival time is determined, we can apply eco-approach and departure algorithm to calculate the optimal speed trajectory to reach the next intersection at the target arrival time.

4.7.2 Summary

During the initial field tests, we found that it is very difficult to follow a speed recommendation that is updated frequently especially when there are other vehicles around. One simple workaround would be not displaying the speed the driver should keep at the moment but the end speed that he/she should get to when hitting the intersection. So the end speed would change much less frequently which makes it easier for driver to follow without giving constant attention to his/her target speed. In order to following the recommended speed trajectories closely, one needs to implement Adaptive Cruise Control (ACC), which will be discussed in detail in Chapter 6.

One limitation of this algorithm for actuated signals is that the actual starting time and ending time of each green phase and red phase are not known in advance, which makes speed planning less effective. In order to improve the prediction of on-set times of

green and red phases, we can look to the historical data to establish the distributions of the phase lengths. These distributions can be further incorporated with real-time pedestrian and vehicle calls to predict the green windows. The both ends of a green window will then be bonded with some confidence level, other than absolute bonds.

Chapter 5
Field Operational Tests

To demonstrate the effectiveness of the eco-approach and departure technology described in the previous chapter, a number of experiments were carried out in real world at various locations with different vehicles. These experiments include testing at the Richmond Field Station (Richmond, California) with BMW, testing at the Turner Fairbanks Highway Research Center in McClan, Virginia, and test in Riverside California. Each of these test programs are described below.

5.1 Richmond Field Station

As part of a FHWA Exploratory Advanced Research project on Advanced Signalization, a testing program was developed to demonstrate the general concept of Eco-Approach and Departure. For these experiments, a test vehicle was outfitted with the eco-approach algorithm and enabling technology and extensively tested at a closed test intersection located at California PATH's Richmond Field Station. Details of the test vehicle are given in the next section followed by a description of the test intersection.

5.1.1 Test Vehicle and Cloud-Based Server Infrastructure

The test vehicle is a BMW 535i sedan model year 2011, as shown in Fig.5.1.

Fig.5.1. Test vehicle at the test intersection.

The test vehicle is equipped with onboard computers which allow the computation of the optimal speed trajectory based on SPaT data in real time, display the recommendation to the driver, and record vehicle data directly from the various CAN buses of the vehicle.

The onboard computing platform is connected with 4G/LTE cellular network linked to the cloud-based server hosted on an EC2 instance at Amazon Web Services as shown in Fig.5.2. It is important to note that compared to the other experiments, the communication was handled by a cellular system, rather than Dedicated Short-Range Communication (DSRC). This has important implications in terms of timing of preview information, which has a significant effect on the performance of the algorithm.

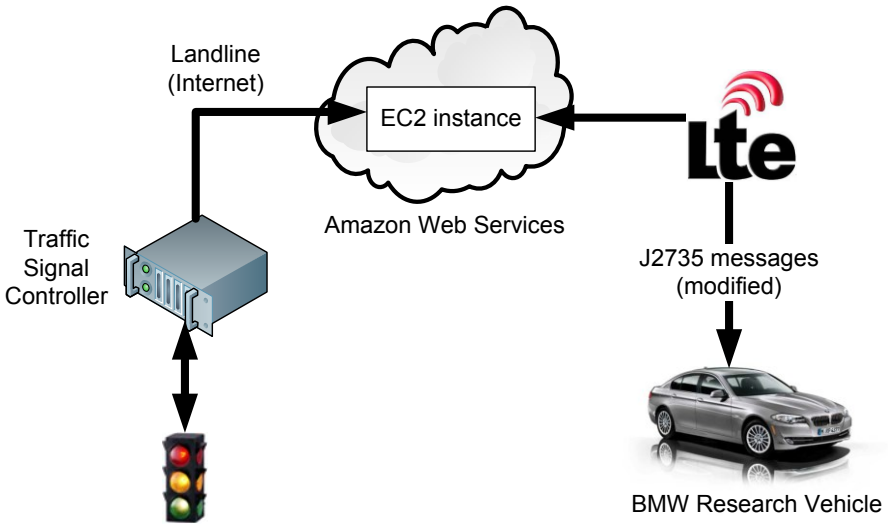

Fig.5.2. Cloud-based server and communication platform.

The test vehicle is equipped with a programmable instrument cluster, shown in Fig.5.3, which allows displaying the recommended speed in an intuitive and non-distractive way. The green bar in the speedometer is where the driver is recommended to keep the speed. The yellow bars outside the green bar are where driver need to adjust the speed to make it into the green bar. The current signal phase and the amount of time left in the current phase are provided at the bottom center of the speedometer as well.

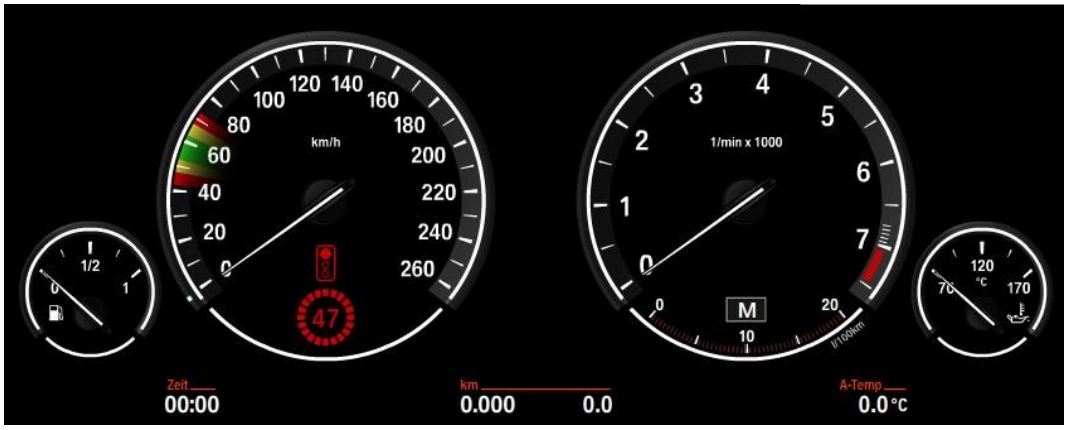

Fig.5.3. Programmable instrument cluster to display SPaT information and speed recommendation

The traffic signal controller at the intersection, shown in Fig.5.4, communicates with the cloud-based server over fast landlines. The server determines the correct SPaT data based on the vehicle's location and heading. The correct SPaT message is then sent to the vehicle over the wireless network link.

Fig.5.4. Traffic Signal Controller

5.1.2 Wireless Communication Channel

The SAE J2735 Standard specifies a message set, and its data frames and data elements to be used by Dedicated Short Range Communications for Wireless Access in Vehicular Environments (DSRC/WAVE) communication systems [28].

As one goal of the test setup was to prove that this type of application can be done with 4G/LTE networks as well, the message set defined in J2735 was adapted to be

usable over a cellular network. The message structures and the ASN.1 encoding were maintained however. The update rate of the SPaT message is 1 Hz.

The SPaT message is a compilation of objects in binary form that describe the signal phase and timing to convey the current status of available lane movements/paths at signalized intersections. To allow the communication of prospective phase changes, the SPaT message defined in J2735 had to be extended by data fields containing the time to the next two state changes of the traffic signal.

5.1.3 Test Site

The map of the test intersection at Richmond Field Station is shown in Fig.5.5. The blue line shows the test segment used in this experimentation. The ideal selection of the test segment is the straight yellow line. However, the driveway marked by the yellow line is not mapped in the digital map of the vehicle's embedded navigation system. As the test setup uses map matched locations only, the yellow driveway was unusable for testing. Therefore, the blue line was chosen as the test segment. The total distance of the entire test "loop" is 307 meters. In each run, we started from the green arrow, passed through the intersection, and then exited the test segment at the red bar downstream, as shown in Fig.5.5. The eco-approach technology equipped vehicle would travel around the test loop, at a nominal speed of around 25 mph, corresponding to the speed limit in the area. The traffic signal controller was set up with fixed-cycle signal timing. The signal cycle length was set to be 60 seconds, with 30 seconds of green, 3 seconds of yellow and 27 seconds of red.

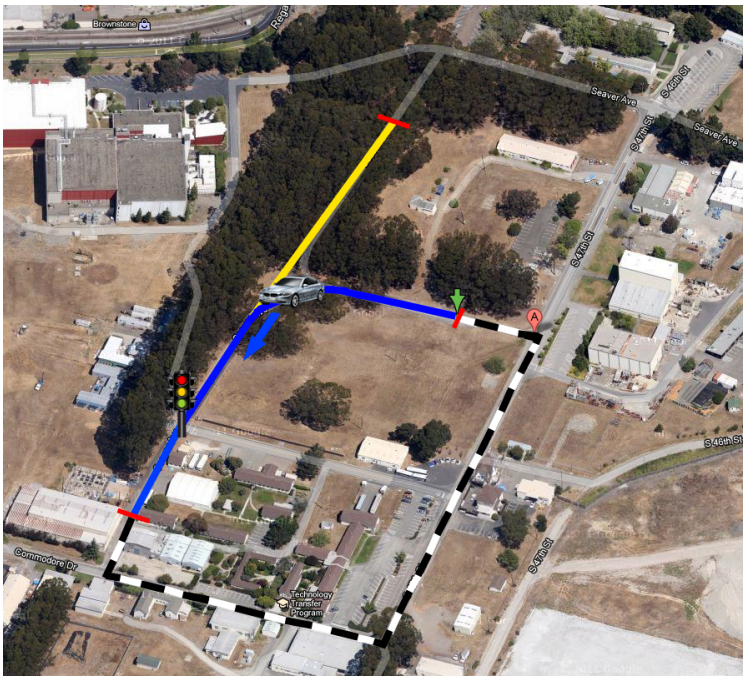

Fig.5.5. Map of test route

5.1.4 Driver and Scenarios

In order to compare the eco-approach technology with regular driving in terms of fuel consumption, two testing scenarios were carried out. One scenario is called "informed driving", where the driver was provided with the recommend speed in the programmable instrument cluster at 1 Hz while driving through the intersection. The other scenario is called "uninformed driving", where the driver drove without any speed recommendations or knowledge of the time left in current signal phase. To have a realistic comparison, the driver drove in a reasonably efficient way as much as possible in the uninformed scenario. A total of 292 runs were made for the informed driving scenario and 270 for the uninformed driving scenario. For each run, the test vehicle entered the test segment randomly in time without knowing the current signal information. Fuel consumption was recorded on a 1 Hz basis, with an accuracy of 10^{-6} liter.

5.1.5 Simulation

The simulation experiments were performed on a fixed-time signalized intersection that is identical to the one at the Richmond Field Station. The total recording distance is 320 meters and the speed limit is 25 mph. Similar to the field experiments, the signal timing at the intersection is fixed, with the signal cycle length set to be 60 seconds, with 30 seconds of green, 3 seconds of yellow and 27 seconds of red.

Once a vehicle entered the test segment, it followed the recommended speed trajectory calculated by the velocity-planning algorithm. Based on the speed trajectory, we calculated the vehicle fuel consumption using a microscopic emission model CMEM. A Typical light-duty vehicle type defined in CMEM was selected and its vehicle/engine parameters were adjusted to match those of the test vehicle as much as possible.

For comparison purposes, we also simulated the uninformed driving scenario. For this scenario, we assumed that the driver attempted to cruise at or around the speed limit until he/she was visually aware of the traffic signal ahead. If the signal was green, the driver simply maintained the cruise speed while crossing the intersection. If the signal was red, the driver slowed down or even stopped, and waited at the intersection until the light turned back to green, and then accelerated back to the speed limit.

In each simulation run, the vehicle entered the test segment at a random time with respect to the signal timing of the intersection. Due to the stochastic nature of traffic micro-simulation, multiple runs were made using different seed numbers. The required number of runs is determined by the same method we discussed in section 3.2. In our

simulation, the significance level was set to 0.05. The allowable error was chosen to be 3%.

Table 5.1 shows the simulation results, where the informed driving has better fuel economy by 14.06% compared with the uninformed driving on average.

Table 5.1. Fuel Economy Analysis

	uninformed	informed	Improvement
Fuel (l/100km)	9.96	8.56	-14.06%

5.1.6 Results and Discussion

Second-by-second fuel consumption data were measured during the real-world experiments for each run from the point the test vehicle entered the test segment until it exited at the other end, as the blue line shows in the map of the test site in Fig.5.5. Note that by driving through the blue curve while maintaining speed, an additional shear force is generated at the wheels that alter the balance of forces and has to be compensated for by the engine. Thus, the engine would consume more fuel. However, this was the case for both the informed and uninformed driving, and thus, the effect on the relative differences between the two scenarios are assumed to be negligible.

After averaging the fuel consumption results over all the runs for both the informed and uninformed driving tests, we found that the informed driving gained a 13.59% of fuel savings compared to the uninformed driving as illustrated in Table 5.2. It's found that the test results are very close to the simulation results presented in Table 5.1. A second driver was also recorded to cross check the results, showing similar fuel

savings compared with the first driver. The results shown in this paper are an average of both drivers. The average travel times of informed driver and uninformed driver are approximately the same. This implies that adopting the velocity-planning algorithm can greatly improve fuel efficiency without sacrificing travel time.

Table 5.2. Fuel efficiency and travel time analysis

	uninformed	informed	Improvement
Fuel (l/100km)	10.23	8.84	-13.59%
Travel time (sec/trip)	40.69	40.3	-0.96%

Further exploring the data of fuel consumption provides more insight on where the fuel was saved. A frequency distribution of fuel economy for each test loop is shown in Fig.5.6. In this figure, an initial peak can be seen in the range of 5 to 9 l/100km, corresponding to the scenario where the driver didn't need to slow down since the vehicle can pass the intersection while the signal is green. This is approximately the same for both the informed and uninformed driving cases. A second set of peaks is observed in the range of 10 to 15 l/100km, corresponding to the case when slowing down is inevitable due to a red light. In this scenario, the informed driver is able to coast down and consume less fuel than the uninformed driver.

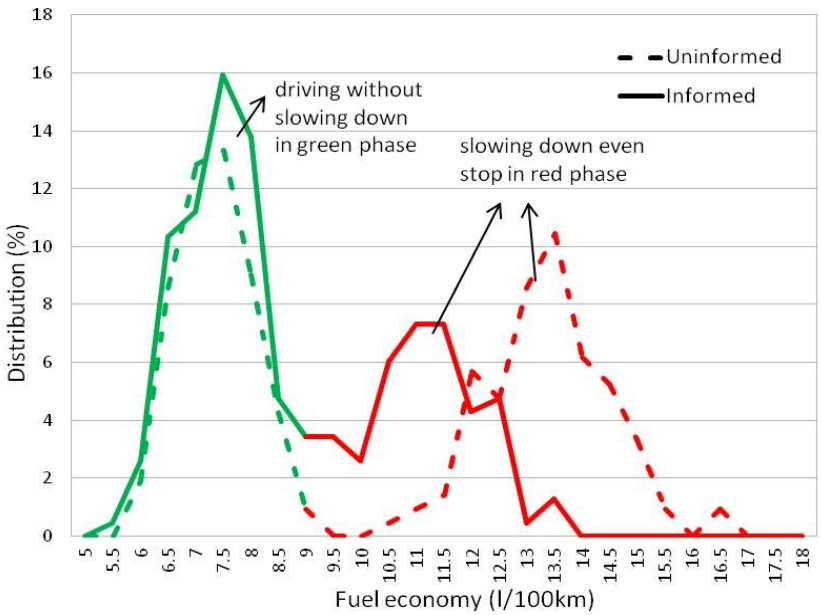

Fig.5.6. Distribution of fuel consumption

Fig.5.7 shows the average speeds of both informed driver and the uninformed driver at different positions of a test loop. A solid line stands for the informed driver, and a dashed line represents an uninformed driver. It is shown in the figure that the informed driver tends to slow down earlier when approaching the intersection, and has a higher average speed to pass the intersection, compared to the uninformed driver. The intersection is located at around 75% of the whole trip.

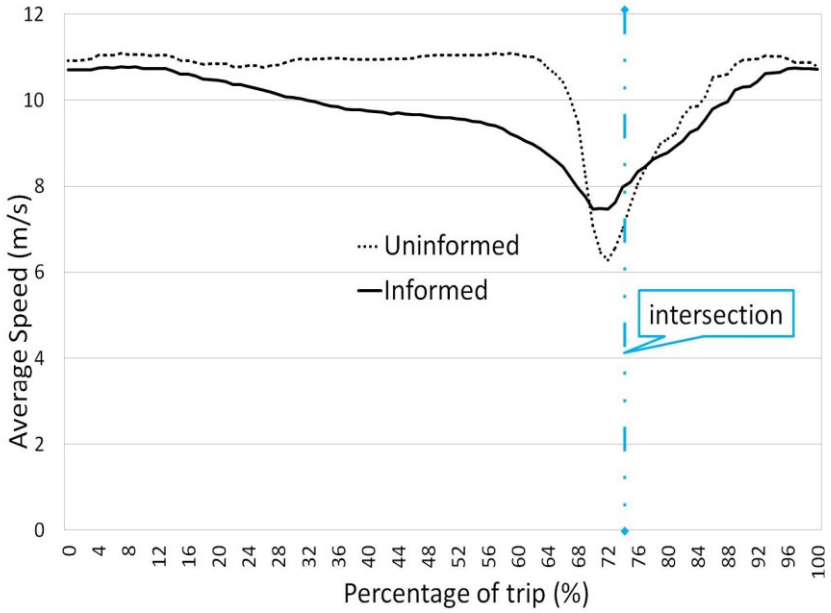

Fig.5.7. Average speed during a trip

Fig.5.8 shows the cumulative average fuel consumption during a trip. From this figure, we can find out where during a trip the fuel was saved by comparing cumulative fuel consumption of informed driver and uninformed driver. It's noted that when vehicle is far before intersection, an informed driver uses a little less fuel than an uninformed driver since the informed driver tends to decelerate earlier. As the vehicle is getting close to the intersection, if the current signal is red, the informed driver has more chance to avoid a complete stop and cruises through the intersection at a constant speed. In contrast, the uninformed driver has to stop in most cases. Therefore, an uninformed driver shows higher fuel consumption in this range. After vehicle passed the intersection, informed driver generally has higher speed than uninformed driver since informed driver tried to avoid full stop at the intersection and kept a constant speed instead. Thus, informed driver doesn't need as much fuel to accelerate back to speed limit as uninformed driver need.

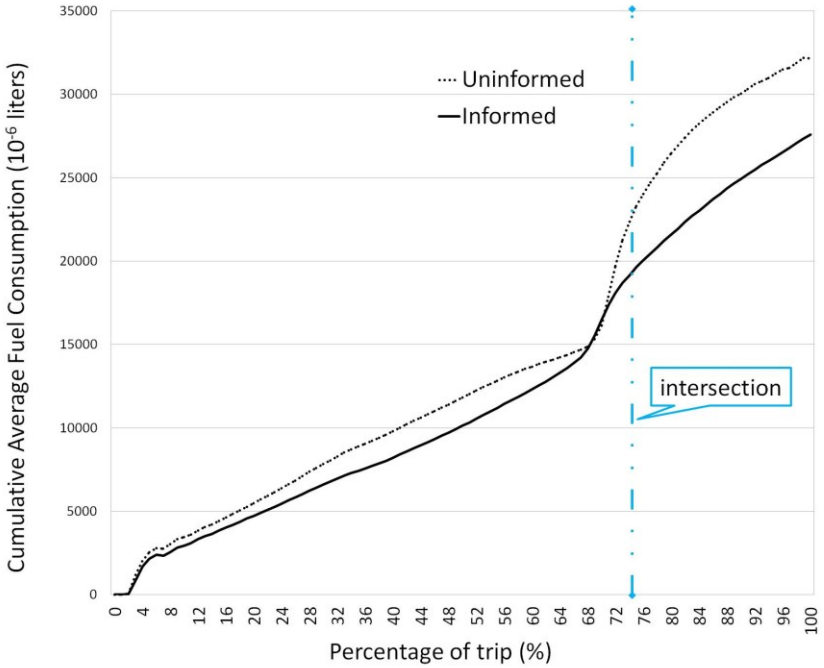

Fig.5.8. Cumulative average fuel consumption during a trip

5.1.7 Summary

In this section, we tested an example of eco-approach technology in a BMW test vehicle at a signalized intersection to determine fuel economy differences. Simulation-based experiments were also carried out for the same test environment to compare the results between simulations and field tests. For comparison purposes, the two testing scenarios included informed driver tests and uninformed driver tests. In the informed driver tests, the driver was provided with speed recommendations, while during the uninformed driver tests, the driver drove without any speed advice. The results show that on average, informed driver saved approximately 13.6% fuel compared with uninformed driver tests. It's also found that fuel savings are mainly from informed driver's early slowing down and cruising through intersection without having to stop at the intersection.

5.2 TFHRC and Riverside

As part of the Identification and Evaluation of Transformative Environmental (AERIS) Applications and Strategies program, two field studies were carried out during the summer of 2012 to examine the potential energy and environmental benefits of an "eco-approach and departure" application as part of the eco-signal operations transformative concept.

The algorithm was then implemented on two test vehicles as part of the field studies: one at the University of California-Riverside, and another at the Turner Fairbanks Highway Research Center in McLean, Virginia. In addition to instrumenting these vehicles, the two test sites were prepared for extensive testing of each vehicle passing through their respective test intersections. Each intersection was set up to broadcast SPaT data for fixed-time signalization to the vehicle; the in-vehicle system would then process the data and carry out velocity planning which resulted in speed advice to the test drivers. The testing was comprehensive in the sense that a number of different approaching speeds were chosen, along with different entry times in the fixed-timed cycle of the traffic signal.

Based on the testing setup, four different scenarios were identified as discussed in section 4.2. Because of the large degree of variability in the results, it is recommended that a comprehensive sensitivity analysis be carried out using traffic simulation modeling tools to identify the key parameters that affect the eco-approach and departure application. Also, it is likely that the benefits shown during the field studies with single-vehicle testing would be reduced when the vehicle was in traffic. Traffic simulation modeling

would be able to show the effectiveness of the algorithm under different levels of traffic congestion. Furthermore, simulation models could evaluate the effectiveness of the algorithm for actuated signal intersections, rather than just fixed-time intersections.

The field studies were carried out to provide a number of benefits:

A. To Assess Practicality of Implementation: On a practical level, these field studies constituted the first rigorous test where DSRC-based SPaT and GID were extended from safety to exclusively deal with AERIS applications. It has provided us feedback on whether this concept is technologically practical and implementable.

B. To Gain Better Understanding of User Experience: During the field studies, the drivers were instructed to carefully follow the speed advice provided by the vehicle. From this, we learned how well our drivers were able to follow a prescribed speed trajectory. This initial driver behavior work can lead to a more rigorous set of experiments to determine how well a wide variety of drivers can follow this type of speed advice to achieve better fuel economy.

C. To Validate Traffic Simulation and Emissions Modeling: The resulting data from the field studies can now be used to validate traffic simulation and emissions models. For example, the vehicle trajectories from the field tests could be compared to vehicle trajectories from traffic simulation models. Further, these second-by-second vehicle trajectories can be used as input to MOVES or CMEM emissions models to quantify the air quality impacts (GHG emissions and particulate emissions) of eco-signals.

To demonstrate the effectiveness of the eco-approach technology, an initial field study was carried out in Riverside California, followed by a second field study in McLean Virginia at the Turner Fairbanks Highway Research Center (TFHRC). The details of those field studies are provided here.

Signal Phase and Timing information is potentially valuable for a number of ITS applications, including those that are being developed for safety, mobility, and the environment. The Society of Automotive Engineers (SAE) has developed and maintains specific standards for vehicle communications, most of which are specified in their J2735 standards document. The SAE J2735 standard specifies a message set, and its data frames and data elements to be used by Dedicated Short Range Communications for Wireless Access in Vehicular Environments (DSRC/WAVE) communication systems [28]. As part of the overall J2735 standard, SPaT communication standards have been developed which are referred to as the "SPAT-blob" and "MAP-blob". The latest SPaT standards are Revision C, published in February 2012 [29]. It is important to note that the SPaT standards were created for a variety of traffic signal operations, however for the current field studies, only fixed-time signalization scenarios were considered. The SPaT messaging was set up to be broadcast from the traffic signal controller at a rate of 10Hz. For further details on the SPaT messaging, please refer to [28][29].

5.2.1 Field Study at Riverside

The initial field testing of the Eco-Approach application took place close to the Center for Environmental Research and Technology at UC –Riverside (CE-CERT). For this field study, Palmyrita Avenue was used where traffic could be carefully controlled, as shown in Fig.5.9. For the testing on the street, different passes through an artificial intersection could be made at different speeds and at different points in the signal timing. As shown in Fig.5.10, a portable traffic signal was set up in the middle of the parking lot.

Fig.5.9. Field study location in Riverside California (Palmyrita Ave, Riverside CA)

For the eco-signal testing, a portable traffic signal was developed, as shown in Fig.5.10. As illustrated in Fig.5.11, this portable traffic signal consisted of traffic signal heads mounted on a trailer that are connected to an Econolite ASC/3-2100 traffic signal controller (same controller as the one operating at TFHRC test intersection). This traffic signal controller is also connected to a separate PC that translates the controller output into the SPaT messages (SPaT blob revision C). These messages are then sent from the

SPaT PC to the Dedicated Short Range Communication (DSRC) modem, and then sent out at 10 Hz.

Fig.5.10. Portable Traffic Signal Trailer used in the Riverside field study.

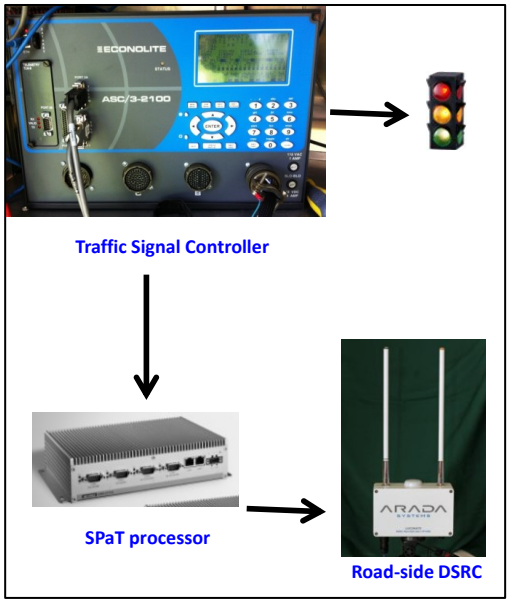

Fig.5.11. Traffic signal system components

A 2008 Nissan Altima research test vehicle was setup to perform the eco-signal testing, as shown in Fig.5.12. This vehicle was equipped with a DSRC modem to receive the SPaT messages, an on-board computer to compute the velocity trajectories, and a 7-inch automotive-grade display to serve as an artificial dashboard (see Fig.5.14).

Fig.5.12. Riverside test vehicle (2008 Nissan Altima)

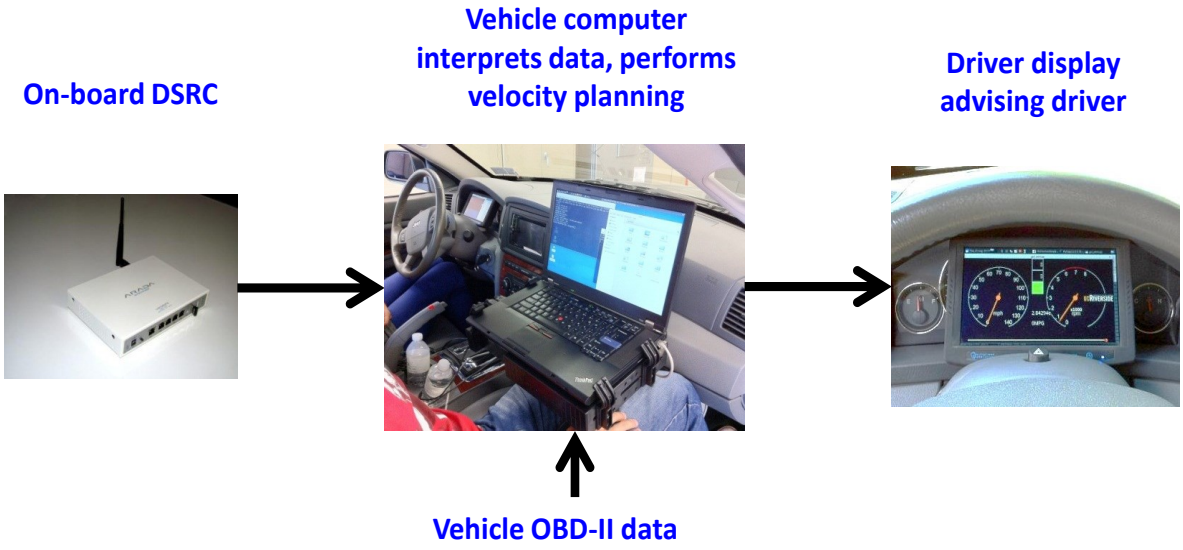

Fig.5.13. Test vehicle components.

In this system architecture, the on-board computer carries out a number of tasks, including: 1) parsing the SPaT message and GID/(or GPS/Position data) received by the DSRC modem at 10 Hz.; 2) acquiring vehicle data from the OBD-II bus (e.g., vehicle speed, RPM, fuel economy); 3) estimating the distance to intersection based on a developed map matching algorithm; 4) calculating a velocity trajectory based on the eco-approach and departure algorithm; and 5) displaying information to the driver through the artificial dashboard display.

For the artificial dashboard, two were designed: 1) a dashboard that presents a number of items to the driver for test and development purposes (see Fig.5.14); and 2) a dashboard with a reduced amount of information that is used for demonstration purposes (see Fig.5.15). For the testing, the full-information dashboard was used for the test

drivers to which they were accustomed and did not result in any distraction. The reduced-information dashboard was used for demonstration purposes with little driver distraction.

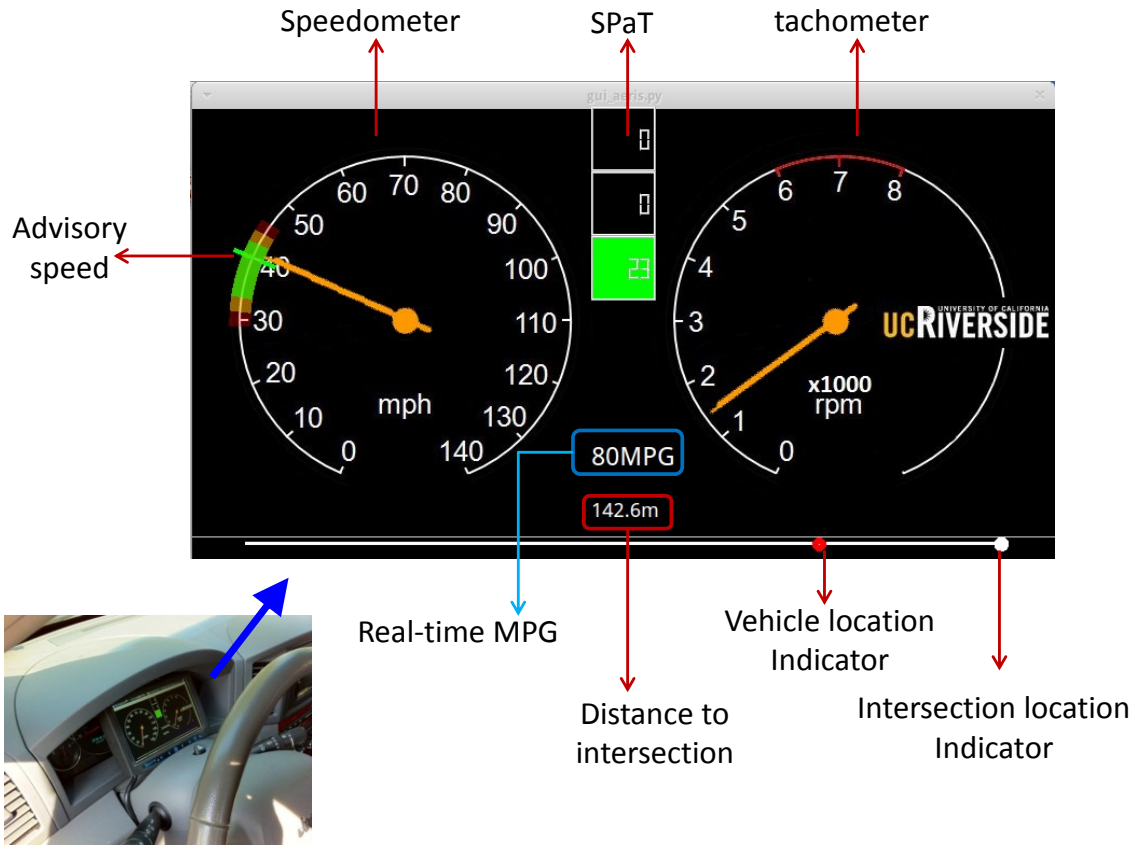

Fig.5.14. Artificial dashboard for testing

In Fig.5.14, a number of items were displayed: 1) the vehicle's current speed (i.e., speedometer); 2) the vehicle's RPM; 3) an "advisory" speed as calculated from the velocity planning algorithm, along with a green-zone, yellow-zone, and red-zone that moved along the edge of the speedometer; 4) the SPaT countdown information for the current signal phase; 5) the real-time fuel economy in MPG; 6) the distance to the intersection (in meters); and 7), vehicle and intersection location indicators. The

demonstration dashboard (Figure 3-7) only contained information on vehicle speed, RPM, target speed, and an arrow to indicate whether to speed up or slow down.

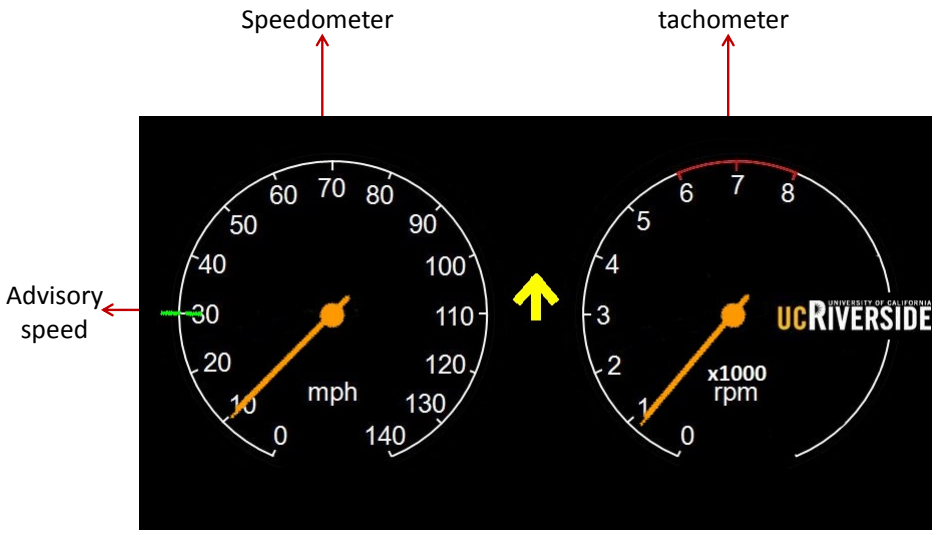

Fig.5.15. Artificial dashboard for demonstration

5.2.2 Field Study at Turner Fairbanks Highway Research Center

Initial eco-approach testing was originally carried out in Riverside California, after which additional experiments were carried out at the TFHRC test facility. This test facility in McLean Virginia is shown in Fig.5.16.

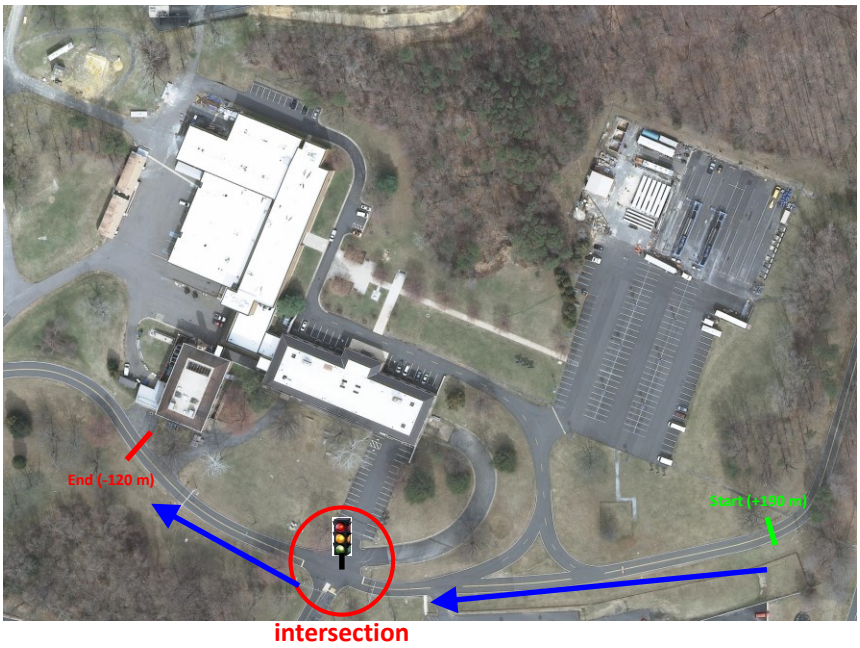

Fig.5.16. TFHRC test facility.

The testing at TFHRC was setup in one direction only, where the vehicles approached the intersection from the east, proceeded through the intersection, and then complete the test run on the west side of the facility. The start of the intersection test zone was at 190 meters to the east of the intersection, and then end of the test zone was 120 meters to the west. This testing area was long enough to carry out vehicle experiments up to 30 mph.

The established test intersection at TFHRC is shown in Fig.5.17. In this figure, the traffic cabinet is shown on the left, which contains the traffic signal controller, the SPaT PC, and an external road-side DSRC modem to broadcast the SPaT information. The intersection is set up as a standard 4-direction intersection with traffic lights in all directions. For more information on the TFHRC intersection, refer to the TFHRC STOL operations manual.

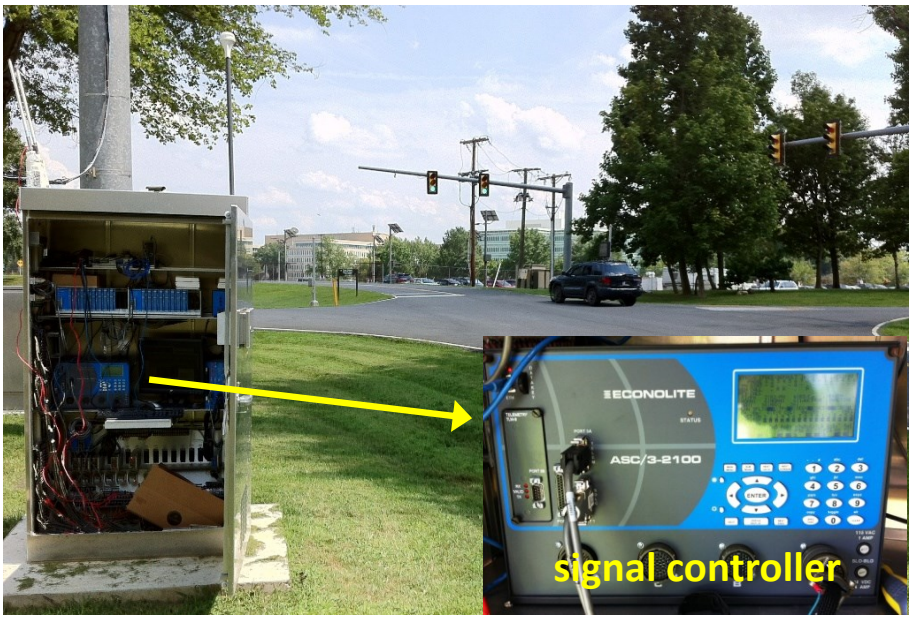

Fig.5.17. Turner Fairbanks Highway Research Center intersection

For the testing at TFHRC, a 2008 Jeep Grand Cherokee test vehicle was utilized. Similar to the test vehicle at Riverside, the Jeep was outfitted with a DSRC modem, an on-board computer, and an artificial dashboard, as shown in Fig.5.18. The equipment and operational capability was set up to be the same as the test vehicle utilized for the Riverside testing.

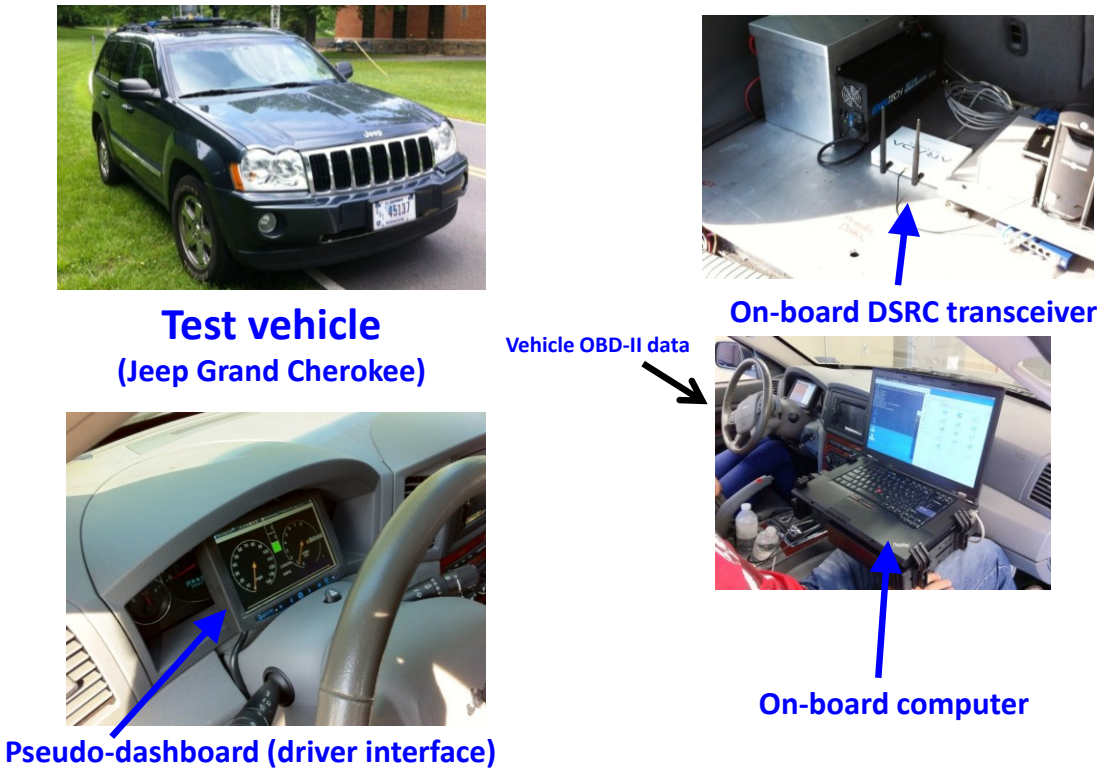

Fig.5.18. Turner Fairbanks Highway Research Center test vehicle and equipment

5.2.3 Experimentation and Results

For the experimentation carried out in Riverside and at TFHRC, the traffic signal controller was set up for fixed timed signal phasing: 26-seconds green, 4-seconds yellow, followed by 30-seconds of red. The total cycle time is 60 seconds. The field experimentation then consisted of two stages. The first stage (Stage I) was the "uninformed" driver stage, where a driver approaches the intersection at different times within the cycle and at different speeds, and travels through the intersection in a normal fashion, stopping as needed without any advice. The vehicle's fuel economy was measured for a large number of driving trajectories, establishing a baseline that can be

used as a point of comparison for the Stage II experiments. In Stage II, the driver again approaches the intersection at different times and speeds; however, this time the driver attempts to follow the "eco-speed advice" provided on the artificial dashboard display.

The field experimentation was designed to be comprehensive in that the test vehicle approached the intersection at different timed intervals throughout the entire cycle (i.e., varying by 5-seconds in the 60 second cycle). Furthermore, the vehicle approached the intersection at different driving speeds, ranging from 20 mph to 40 mph. The overall vehicle fuel economy and CO_2 emissions are then compared between the Stage I experiments (uninformed driver) and the Stage II experiments (informed driver).

In order to cover every possible driving scenario, a field study matrix was developed that varies the vehicle's intersection entry speed and entry time with respect to the overall cycle of the traffic signal. This field study matrix is shown in Fig.5.19. This test matrix consists of the entry speed along the vertical axis, and the delay in the signal cycle across the horizontal access. In this matrix, there are a total of 12 x 5 = 60 test cells. Fig.5.20 illustrates an overlay of the four different scenarios aforementioned on the field study matrix for the Riverside tests, and Fig.5.21 corresponds to the TFHRC tests. The overlay of scenarios in these field study matrices is different because of the geometry of the test (i.e., distance of receiving SPaT messages, define intersection zone, etc).

V/T	0	5	10	15	20	25	30	35	40	45	50	55
20 mph												
25 mph												
30 mph												
35 mph												
40 mph												

Fig.5.19. Field study test matrix

V/T	0	5	10	15	20	25	30	35	40	45	50	55
20 mph	Scenario 4			Scenario 1							Scenario 3	
25 mph	S 3	Scenario 4			Scenario 1						S 2	S 3
30 mph	S 3	Scenario 4			Scenario 1					S 2	Scenario 3	
35 mph	Scenario 3		Scenario 4			Scenario 1						S 2
40 mph	Scenario 3			Scenario 4		Scenario 1					S 2	S 3

Fig.5.20. Field study test matrix with overlaid driving scenarios for Riverside tests

V/T	0	5	10	15	20	25	30	35	40	45	50	55
20 mph	S 1	Scenario 2						Scenario 4				S 3
25 mph	S 4	Scenario 1						Scenario 3			Scenario 4	
30 mph	Scenario 4		Scenario 1						Scenario 3			S 4
35 mph												
40 mph												

Fig.5.21. Field study test matrix with overlaid driving scenarios for TFHRC tests

For the experiments, the driver drives through the intersection a minimum of three times for each cell in the test matrix. If there is a high degree of variance between the tests, additional test runs are made. After the uninformed driving stage (Stage I) was completed, similar testing was conducted for the informed driving stage (Stage II). In this stage, the eco-approach algorithm is activated and the test driver followed the eco-speed advice as closely as possible. Some test cells were tested several times to reduce the uncertainty between repeated measurements. For each data run, second-by-second vehicle velocity and fuel economy were measured. These were later integrated to give an average value for each test cell. In addition, a "driver score" was measured for each test run, providing a measure of how well the driver followed the suggested velocity trajectory.

The results of the Riverside testing are shown in Fig.5.22. This matrix shows the average amount of fuel savings (ml) for the different test runs within each test cell. The fuel savings are calculated by subtracting the average fuel consumption of the eco-approach driving tests from the average of the uninformed driving tests, for all three drivers. The column on the far right shows the overall percent improvement in fuel economy for the entire row.

Vel\Time	0 s	5 s	10 s	15 s	20 s	25 s	30 s	35 s	40 s	45 s	50 s	55 s	saving %
20 mph	11.4	15.3	21.4	6.59	5.05	3.12	0.22	2.13	-2.7	1.67	2.2	6.03	16.447
25 mph	3.31	13.8	19.6	15.3	0.67	1.99	0.45	0.49	-1.52	3.35	6.83	2.36	17.7178
30 mph	-1.9	9.51	16	13	0.78	0.64	2.19	3.35	3.5	19.6	11	10.1	25.6451
35 mph	7.07	9.29	7.22	25.1	29.3	1.04	0.19	-1.3	1.31	-1.1	2.26	6.55	28.361
40 mph	-3.5	3.94	-1.64	12.8	5.76	1.02	1.64	3.44	0.58	0.71	4.52	4.81	11.002

Fig.5.22. Riverside testing results

The results of the TFHRC testing are shown in Fig.5.23. Again, this matrix shows the amount of fuel savings (ml) for the different test runs within each test cell. Because of the constrained roadway system of TFHRC, it was not possible to safely test at 35 mph and 40 mph. As before, the average fuel savings are calculated by subtracting the average fuel consumption of the eco-approach driving tests from the average of the uninformed driving tests. The column on the far right shows the overall percent improvement in fuel economy, for all drivers combined. The results are slightly different than that of the Riverside testing, primarily due to the geometry differences, including significantly more road grade at the TFHRC test site.

delay into cycle (sec)

mph V/T	0	5	10	15	20	25	30	35	40	45	50	55	% savings
20	8.6	-11.3	-10.2	-5.2	-9.3	-13.1	13.8	7.1	9.4	-13.2	12.5	24.0	2.5%
25	17.8	22.5*	7.0	0.9	6.4	-9.4	-11.1	16.0	12.2	18.9	14.7	14.8	18.1%
30	-1.2	4.3	1.5	2.3	-1.2	6.7	-4.4	8.8	16.3	10.3	21.9	10.6	11.2%
35													
40													

Fig.5.23. TFHRC testing results

As can be seen in the matrices, some negative savings exist in some of the cells. This implies that there were certain cases (especially in Driving Scenario No. 1), where the uniformed driving runs were smoother during the "cruise" portion of the driving (perhaps based on less distraction following the advisory speed) compared to the eco-approach driving runs. Nevertheless, the overall trend in the results shows a fuel economy improvement.

A driving score was calculated for each driver by examining the target velocity trajectory generated by the eco-approach algorithm and the actual vehicle velocity trajectory that was driven. An example of these two velocity trajectories is shown in Fig.5.24.

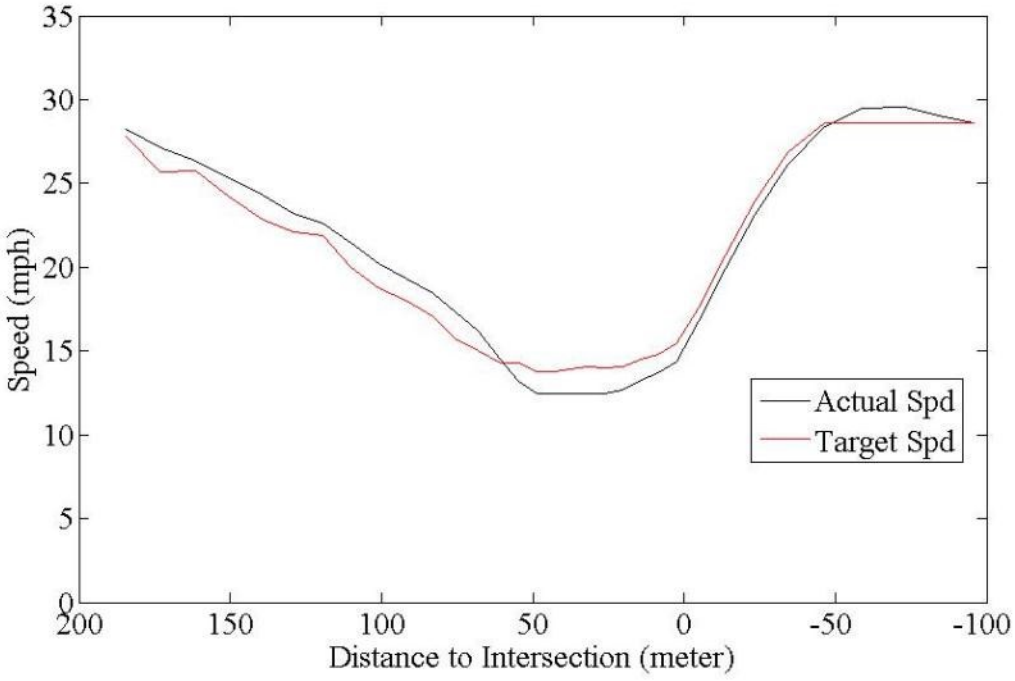

Fig.5.24. Example velocity trajectories for target speed and actual speed

Given the two data sets, one heuristic way to evaluate the driver's compliance with the advisory speed is to set up the following normalized driving score system equation:

$$SCORE = 100(1 - \frac{1}{n}\sum_{i=1}^{n}\frac{|A-T|}{A+T})$$

where A is the instantaneous actual speed and T is the instantaneous target speed, and n is the number of samples. This measure is normalized so that a perfect score results in 100, and the worst score is 0. This driving score evaluation was valuable in eliminating bad runs in the data set. As an example, the average driving score for the three drivers for the TFHRC testing (30 mph case) were 87.9, 90.1 and 89.3 respectively.

The primary data collected and reported for the eco-approach application focused on fuel consumption. As another part of the analysis, we also examined emissions of greenhouse gases (primarily CO_2) and the criteria pollutants of HC, NO_x and CO.

It is well established that CO_2 emissions are directly proportional to fuel consumption. Therefore, the percentage savings of CO_2 for the different tests are the same as the percentage savings of fuel.

For this analysis, the second-by-second vehicle trajectories for each test cell are used as input to the CMEM. CMEM is capable of processing each trajectory and calculating the total emission for each run. The emissions are then aggregated for each cell, and the emission savings are calculated by subtracting the emissions of the eco-approach driving from the uninformed driving. As part of this analysis, the trajectories from the Riverside testing were used. The CMEM model was calibrated for an average vehicle found on the road today, by compositing vehicle types through a weighting process based on current 2012 vehicle population statistics for Riverside California. The results for the different emissions savings are shown in Fig.5.25.

Vel\Time	0 s	5 s	10 s	15 s	20 s	25 s	30 s	35 s	40 s	45 s	50 s	55 s	%
20 mph	19.23	18.59	19.75	4.86	3.24	2.12	1.00	4.36	-2.73	9.59	12.80	16.14	21.42
25 mph	15.34	21.14	23.02	12.23	1.87	-0.77	0.56	0.94	0.73	7.20	13.72	11.79	22.24
30 mph	15.62	-0.97	6.55	7.09	-1.96	0.16	0.35	-0.62	-0.11	29.70	11.45	11.99	18.42
35 mph	7.77	18.75	13.74	19.42	10.70	1.12	-1.02	-0.36	-0.13	4.68	6.61	9.86	25.45
40 mph	-4.24	4.56	11.58	10.24	3.21	0.03	5.31	3.40	2.70	0.14	0.29	7.64	15.82

Vel\Time	0 s	5 s	10 s	15 s	20 s	25 s	30 s	35 s	40 s	45 s	50 s	55 s	%
20 mph	1.3	1.4	1.5	2.1	0.6	0.3	0.2	5.9	-0.1	0.8	1.0	1.3	47.6
25 mph	1.3	2.5	1.8	1.1	0.3	0.1	0.1	0.2	0.1	0.5	1.2	1.0	37.1
30 mph	0.7	0.0	0.2	0.4	-0.3	0.0	0.2	-0.2	0.1	0.0	0.4	0.8	12.1
35 mph	2.4	7.5	5.3	2.1	5.9	-0.3	-0.2	0.0	0.1	0.4	1.0	0.9	61.9
40 mph	-0.1	0.9	1.1	0.9	0.1	0.0	0.9	0.1	0.7	0.0	-0.1	0.1	36.2

Vel\Time	0 s	5 s	10 s	15 s	20 s	25 s	30 s	35 s	40 s	45 s	50 s	55 s	%
20 mph	0.10	0.11	0.10	0.09	0.05	1.15	0.01	0.06	-0.01	0.06	0.08	0.10	52.22
25 mph	0.07	0.13	0.14	0.09	0.06	0.02	-0.01	0.02	0.01	0.03	0.07	0.07	27.26
30 mph	0.04	0.00	0.00	0.01	0.03	0.05	0.00	0.01	-0.01	0.00	0.04	0.00	7.05
35 mph	0.06	0.13	0.10	0.14	0.11	-0.05	-0.01	-0.01	0.00	0.00	0.07	0.07	27.90
40 mph	-0.01	-0.10	0.02	-0.01	-0.02	-0.02	0.08	0.01	0.30	0.06	0.09	0.05	16.87

Vel\Time	0 s	5 s	10 s	15 s	20 s	25 s	30 s	35 s	40 s	45 s	50 s	55 s	%
20 mph	0.3	0.3	0.3	0.2	0.1	1.1	0.1	0.2	0.0	0.1	0.2	0.2	52.2
25 mph	0.2	0.3	0.3	0.2	0.1	0.0	0.0	0.1	0.0	0.1	0.2	0.2	38.5
30 mph	0.1	0.0	0.1	0.1	0.0	0.0	0.0	0.0	0.0	0.0	0.1	0.1	12.2
35 mph	0.2	0.3	0.3	0.3	0.3	-0.1	0.0	0.0	0.0	0.1	0.1	0.1	40.6
40 mph	0.0	0.1	0.2	0.2	0.3	0.0	0.1	-0.1	0.1	0.0	0.0	0.0	22.8

Fig.5.25. Fuel and Emission Savings for Composite Vehicle

5.2.4 Summary

As part of the AERIS field study program, an eco-approach and departure application to traffic signals was extensively evaluated using several test vehicles and test sites to determine potential fuel economy and emissions impacts. For comparison purposes, two testing stages were carried out that included informed driver tests and uninformed driver tests.

Two test sites and two vehicles were utilized in the experiments; at each test intersection, SPaT data were broadcast for fixed-time signalization to the vehicle. The testing was performed for a variety of intersection entry and exit speeds, and at entering the intersection at various times in the overall signal cycle.

The results show that on average, informed drivers had fuel savings in the range of 10% to 25%, depending on the entry and exit speed of the vehicle traveling through the intersection. For the Riverside-based testing using a light-duty passenger vehicle (Nissan Altima), there was approximately 19.8% reduction of fuel and CO_2 emissions averaged across all speed ranges. For the TFHRC testing using a SUV (Jeep Grand Cherokee), the average reduction was approximately 10.7%; however, higher speed testing was not conducted at TFHRC. It should be noted that most savings occur around an entry/exit speed of around 30 mph. Savings at slower speeds aren't as great since vehicles traveling slowly can typically adjust better to make it through a green light, for both informed and uninformed driving scenarios. Savings at higher speeds are also reduced since an informed driver can't drastically modify their overall driving trajectory to achieve significant savings. Another key difference between Riverside and TFHRC testing is the range of the DSRC signal. Because of various trees and terrain, the reliable DSRC range at TFHRC was approximately 190 meters. The reliable DSRC range at Riverside was approximately 500 meters. With a longer DSRC range, the vehicle has more time to plan an effective trajectory, resulting in greater fuel savings.

It is important to note that there are many other factors affecting the results besides entry and exit speed. Examples include vehicle type, driver variability and their ability to follow the eco-advice, and road terrain. It was found that at TFHRC, small road grade differences had a noticeable effect, particularly when the vehicle is coasting or accelerating towards the intersection.

From a pollutant emissions perspective, emissions were estimated by combining the vehicle trajectories from the testing with a modal emissions model that predicts second-by-second emissions. For this part of the analysis, the emissions model was calibrated for a 2011 composite-year vehicle. This means that given a typical fleet on the road in 2011, the emission characteristics reflect that of the entire fleet as a single "composite" vehicle. The overall pollutant emissions reductions across all speeds in this case were calculated to be 20.6% for CO_2, 38% for CO, 26% for HC, and 33% for NO_x.

These results are mostly consistent with traffic simulation modeling studies examining the eco-approach and departure application. For example, [26] and [32] showed typical fuel savings of around 12% - 16%. Another study with BMW showed a fuel savings of around 14% [33]. The results are comparable to 19% for the Riverside testing and 11% for the TFHRC testing.

Chapter 6
Related Eco-ITS Applications

The Eco-Approach and Departure algorithm fits in well will other eco-friendly ITS applications, several of which were evaluated as part of the AERIS research program. One of the key combined applications is Connected Eco-Driving, which includes as a key component the Eco-Approach and Departure algorithm, described in Section 6.1. Another is Cooperative Adaptive Cruise Control (CACC), described in Section 6.2.

6.1 Connected Eco-Driving Algorithm

Connected Eco-Driving algorithm consists of three major components as shown in Fig.6.1: 1) Eco-Approach and Departure (for a signalized arterial), 2) Eco-Speed Harmonization (for both freeways and arterials), and 3) General Eco-Driving Principles (for both freeways and arterial). Each component has its own effective region, as depicted in Fig.6.2. For example, the Eco-Approach and Departure module is effective within the communication range of traffic signal infrastructure (typically a radius of 300 meters at a signal, based on the typical range of dedicated short range communications), because of the availability of signal phase and timing (SPaT) information. The description of each component is elaborated in the following section.

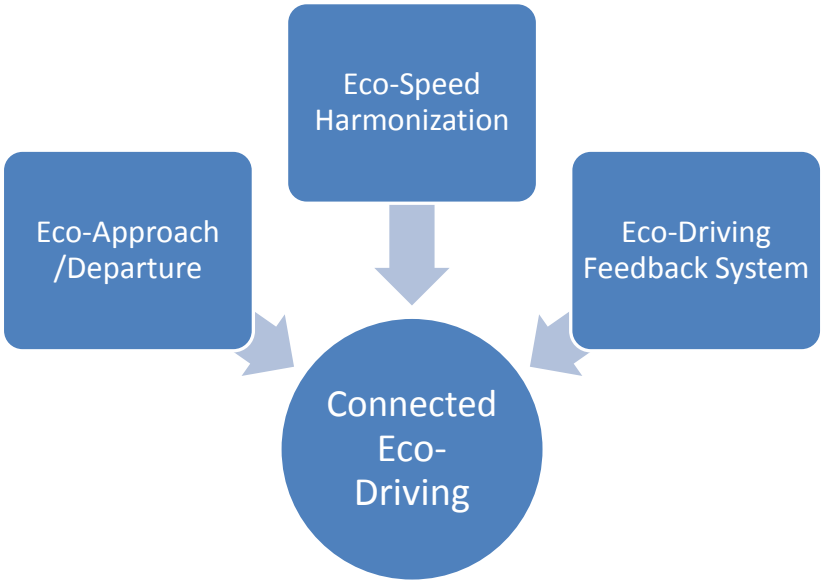

Fig.6.1. Components of Connected Eco-Driving application

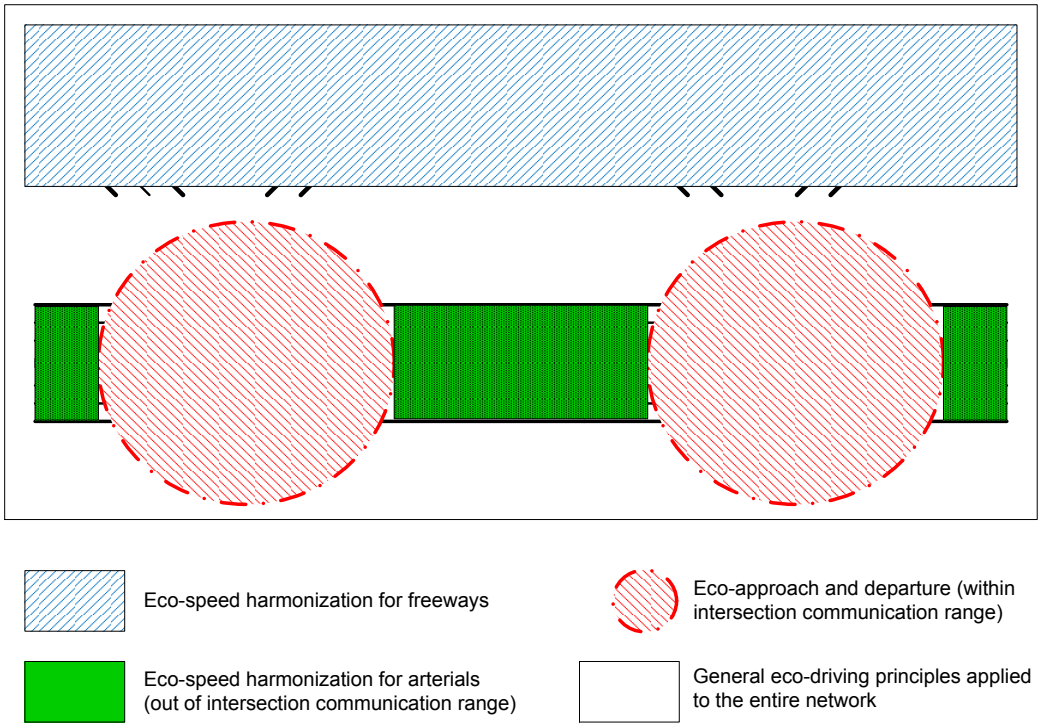

Fig.6.2. Effective region of each component of Connected Eco-Driving application

There are two new components that need to be addressed: Eco-Speed Harmonization and General Eco-Driving Principles.

6.1.1 Arterial-Based Eco-Speed Harmonization

It is well known that speed and acceleration have a major impact on a vehicle's fuel economy and tailpipe emissions. With the availability of real-time traffic information or other external conditions (e.g., roadway grade and road weather conditions), speed advice at particular locations and time instances can be dynamically provided to drivers allowing them to reduce the unnecessary stop-and-go maneuvers while meeting specific driving requirements (e.g., travel time). For drivers, it is not realistic to sacrifice travel time to gain marginal environmental benefits. It also cannot be assumed that the reduction in travel time saves energy. It is noted that the speed advice can be disseminated through at least two channels: 1) the TMC provides a speed recommendation to all vehicles to harmonize speed of the entire roadway; or 2) each individual vehicle optimizes its speed based on data (i.e., traffic conditions) collected from infrastructure and data from the vehicle's CAN BUS.

This module can be implemented in a variety of ways, depending on how the set speed is determined. In this application, the speed is calculated based on the average link speed, which can be directly measured and estimated by using the CV technology. For link i, within time interval ΔT, the average link speed is:

$$\bar{V}_i = \begin{cases} V^{ff}, & no\ vehicle\ within\ \Delta T\ along\ link\ i \\ \dfrac{Vehicle\ miles\ traveled\ within\ \Delta T\ along\ link\ i}{Vehicle\ hours\ spent\ within\ \Delta T\ along\ link\ i}, & otherwise \end{cases}$$

where V^{ff} is the free-flow speed or speed limit of that roadway segment.

With the measured average link speed, a simple regression model is developed to determine the recommended speed for vehicle j, within ΔT,

$$V_j^{ctrl} = a \cdot \bar{V}_i + b$$

Based on the collected data, Fig.6.3 provides a candidate set of values that a's and b's can choose.

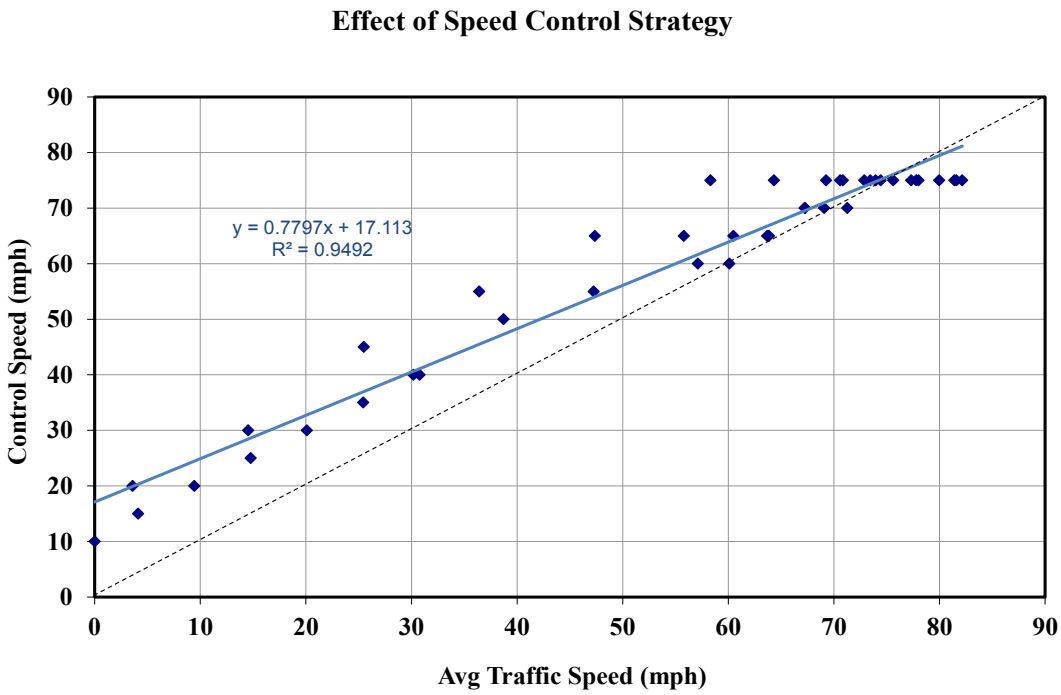

Fig.6.3. A candidate strategy for the control speed determination [38]

6.1.2 General Eco-Driving Principles

Another way to reduce fuel consumption and pollutant emissions is to provide feedback to drivers on their driving behavior to encourage them to drive in a more environmentally efficient manner. To model the impacts resulting from use of the General Eco-Driving Principles system, the research team modified the

acceleration/deceleration profiles in Paramics based on the field data collected from equipped vehicles.

More specifically, Fig.6.4 illustrates the iterative procedure to calibrate the acceleration/deceleration profiles. As shown in Fig.6.5, the accelerations under eco-scenarios (blue) are milder than the default values (red) across different speeds. Similar procedures have been applied to deceleration-speed profile.

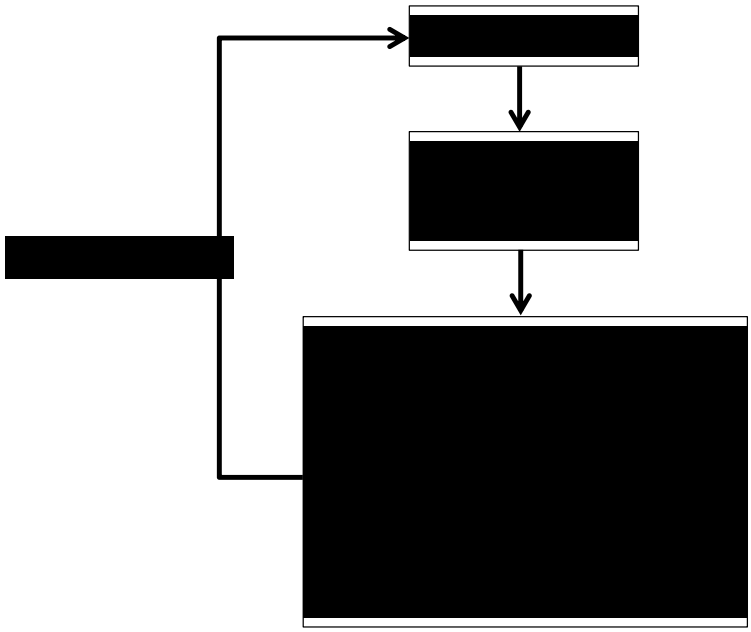

Fig.6.4. Procedure to calibrate eco acceleration/deceleration profiles in Paramics

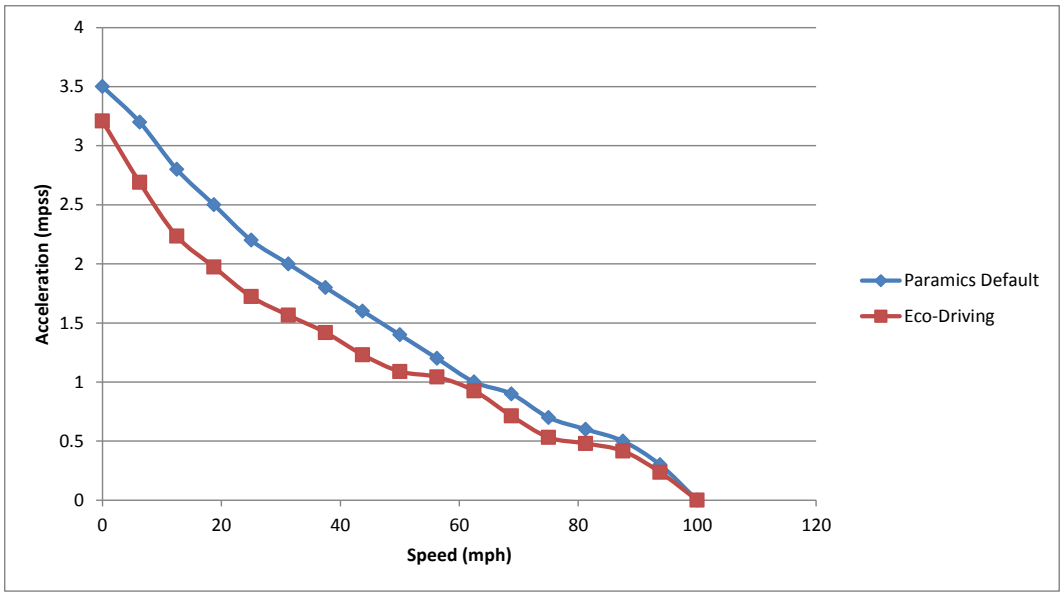

Fig.6.5. Example acceleration/deceleration profiles in Paramics for cars: default vs. eco-driving

6.1.3 Simulation Site

As shown in Fig.6.6, the model region in this study is the 27-intersection (6-mile) segment of El Camino Real between Churchill Avenue in Palo Alto, California, and Grant Road in Mountain View, California. El Camino Real is a major north–south arterial connecting San Francisco and San Jose and is parallel to the US-101 freeway.

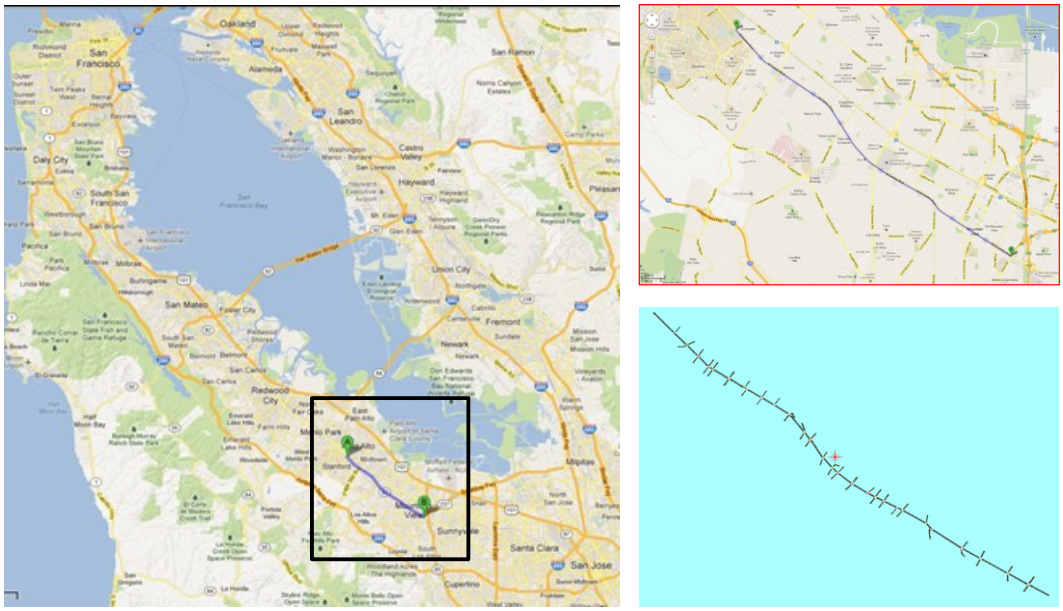

Fig.6.6. Modeled segment of El Camino Real corridor (27 intersections) in California

This 6-mile segment of El Camino Real has been coded in Paramics, a microscopic traffic simulation tool, and is readily available for use in this project. This segment has three lanes in each direction and consists of 27 signalized intersections. The intersection spacing varies from 50 to 760 meters, and the speed limit is 40 mph. Fig.6.7 shows a detailed map and sketch plot for the study corridor. Vehicle demands and their origin-destination (OD) patterns were calibrated for a typical weekday morning between 7:15 a.m. and 9:30 a.m. in summer 2005. The traffic signals along the segment are both actuated and coordinated. Signal settings in the model are based on the parameter values exported from the actual traffic signal system in July 2005. Traffic signals in the existing simulation network are coded as fixed-time signals.

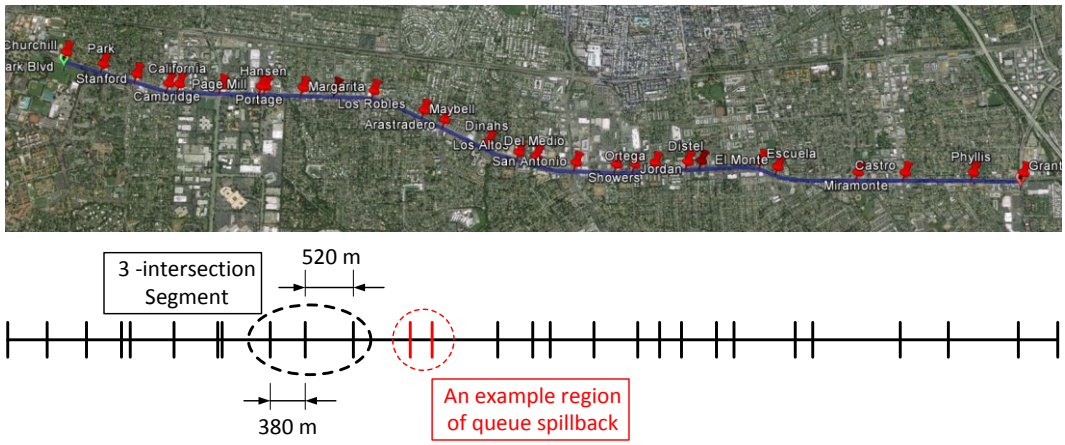

Fig.6.7. Detailed map and sketch plot for the modeled segment of El Camino Real corridor (27 intersections)

6.1.4 Simulation Approach

The microscopic traffic simulation software Paramics was used to model the movement of individual vehicles and their interactions in detail. As part of the evaluation, detailed speed profiles of every vehicle were examined to estimate emissions and energy consumption. As part of the programming environment, Paramics supports the development of plugins using its API, which enables users to interface with its core simulation engine to perform specific tasks. The interaction between different models and the API used in this application is shown in Fig.6.8. The Connected Eco-Driving application plugin is designed to fulfill the following functions:

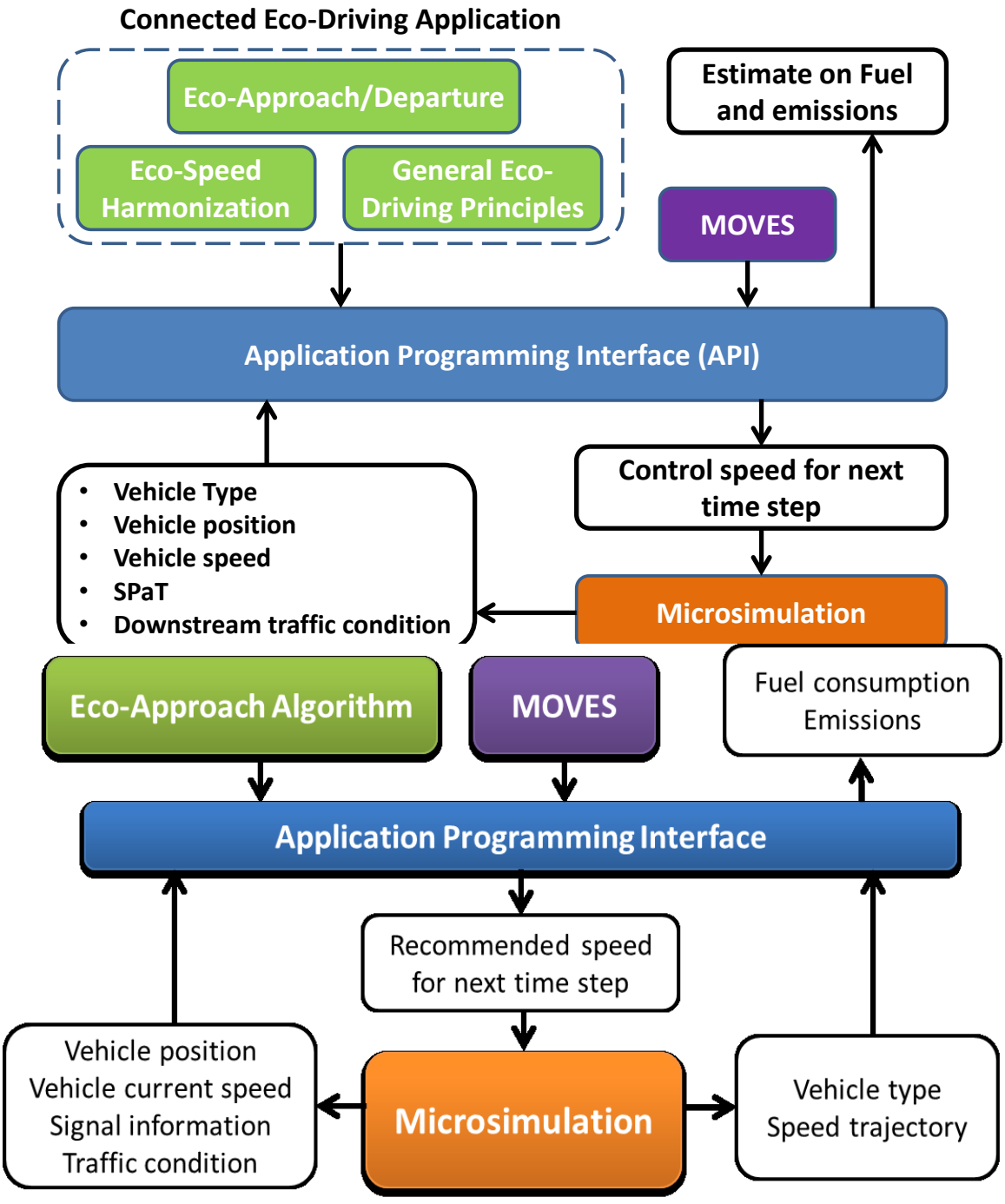

Fig.6.8. Diagram of interactions among the models and API

A. Collect vehicles' characteristics (e.g., type) and second-by-second speed data.
B. Collect SPaT information.
C. Estimate vehicles' energy consumption and pollutant emissions based on the MOVES model.
D. Generate vehicles' advisory speeds.
E. Update link average speed.
F. Calculate vehicles' control speeds.
G. Modify vehicles' acceleration profile.

Prior to modeling the application, the Paramics model was carefully calibrated for the networks. Because of the stochastic nature of the microsimulation, multiple runs were conducted using different seed numbers. In this simulation, the significance level was set to 0.05. The allowable error was set at 2%.

6.1.5 Results and Discussion

As described previously, the Connected Eco-Driving application is composed of three modules: 1) Eco-Approach and Departure, 2) Eco-Speed Harmonization, and 3) General Eco-Driving Principles—each of which has a different effective region. To gain more in-depth insight into the application as well as to access its benefits, the research team used the 27-intersection El Camino Real network model (in Paramics) and conducted sensitivity analysis on different roadway congestion levels, or volume to capacity ratios (V/C = 0.83 for the baseline traffic demand), by applying each individual

module as well as the combined Connected Eco-Driving strategy. The environmental and mobility impacts were estimated by the aforementioned plugins.

Fig.6.9 summaries the energy savings results from the simulation study for each individual module and the combined Connected Eco-Driving application. It can be observed that benefits from the General Eco-Driving Principles module varies from 0% to 3%, depending on the volume to capacity ratio (i.e., V/C). The Eco-Approach and Departure module can reduce energy consumption by up to 8%, especially in the light traffic condition (e.g., V/C = 0.2). On the other hand, Eco-Speed Harmonization can achieve up to 18% of energy savings.

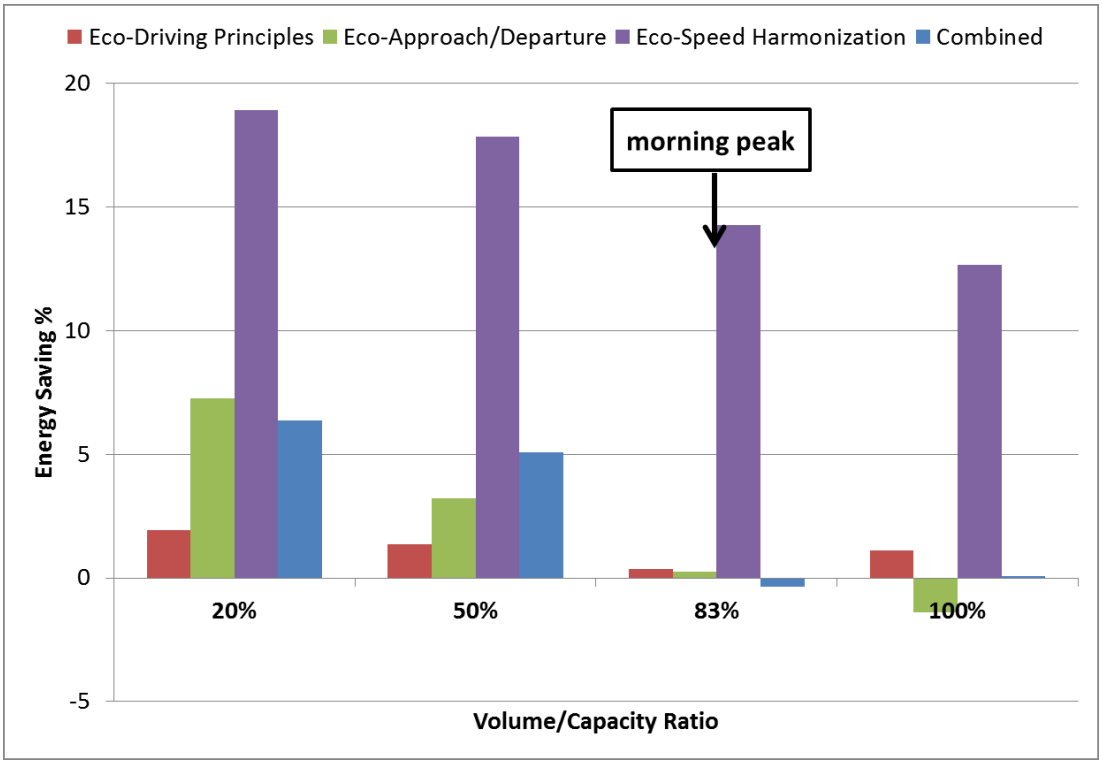

Fig.6.9. Performance of different modules and Connected Eco-Driving application on 27-intersection El Camino Real network under 100% penetration rate: energy savings

On the other hand, as shown in Fig.6.10, the General Eco-Driving Principles module is quite robust to the demand variations in terms of penalizing the mobility of entire network. It gives rise to slight increase in vehicle-hour-traveled (less than 3%). However, mobility impacts due to the Eco-Approach and Departure module are very sensitive to travel demands. When the network-wide V/C = 0.83 (i.e., baseline demand), VHT can be increased by around 20%.

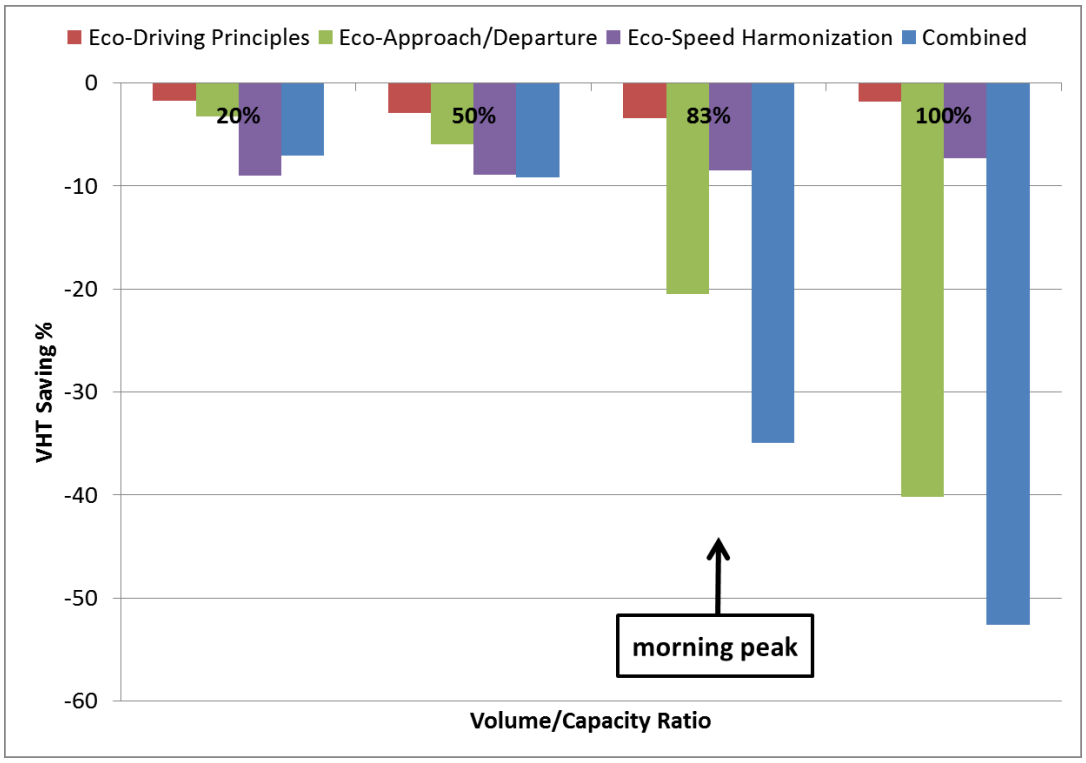

Fig.6.10. Performance of different modules and Connected Eco-Driving application on 27-intersection El Camino Real network under 100% penetration rate: changes in vehicle-hour-traveled or VHT (%)

By further investigating the simulation tests, the research team realized that vehicles equipped with the Eco-Approach/Departure module may travel as a "moving bottleneck" when it has to be stopped by the signal, due to the deceleration /acceleration

smoothing effects. If the intersection spacing is not long enough, then it is very likely that the equipped vehicle will "push" its followers back to the upstream intersection, resulting in queue spill-back. Fig.6.11 presents example snapshots from one microscopic simulation test, showing that queue spill-back does occur (and often) when the Eco-Approach/Departure module is applied, especially in congested scenarios. However, such queue spill-back issue can be hardly witnessed in the baseline case (no equipped vehicles).

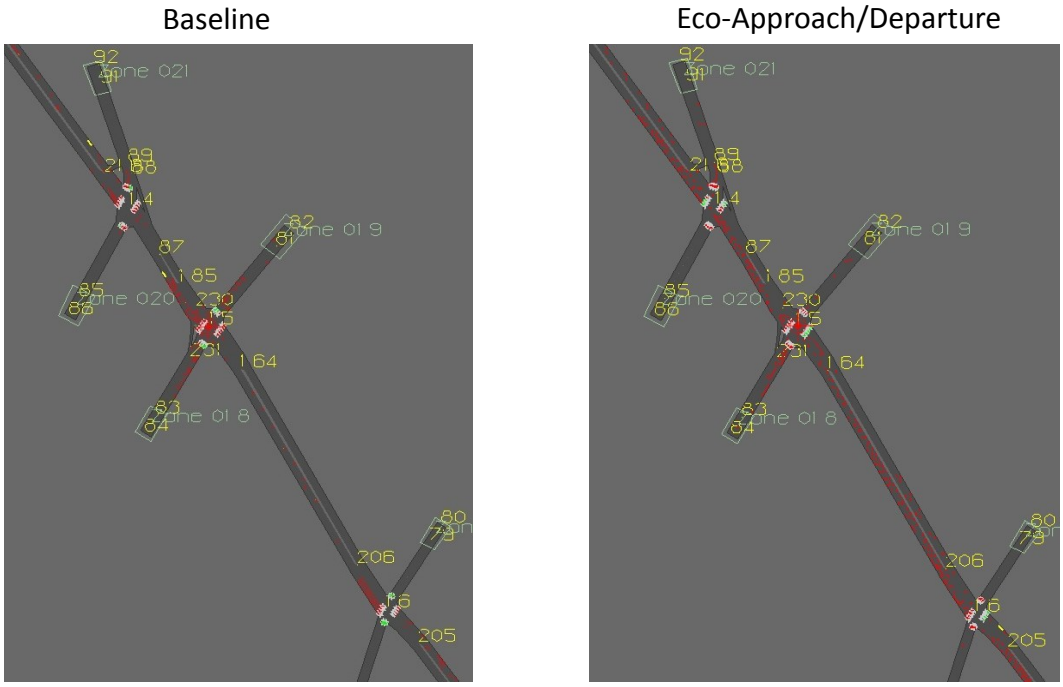

Fig.6.11. Snapshots from simulation study to show "queue spill-back" along the short link due to the Eco-Approach/Departure module

In addition, the overall benefits of Connected Eco-Driving (combined) are not simply the summation of two modules, but there are offsets in benefits when integrated. In this particular network, most of the intersection spacings are around 300 meters, so the effectiveness of Eco-Approach/Departure module dominates. The changes in measures of

effectiveness (MOEs) over different congestion levels have been summarized in Table 6.1. As shown in the Table, if the traffic demand is low (e.g., V/C = 0.20), the proposed Connected Eco-Driving application can provide around 6.4% savings in energy consumption and significant reduction in other criteria pollutants (ranging from 8.5% to 32.6%), while the vehicle-hour-travelled per vehicle may increase by 7.1%. As the network get more and more congested, the benefits drop. For example, under the baseline (morning peak) traffic demand, where V/C = 0.83, there is no improvement in energy consumption, although there are still significant reductions in other criteria pollutants. However, the VHT increases by about 35%.

Table 6.1. Changes (%) in Measures of Effectiveness (MOEs) Due to the Connected Eco-Driving Application along 27-intersection El Camino Real Corridor (100% penetration rate)

V/C	Energy (KJ/mi)	CO_2 (g/mi)	CO (g/mi)	HC (g/mi)	NO_x (g/mi	PM2.5 (g/mi)	VHT (s/veh)	VMT (mi/veh)
0.20	6.36	6.36	32.56	10.32	8.50	21.71	-7.09	-0.91
0.50	5.09	5.10	30.47	9.08	7.63	22.75	-9.14	-1.78
0.83	-0.35	-0.26	26.52	3.03	2.17	18.01	-34.95	0.23
1.00	0.07	0.10	24.45	2.02	6.73	22.12	-52.61	0.73

To get better understandings on the interaction between different modules, the research team conducted additional sensitivity analysis on module combination. The results have been summarized in Table 6.2, where the baseline traffic demand (i.e., V/C = 0.83) is modeled. As illustrated in the Table, under the baseline traffic demand, there is no significant benefits in energy savings from combined modelling. Only Eco-Speed Harmonization again shows significant benefit under this level of demand.

Table 6.2. Changes (%) in MOEs under Different Module Combinations (morning peak, baseline traffic demand where V/C is 0.83) along 27-intersection El Camino Real Corridor (100% penetration rate)

Module Comb.	Energy (KJ/mi)	CO_2 (g/mi)	CO (g/mi)	HC (g/mi)	NO_x (g/mi	PM2.5 (g/mi)	VHT (s/veh)	VMT (mi/veh)
Baseline	0.00	0.00	0.00	0.00	0.00	0.00	0.00	0.00
A	0.26	0.37	9.32	0.39	3.57	8.86	-20.53	-0.11
H	14.27	14.37	40.56	14.60	19.23	34.78	-8.47	-0.23
P	0.36	0.45	18.43	6.17	1.04	11.54	-3.42	-0.50
A + H	-0.25	-0.15	15.57	0.28	3.60	12.80	-32.00	-0.72
A + P	0.73	0.85	24.51	4.45	5.59	19.86	-33.47	-0.21
H + P	13.97	14.07	42.57	14.47	19.82	38.03	-10.93	-0.70
A + H + P	-0.35	-0.26	26.52	3.03	2.17	18.01	-34.95	0.23

A: eco-approach/departure; P: eco-driving principles

6.1.6 Summary

The analyses on 27-intersection El Camino Real network show that as traffic becomes more and more congested, the benefits from the Connected Eco-Driving application decrease. This is logical since there is less room along the arterial for the application to improve the system performance when the traffic demand increases. In addition, the implementation of this overall application may cause "moving bottlenecks" under high traffic volumes due to the smoothed deceleration/acceleration by the leading/preceding vehicles, which may result in queue spill-back when the storage space (intersection spacing) is not long enough. This has been verified by the snapshots of simulation runs (see Fig.6.11).

The benefits of Connected Eco-Driving are NOT simply the summation of benefits from each individual component. There are interactions between different modules, which may offset their own benefits when integrated. For example, the

progression speeds of traffic flows may be changed due to the implementation of some modules (e.g., General Eco-Driving Principles), which may affect the coordination levels along the corridor.

By investigating each module of the Connected Eco-Driving application, it can be shown that the modified Eco-Approach/Departure module works well in the light traffic condition. However, its effectiveness diminishes when the network gets congested. The General Eco-Driving Principles component is quite robust to the demand variations, and the changes in energy consumption and VHT are within 3%.

The sensitivity analyses on penetration rate show that there is not too much variation in MOE changes for General Eco-Driving Principles module when applying the 27-intersection ECR corridor (baseline traffic demand).

6.2 Cooperative Adaptive Cruise Control

In order to relieve drivers from driving fatigue and enhance drivers' comfort and performance, reduce risks of accidents, increase capacity, there has been extensive research of automating some tasks in vehicle [39], such as adaptive cruise control [37] which has been introduced in consumer vehicles for more than a decade. It automatically adjusts vehicle's speed to keep a safe headway distance from its proceeding vehicle by using distance-detecting sensors, satellite signal, roadside infrastructures (V2I or I2V), or information broadcast from other surrounding vehicles. The latter two types of information can be achieved by connected vehicle technology [36]. CACC is one of the ACC concepts that build on top of connected vehicle.

There are different levels in the control system. The highest level determines the optimal motion of vehicle that is subject to some constraints, while the lower levels controls engine, brakes and steering, etc. [40]. Most research has been focused on high level since the low level control is similar across different systems. One of such high-level control design proposed by Raza etc. [41][42] takes the information from onboard sensors, roadside infrastructure and other vehicles as inputs and sends commands to vehicle's brake and throttle.

Although they may produce some similar outcomes, platooning and ACC have different objectives. In a platoon, the objective is to maintain string stability so that the spacing between vehicles doesn't grow to the end of the platoon [43][44][45]. It was found that V2V communication [46][47][48] and onboard sensor [49] can be utilized to achieve the string stability. Such model is designed to increase road capacity. On the other hand, ACC is designed to keep safety headway between vehicles, and meanwhile ensuring driving comfort. Fuzzy and neurocontrollers [50][51][52] can be trained for such purpose. Other mathematical models include sliding mode control [53] and optimal dynamic back-stepping control [54].

In this section, the key question we will discuss is how ACC can contribute to increasing energy efficiency and reducing vehicle emissions. Barth and Boriboonsomsin [55] have examined the impact on energy and emissions by vehicle automation, as shown in Fig.6.12. The solid line showing real-world driving data is drawn from many trips from different types of vehicle. The dashed red line represents the lowest energy and emissions that a vehicle can achieve. The high emissions at low speeds is due to the fact

that vehicles stay on the road for longer; and the high emissions at high speed is due to the aerodynamic drag forces are higher.

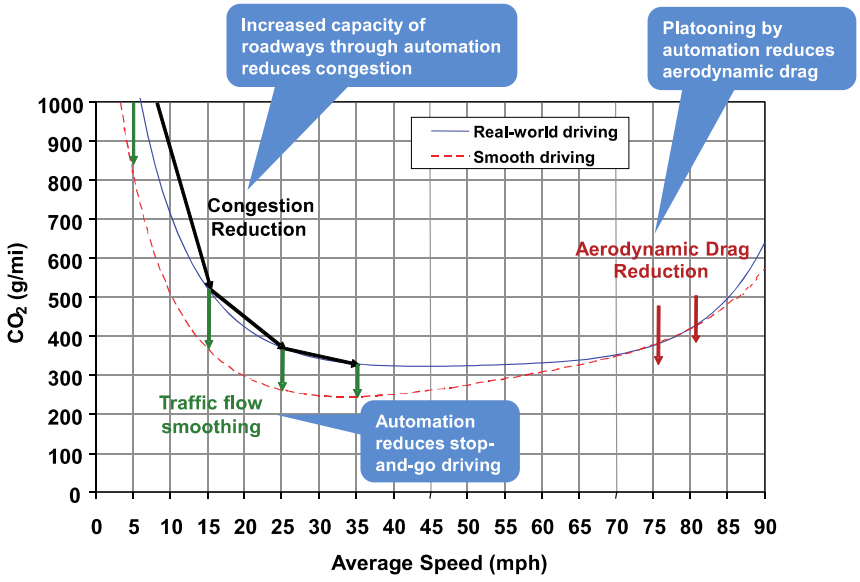

Fig.6.12. Energy and Emissions as a function of average traffic speed

Aforementioned, CACC is ACC for connected vehicles that are capable of V2I or V2V communications. With V2I and V2V communications, assuming zero-delay of such communications, every vehicle in a queue can be informed the moment the queue starts to release. If all the vehicles in a queue start to move at the same time in platoons, traffic throughput will be improved. To mimic such scheme in simulation, we chose to tune one parameter in Paramics: driver's reaction time. Assuming the driver's reaction time is zero, vehicles in a queue are expected to move at the same time when the queue starts to release, thus network capacity is also expected to increase.

With the purpose of increasing network capacity, mitigating congestions and reducing energy consumption and emissions, CACC can be potentially coupled with

EAD to further improve energy efficiency and reduce emissions when applying on a signalized corridor.

6.2.1 Simulation Setup

Simulation was conducted on an isolated intersection with single lane in each direction, as shown in Fig.6.13. The link lengths on both side of the intersection (mainline) are both 650 meters. Only the traffic on the mainline are considered, and turning traffic are omitted at first.

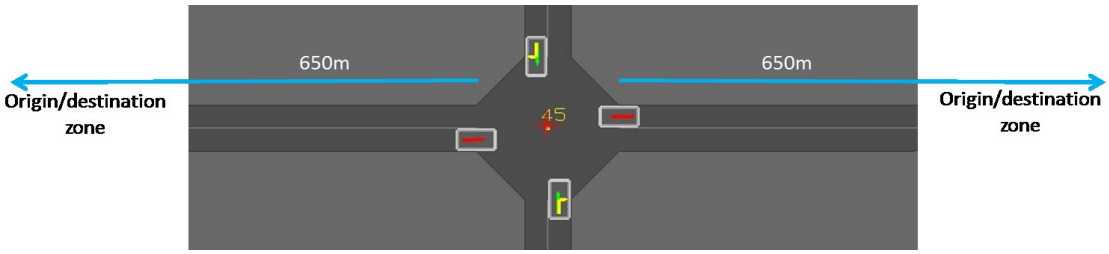

Fig.6.13. Network of an isolated intersection

6.2.2 Results and Discussion

As discussed earlier in this section, when a queue starts to release, vehicles within the queue will start to move at the same time as a whole, due to the zero driver reaction time. Fig.6.14 shows the speed-time diagrams of a queue of 3 vehicles starts to release from the intersection before and after applying CACC. It can be seen that under CACC, vehicles start to move at the same time and follow more closely with each other compared to baseline ACC. The distance-time diagram in Fig.6.15 also shows CACC can smoothen the vehicles' trajectories, potentially beneficial to improving energy efficiency.

CACC mainly takes effect when vehicles are close to each other, especially when vehicles are in a queue or a platoon. Thus traffic demand is expected to have the most impact on travel time and energy efficiency after applying CACC on vehicles.

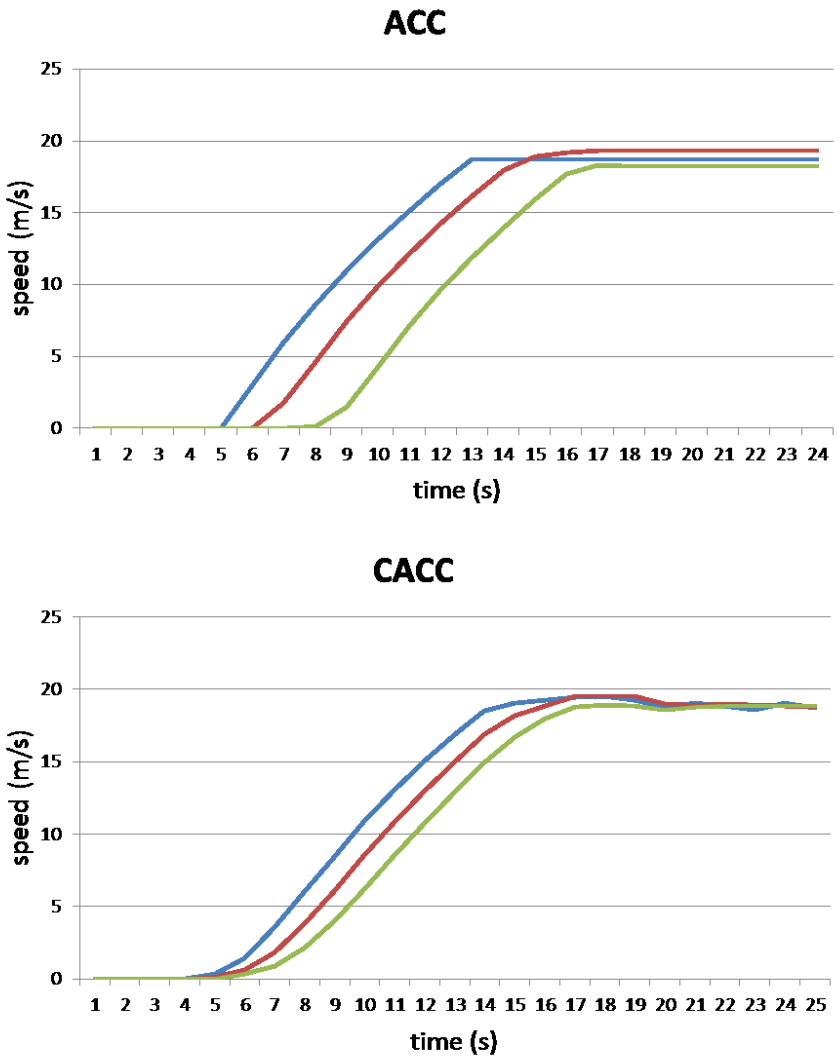

Fig.6.14. Speed-time diagrams of a releasing queue

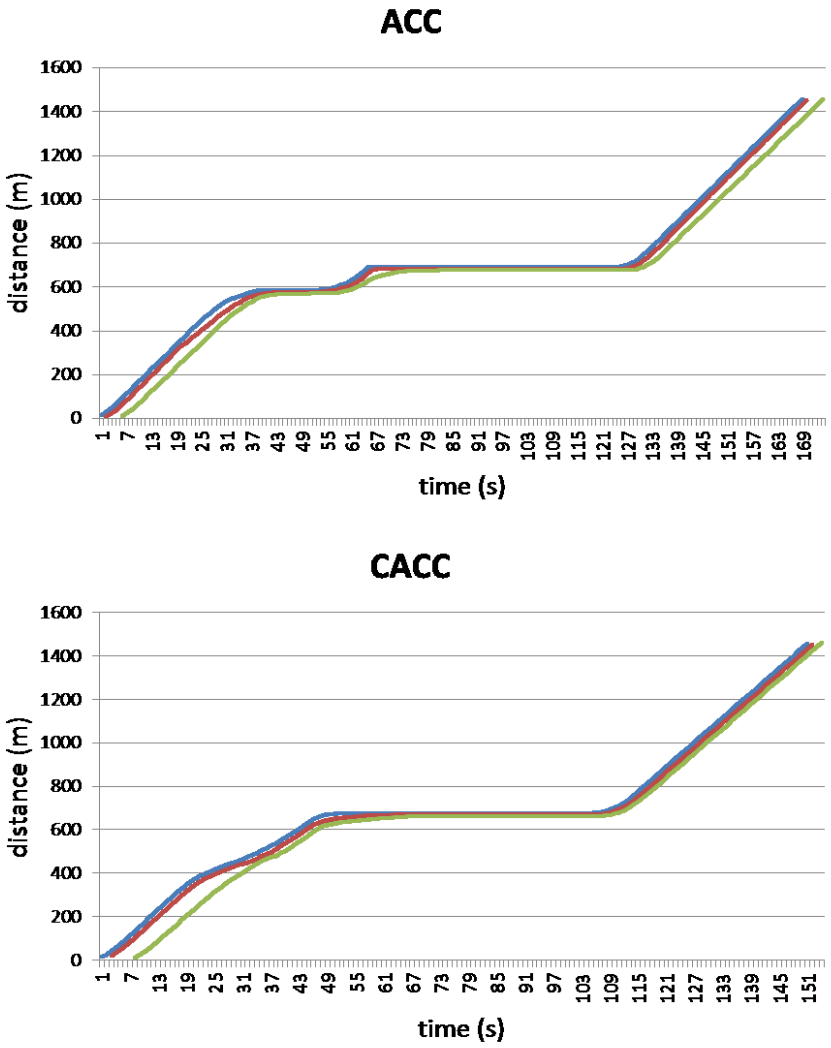

Fig.6.15. Distance-time diagrams of a releasing queue

It was argued that network capacity is sensitive to driver's reaction time. Another important factor affecting network capacity is safety headway. In order to investigate how these two factor impact the mobility and energy efficiency, we conducted a set of simulation runs. The results are shown in Fig.6.16, Fig.6.17, Fig.6.18 and Fig.6.19. These plots generally show that lower reaction time and shorter headway contributes to lower energy rate and shorter VHT. It is also shown that as traffic gets more congested, this

trend is more significant, which is due to the longer queue lengths under higher traffic demand. The longer the queue lengths are, the longer time CACC will take effect.

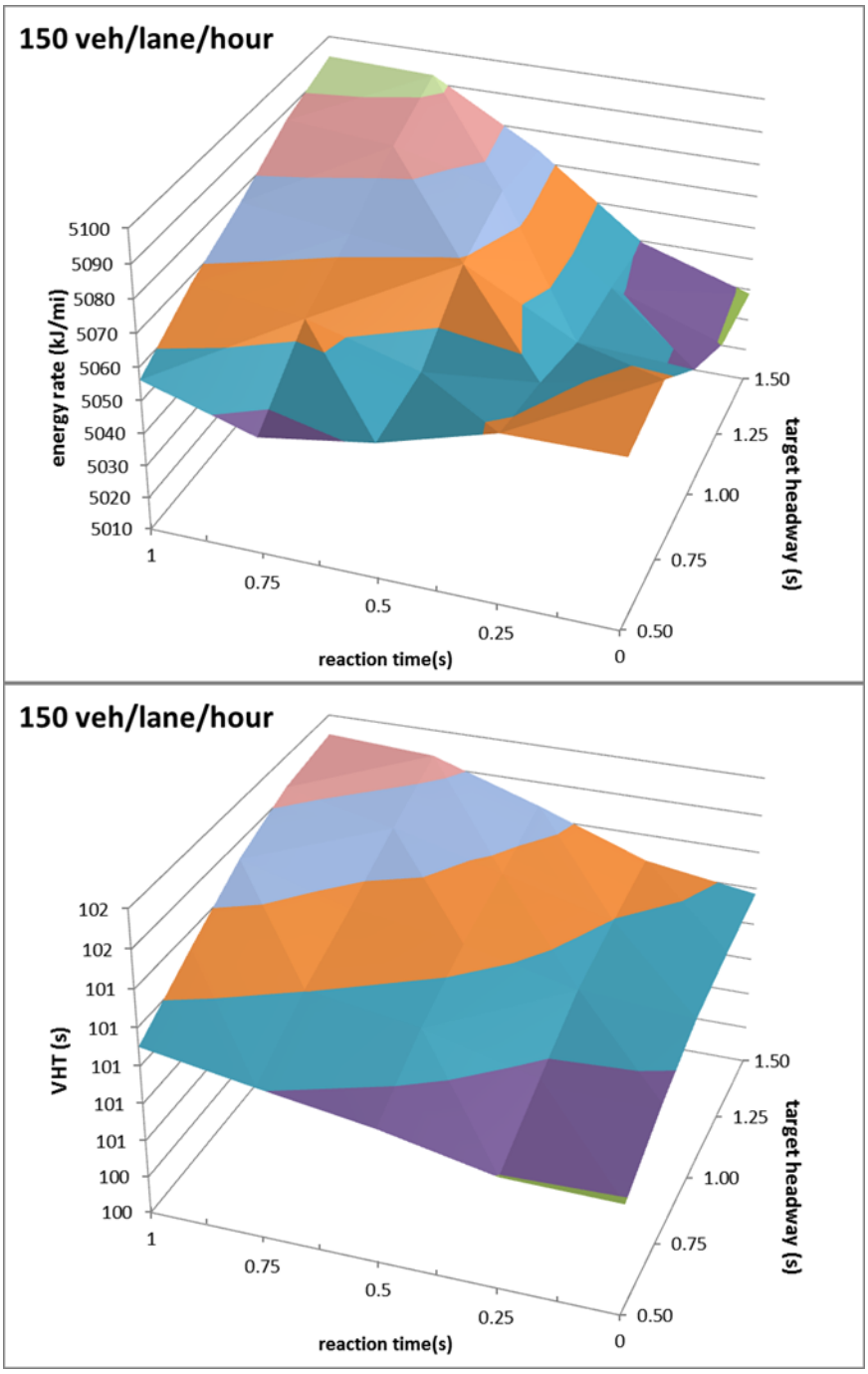

Fig.6.16. Energy rate and VHT at 150 veh/lane/hr

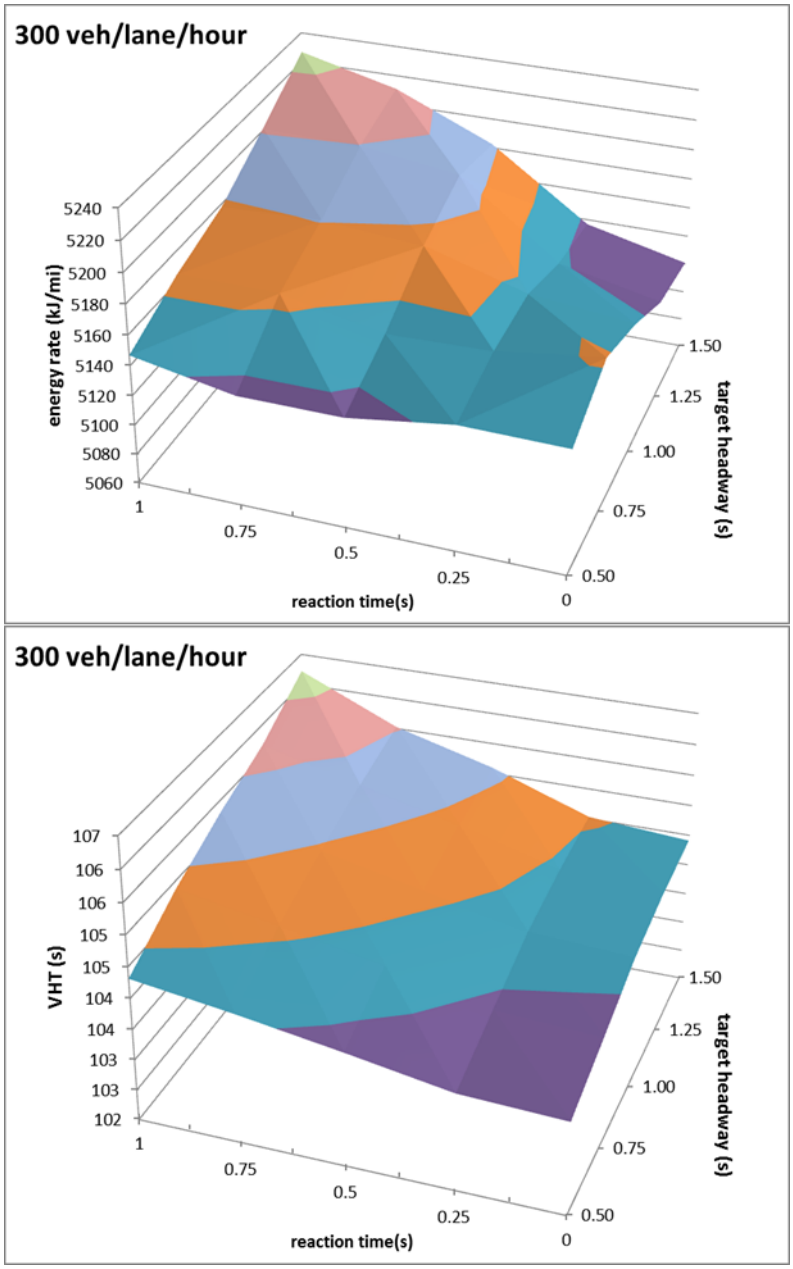

Fig.6.17. Energy rate and VHT at 300 veh/lane/hr

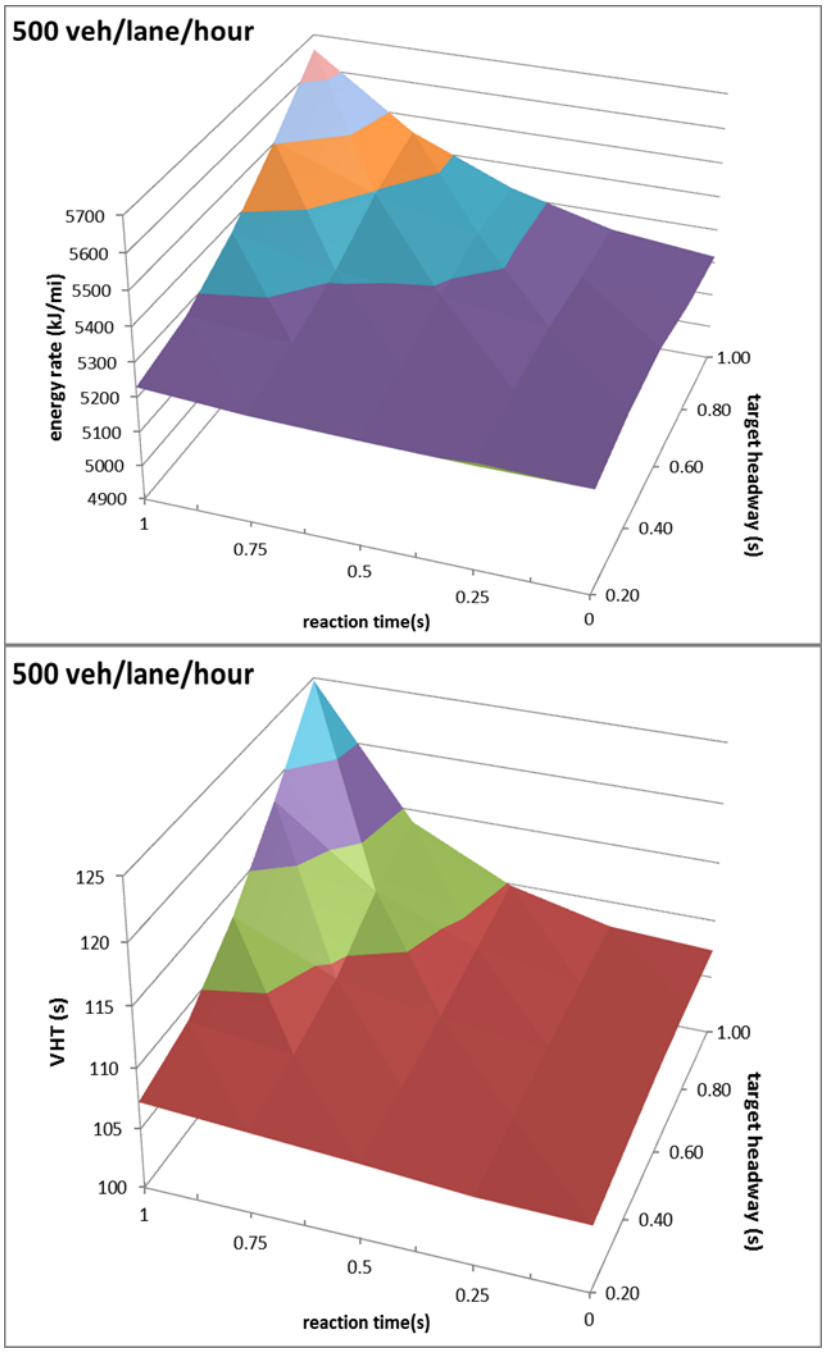

Fig.6.18. Energy rate and VHT at 500 veh/lane/hr

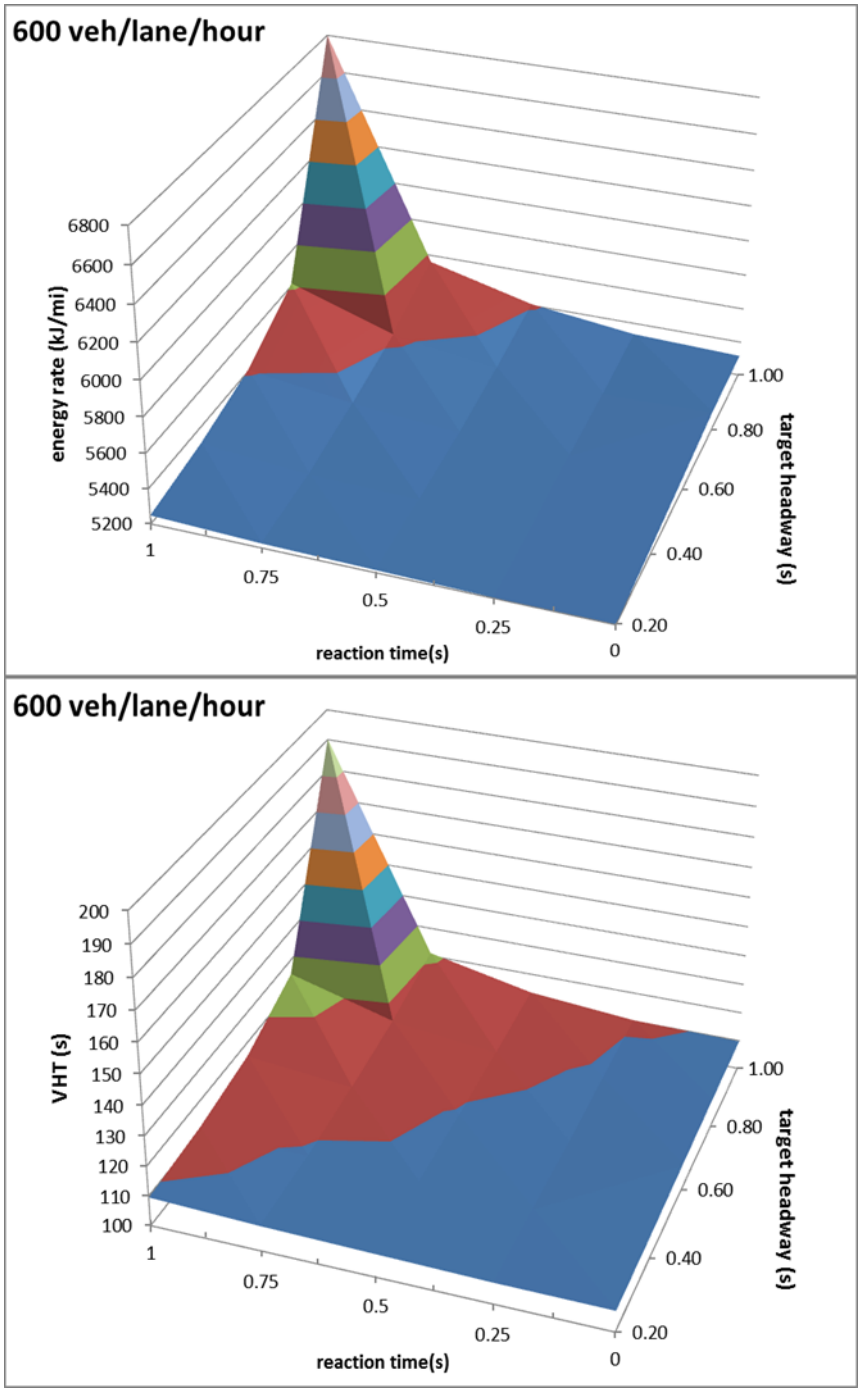

Fig.6.19. Energy rate and VHT at 600 veh/lane/hr

Previous simulations are based on a single-lane intersection. In the following simulations, multiple lanes (up to 4 lanes each direction) are modeled. Table 6.3 and

Fig.6.20 show the energy rate with different reaction times and number of lanes. It is found that there is no clear relation between energy efficiency and number of lanes.

Table 6.3. Energy rate as a function of reaction time and number of lanes

energy rate (kJ/mi)		target headway (s)			
		1.00	1.00	1.00	1.00
		1-lane	2-lane	3-lane	4-lane
reaction time(s)	0.00	5309.43	5252.69	5274.77	5273.12
	0.25	5324.55	5282.53	5288.56	5295.23
	0.50	5407.38	5341.13	5344.76	5358.95
	0.75	5559.16	5461.34	5536.19	5525.45
	1.00	6815.49	6271.64	6662.63	6361.14

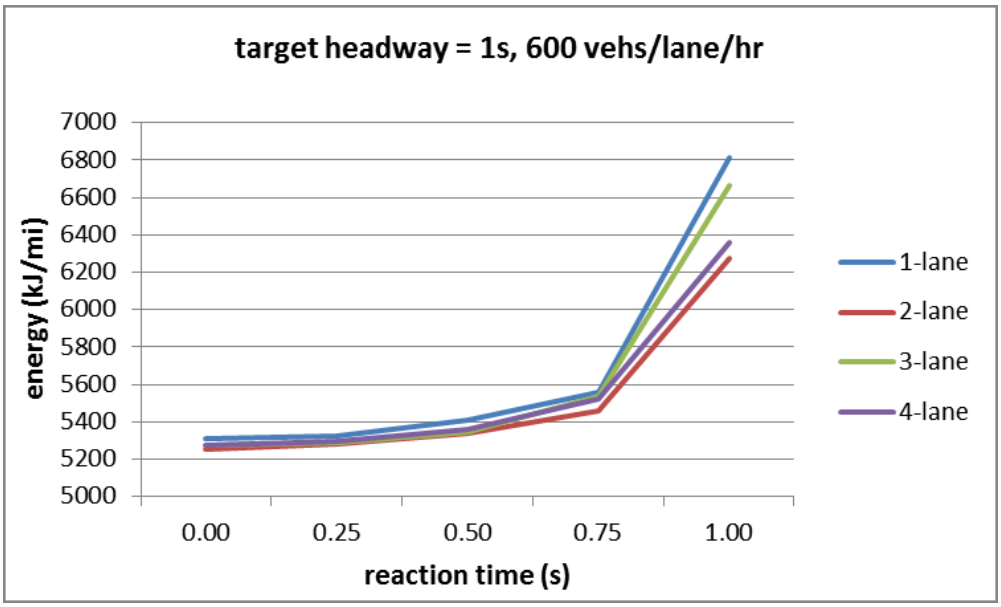

Fig.6.20. Energy rate vs. reaction time

6.2.3 Summary

There is a general trend that energy consumption rate increases as driver's reaction time and target headway increases. This trend is more obvious at higher

congestion levels, which may be due to the longer queue length in more congested traffic. It is also found number of lanes doesn't have direct effect on energy efficiency.

Varying driver's reaction time is a passive way to simulate CACC. One of the more active methods is to regulate vehicles' longitudinal gap by adjusting the following vehicles' speeds within a platoon. We also needs to address vehicles' lateral maneuver, such as when a vehicle decides to follow its proceeding vehicle to form or join a platoon, and when to unfollow the proceeding vehicle to leave the platoon, etc.

It would also be valuable to conduct some sensitivity analyses to have more insight into the CACC through simulation before field operational tests. The parameters we can vary include target headway, communication delay, penetration rate of connected vehicles, etc.

The natural last step is to implement the algorithms and communication scheme on test vehicles and roadside infrastructures in order to verify our simulation results and more importantly, improve our algorithm to adapt to the real-world scenarios.

Since CACC is focused on defining the following vehicles' behaviors within a platoon, which are essentially replicas of the leading vehicle's behavior, the natural next step is to apply the EAD algorithm on the leading vehicle to further increase the eco-benefits of the total traffic. More detail about the future work of integrating CACC with EAD and even other Eco-Driving applications can be found in Chapter 7.

Chapter 7

Conclusions and Future Work

In this dissertation, fundamental algorithm design and development has been carried out in a number of eco-friendly connected vehicle applications. The majority of the development has been on the concept of Eco-Approach and Departure at a signalized intersection. Before diving into the main topic, the calibration strategy for micro-scale traffic simulation was discussed and a new method to calibrate the micro-scale simulations was proposed. After justifying the validity of micro-scale traffic simulation, a few different types of eco-driving applications were proposed and evaluated, including Eco-Approach and Departure, Connected Eco-Driving applications and Connected Adaptive Cruise Control. The first two applications were evaluated both in simulations and field tests.

Section 7.1 provides general conclusions based on the research and results provided in this dissertation. Section 7.2 sheds some light on possible future work.

7.1 Conclusions

Chapter 3 discussed the limitation of traditional calibration practice and proposed an improved method to calibrate micro-scale traffic simulations. As the current state-of-the-practice calibration criteria for micro-simulation models are based only on macroscopic traffic parameters, it is of interest to examine whether these criteria are sufficient to make the simulated vehicle trajectories at the micro scale represent those in

the real-world or not. This chapter investigates this issue using an NGSIM dataset as a ground truth. It is found that the microsimulation calibration criteria based on macroscopic traffic parameters alone are not adequate to represent vehicle trajectories at the micro scale. After carefully calibration on the microscopic parameters including mean target headway time, mean reaction time, mean acceleration/deceleration profiles, speed memory and simulation time step, it is found that after micro-scale calibration, not only the macroscopic criteria were met, the VSP distribution from simulation has much better match to that from NGSIM data, which means after micro-scale calibration, the simulation can capture real-world driving behaviors more accurately. The emission results further prove that micro-scale calibration can make simulation better at capturing microscopic behaviors in real world.

Chapter 4 proposed the eco-approach and departure algorithm and its enhanced version to deal with intersection congestion. Based on this research, there are several key findings that are counter-intuitive when compared to typical eco-driving advices. When traveling on a roadway where there are specific points where traffic is controlled (traffic lights), specific constraints emerge in time and space; as a result, it has been found that hard accelerations that quickly get a vehicle up to a target speed and then have a steady cruise to reach a specific location at a specific time are less fuel consuming compared to a velocity profile that takes a longer period of time of acceleration to reach the same point of time and space. Similarly, it is beneficial to decelerate quickly, and then hold a steady state cruise speed when reaching a traffic signal just as it is turning green. At that point, it takes less energy to accelerate back up to typical speed traversing the corridor, compared

to starting from a stop. Results of our algorithms show approximately 12% fuel economy improvement and 13% emission reductions in individual vehicles over a standard baseline case without the velocity planning. In addition to these individual vehicle benefits, a set of experiments were also carried out to determine if there is a network-wide energy/emissions savings from having a low penetration rate of dynamic eco-driving technology equipped vehicles in the traffic stream. It is concluded that there is indeed additional network-wide fuel savings and emission reductions, due to the fact that unequipped vehicles are forced to follow the trajectories of the dynamic eco-driving vehicles in front, based on the car following logic. In the experiments, the maximum fuel saving and emission reduction occur during low congestion condition (corresponding to traffic volume of 100 vehicles/hour/link). Even at low technology penetration rates, significant fuel savings and emission reductions were still achieved. Under these low-penetration conditions, the total traffic energy/emission savings typically double what is saved from the technology-equipped vehicles alone (e.g., total 3.39% savings compared to 1.57% savings from equipped vehicles at the penetration rate of 20%). We also tested our algorithm in a multiple-lane network with different signal cycle lengths. As both the cycle lengths and green phase duration increase, vehicles have more chances to pass intersections without stop or slowing down. Also since vehicles have more flexibility to change lanes, indirect network energy/emission benefit from car-following logic is weakened. Therefore, fuel savings are not as high as in previous simulations.

The enhanced version of this eco-approach and departure algorithm was also proposed in Chapter 4. This enhanced algorithm considers not only the phase and timing

of the signal but also the estimated intersection delay in front of the subject vehicle. The comparative study in a simulation environment exhibits that the proposed application outperforms its predecessor, which does not account for the estimated intersection delay, especially when traffic gets more congested. Simulation results also show that the network-wide fuel saving benefits of the proposed application are not sensitive to the congestion level, but to the penetration rate, communication range, and communication delay.

Chapter 4 also discussed an eco-approach and departure model optimized for improving fuel consumption in situations where the car is facing multiple traffic lights in a row on its route. The main goal is to find an optimal speed trajectory that prefers leading the car through green phases while optimizing a weighted cost function of fuel consumption and time saving for the whole route. Furthermore, several weak and strong constraints that have to be considered have to be worked out and analyzed. This research was done with BMW. Due to the time constraint, we couldn't finish implementing the algorithm in simulations. This chapter will give a brief description of the algorithm used for multiple fixed-time intersections.

Chapter 5 includes all the field studies we have conducted for Eco-Approach and Departure application. The first section discussed the field tests at Richmond Field Station. In this section, we tested an example of eco-approach technology in a BMW test vehicle at a signalized intersection to determine fuel economy differences. Simulation-based experiments were also carried out for the same test environment to compare the results between simulations and field tests. For comparison purposes, the two testing

scenarios included informed driver tests and uninformed driver tests. In the informed driver tests, the driver was provided with speed recommendations, while during the uninformed driver tests, the driver drove without any speed advice. The results show that on average, informed driver saved approximately 13.6% fuel compared with uninformed driver tests. It's also found that fuel savings are mainly from informed driver's early slowing down and cruising through intersection without having to stop at the intersection. In the second section, two test sites and two vehicles were utilized in the field experiments; at each test intersection, SPaT data were broadcast for fixed-time signalization to the vehicle. The testing was performed for a variety of intersection entry and exit speeds, and at entering the intersection at various times in the overall signal cycle. The results show that on average, informed drivers had fuel savings in the range of 10% to 25%, depending on the entry and exit speed of the vehicle traveling through the intersection. For the Riverside-based testing using a light-duty passenger vehicle (Nissan Altima), there was approximately 19.8% reduction of fuel and CO_2 emissions averaged across all speed ranges. For the TFHRC testing using a SUV (Jeep Grand Cherokee), the average reduction was approximately 10.7%; however, higher speed testing was not conducted at TFHRC. It should be noted that most savings occur around an entry/exit speed of around 30 mph. Savings at slower speeds aren't as great since vehicles traveling slowly can typically adjust better to make it through a green light, for both informed and uninformed driving scenarios. Savings at higher speeds are also reduced since an informed driver can't drastically modify their overall driving trajectory to achieve significant savings. Another key difference between Riverside and TFHRC testing is the

range of the DSRC signal. Because of various trees and terrain, the reliable DSRC range at TFHRC was approximately 190 meters. The reliable DSRC range at Riverside was approximately 500 meters. With a longer DSRC range, the vehicle has more time to plan an effective trajectory, resulting in greater fuel savings. It is important to note that there are many other factors affecting the results besides entry and exit speed. Examples include vehicle type, driver variability and their ability to follow the eco-advice, and road terrain. It was found that at TFHRC, small road grade differences had a noticeable effect, particularly when the vehicle is coasting or accelerating towards the intersection. The overall pollutant emissions reductions across all speeds in this case were calculated to be 20.6% for CO_2, 38% for CO, 26% for HC, and 33% for NO_x. These results are mostly consistent with traffic simulation modeling studies examining the eco-approach and departure application. The results are comparable to 19% for the Riverside testing and 11% for the TFHRC testing.

Connected Eco-Driving application is discussed in Chapter 6. The analyses on 27-intersection El Camino Real network show that as traffic becomes more and more congested, the benefits from the Connected Eco-Driving application decrease. This is logical since there is less room along the arterial for the application to improve the system performance when the traffic demand increases. In addition, the implementation of this overall application may cause "moving bottlenecks" under high traffic volumes due to the smoothed deceleration/acceleration by the leading/preceding vehicles, which may result in queue spill-back when the storage space (intersection spacing) is not long enough. This has been verified by the snapshots of simulation runs (see Fig.6.11). The

benefits of Connected Eco-Driving are NOT simply the summation of benefits from each individual component. There are interactions between different modules, which may offset their own benefits when integrated. For example, the progression speeds of traffic flows may be changed due to the implementation of some modules (e.g., General Eco-Driving Principles), which may affect the coordination levels along the corridor. By investigating each module of the Connected Eco-Driving application, it can be shown that the modified Eco-Approach/Departure module works well in the light traffic condition. However, its effectiveness diminishes when the network gets congested. The General Eco-Driving Principles component is quite robust to the demand variations, and the changes in energy consumption and VHT are within 3%. The sensitivity analyses on penetration rate show that there is not too much variation in MOE changes for General Eco-Driving Principles module when applying the 27-intersection ECR corridor (baseline traffic demand).

Chapter 6 also provides some simulation analyses on Connected Adaptive Cruise Control. It is found that there is a general trend that energy consumption rate increases as driver's reaction time and target headway increases. This trend is more obvious at higher congestion levels, which may be due to the longer queue length in more congested traffic. It is also found number of lanes doesn't have direct effect on energy efficiency.

7.2 Future Work

Through the research on the various topics in this dissertation, we have accumulated some insight into how to improve our current research and some new

directions we can try in the future. We broke the discussion into different topics in the following subsections.

7.2.1 Micro-Simulation Calibration

The micro-scale calibration proposed in Chapter 3 focuses on calibrating mean target headway time, mean reaction time, mean acceleration/deceleration profiles, speed memory and simulation time step. There are other micro-scale parameters that can be fine-tuned as well, such as driver's aggressiveness, awareness, patience threshold and familiarity to the road network. The first three parameters are correlated to the driver's driving behaviors, which have a big impact on energy consumption and emissions. The last parameter is related to driver's routing choices, which affect energy consumption and emissions on a large network. Calibration on these parameters is expected to help further reduce the error of energy consumption and emission, and better match the simulated VSP distribution with NGSIM data.

7.2.2 Eco-Approach and Departure Application

The current algorithm we are using for Eco-Approach and Departure does not take into account the vehicle's engine specification. Since heavy-duty vehicles have very different engine maps compared to light-duty vehicles, heavy-duty vehicles should have different optimized trajectories, even different approaching and departing strategies from the light-duty vehicles. The natural next step is to integrate vehicle's specific engine map into the optimization process to further increase the fuel economy. The challenge would be the much higher computation complexity when applying such algorithm in simulations

and real-world tests, since it requires a look-up of the engine map table every time step for each vehicle and the optimization will be much more complicated.

On the other hand, even the current algorithm does not penalize vehicle mobility significantly; it is worthwhile to develop a weighted cost function to take into account both the energy cost and the travel time cost to increase the flexibility of the algorithm.

In current algorithm, the through traffic and the turning traffic at the intersection are treated equally when the vehicles do not have to stop at the intersection. The next step on this is to treat the through traffic and the turning traffic differently since the turning speed for turning vehicles should be capped based on the radius of the turning curve to ensure the driving comfort.

In order to apply Eco-Approach and Departure algorithm on actuated signals, current algorithm adapted constant-acceleration/deceleration profiles due to the time constraint of the EAR project. In the future, the sinusoidal function and even trajectory optimized for specific vehicle engine map can be utilized to improve the fuel efficiency and reduce emissions. Since the actuated signals are unpredictable, one vehicle's optimal approaching strategy calculated in last time step may not be optimal in current time step, we should optimize vehicle's trajectory to one intersection at a time as our first next step.

One limitation of this algorithm for actuated signals is that the actual starting time and ending time of each green phase and red phase are not known in advance, which makes speed planning less effective. In order to improve the prediction of on-set times of green and red phases, we can look to the historical data to establish the distributions of the phase lengths. These distributions can be further incorporated with real-time

pedestrians and vehicles calls to predict the green windows. The both ends of a green window will then be bonded with some confidence level, other than absolute bonds.

7.2.3 Cooperative Adaptive Cruise Control

In section 6.2, we proposed a way to simulate Cooperative Adaptive Cruise Control (CACC) by reducing driver's reaction time in Paramics. By setting the reaction time to zero, we can assume the following vehicles in a platoon will follow leading vehicle of the platoon without any time delay. However there is one problem in this method. The reaction time parameter in Paramics is driver's mean reaction time, so when this time is set to zero, it's not guaranteed that all the following vehicle's driver's reaction times are zero all the time.

One of the alternative methods is to have full control of each vehicle's movement so that we can regulate the gap between current vehicle and its proceeding vehicle in a platoon based on the behavior of proceeding vehicle and the leading vehicle (if it is not the same as the proceeding one). This method also needs to identify when a vehicle decides to follow its proceeding vehicle to form or join a platoon, and when to split from the proceeding vehicle to leave the platoon. For example, when a vehicle is approaching a proceeding vehicle, it could choose to change lane to overtake it or to exit the freeway; it could also choose to follow it to join the platoon. On the other hand, when a vehicle needs to change lane or when the leading vehicle decides to exit the freeway, it may need to unfollow the proceeding vehicle.

Besides the simulation methodology, it would also be valuable to conduct some sensitivity analyses to have more insight into the CACC through simulation before field operational tests. The factors we can vary include target headway, communication delay, penetration rate of connected vehicles, etc.

As mentioned early, simulations are tools for us to gain insight of how CACC would impact the mobility and fuel economy of the traffic. As a natural step after preliminary simulations, we need to implement the algorithms and communication scheme in the vehicles and roadside infrastructures in order to verify our simulation results and more importantly improve our algorithm to adapt to the real-world scenario based on the field test results.

7.2.4 Integration of CACC with Connected Eco-Driving application

With the purpose of increasing network capacity, mitigating congestions and reducing energy consumption and emissions, CACC can be coupled with EAD to further improve energy efficiency and reduce emissions when applying on a signalized corridor. Since CACC is focused on defining following vehicles' behaviors within a platoon, which are essentially replicas of the leading vehicle's behavior, it is natural to apply the EAD algorithm on the leading vehicle to increase the eco-benefits of the total traffic.

To further improve energy efficiency, for each following vehicle in a platoon, the time it passes through the next intersection can be estimated based on its position within the platoon and the leading vehicle's trajectory, in a similar way we calculated intersection delay in our enhanced EAD algorithm described in Chapter 4. Therefore, if one following vehicle finds out it cannot pass the next intersection within the green phase

if it keeps staying in the platoon, it should break away from the platoon, become a leader and follow a new trajectory calculated by EAD algorithm.

Since Eco-Speed Harmonization and General Eco-Driving Principle have their own effective zones, which are different from EAD's effective zone, one way to integrate all the four components (EAD, Eco-Speed Harmonization, General Eco-Driving Principles and CACC) together and not having any two components compromising each other is to apply both EAD and Eco-Speed Harmonization only on the leading vehicle in each platoon with the rest of the platoon obeying CACC-defined behaviors, and all the vehicles' acceleration/deceleration behaviors are regulated by General Eco-Driving Principles.

Bibliography

[1] International Energy Agency, "Energy efficiency policy recommendations in support of the G8 plan of action", Paris, 2008.

[2] T. Onoda, "IEA policies – G8 recommendations and an afterwards", Energy Policy, 37(10), 3823-3831.

[3] "AERIS (Applications for the Environment: Real-Time Information Synthesis) ConOps and Modeling Workshop", U.S. DOT, Washington, D.C., 2013.

[4] Bureau of Transportation Statistics (BTS), 2011.

[5] US Environmental Protection Agency (EPA), 2011.

[6] "Eco-Signal Operations, Concept of Operations. Applications for the Environment: Real-Time Information Synthesis (AERIS)", U.S. DOT. 2013.

[7] "Eco-Lanes, Concept of Operations. Applications for the Environment: Real-Time Information Synthesis (AERIS)", U.S. DOT. 2013.

[8] "Low Emissions Zones, Concept of Operations. Applications for the Environment: Real-Time Information Synthesis (AERIS)", U.S. DOT. 2013.

[9] E. Brockfeld, R. Barlovic, A. Schadschneider, M. Schreckenberg, Phys. Rev. E 64 (2001) 056132.

[10] Barth M. and Boriboonsomsin, K. "Real-world carbon dioxide impacts of traffic congestion," Transportation Research Record, vol. 2058, pp. 163-171, 2008.

[11] Li, M., Boriboonsomsin, K., Wu, G., Zhang, W.-B. and Barth, M. "Traffic energy and emission reductions at signalized intersections: a study of the benefits of advanced driver information," International Journal of Intelligent Transportation Systems Research, vol. 7(1), pp. 49-58, 2009.

[12] Yi, K. S. and Chung, J. T. "Nonlinear brake control for vehicle CW/CA systems," Ieee-Asme Transactions on Mechatronics, vol. 6, no. 1, pp. 17-25, Mar, 2001.

[13] M. Barth, F. An, T. Younglove, G. Scora, C. Levine, M. Ross, and T. Wenzel, "The development of a comprehensive modal emissions model," NCHRP Web-Only Document 122, Contractor's final report for NCHRP Project 25-11, National Cooperative Highway Research Program, 307 p., April 2000.

[14] M. Barth, G. Scora, and T. Younglove, "Modal emissions model for heavy-duty diesel vehicles," Transportation Research Record, vol. 1880, pp. 10-20, 2004.

[15] M. Barth, N. Davis, G. Scora, J. Collins, and J. Norbeck, "Measuring and modeling emissions from extremely low emitting vehicles," Transportation Research Record, vol. 1987, pp. 21-31, 2006.

[16] D. Schulz, T. Younglove, and M. Barth, "Statistical analysis and model validation of automobile emissions," Journal of Transportation and Statistics, vol. 3(2), pp. 29-38, 2000.

[17] M. Barth, C. Malcolm, T. Younglove, and N. Hill, "Recent validation efforts for a comprehensive modal emissions model. Transportation Research Record, vol. 1750, pp. 13-23, 2001.

[18] K. Boriboonsomsin and M. Barth, "Impacts of freeway high-occupancy vehicle lane configuration on vehicle emissions," Transportation Research Part D, vol. 13(2) , pp. 112-125, 2008.

[19] R.T. van Katwijk, T. Bakri, D. Vukovic, J.H. Hogema, L.J.J. Steendijk, "Providing Speed Advice to Vehicles Approaching an Intersection: Evaluation and Lessons Learned", Transportation

[20] "EAR Project: Advanced Traffic Signal Control", BMW, March 11, 2011

[21] Stevanovic, A.Z., Stevanovic J. and Kergaye, C., "Impact of Signal Phasing Information Accuracy on Green Light Optimized Speed Advisory Systems." Accepted for publication in Transportation Research Record, Journal of the Transportation Research Board, 2013

[22] Stevanovic, A.Z., Stevanovic J. and Kergaye, C., "Comparative Evaluation of Benefits from Traffic Signal Retiming and Green Light Optimized Speed Advisory Systems." Accepted for publication in Transportation Research Record, Journal of the Transportation Research Board, 2013

[23] Tsugawa, S. "The current trends and issues on ITS in Japan: Safety, energy and environment". Intelligent Radio for Future Personal Terminals (IMWS-IRFPT), 2011 IEEE MTT-S International Microwave Workshop Series.

[24] http://www.tmleuven.be/project/ecostand/.

[25] http://www.its.dot.gov/aeris/.

[26] Barth, M., Mandava, S., Boriboonsomsin, K., Xia, H, "Dynamic ECO-driving for arterial corridors," Integrated and Sustainable Transportation System (FISTS), 2011 IEEE Forum on , vol., no., pp.182-188, June 29 2011-July 1, 2011

[27] Xia, H., Boriboonsomsin, K., Barth, M., "Indirect Network-wide Energy/Emissions Benefits from Dynamic ECO-Driving on Signalized Corridors", Intelligent Transportation Systems (ITSC), 14th International IEEE Conference, pp 329 – 334, 2011

[28] "Dedicated Short Range Communications (DSRC) Message Set Dictionary: J2735". Society of Automotive Engineers International, Warrendale, Pa., 2009.

[29] Battelle, "Signal Phase and Timing and Related Message Binary Format (BLOB) Details", Technical report provided to FHWA Office of Operations Research and Development, TFHRC, 2012.

[30] B. Asadi, A. Vahidi, "Predictive Use of Traffic Signal State for Fuel Saving". 12th IFAC Symposium on Transportation Systems Redondo Beach, CA, USA, September, 2009.

[31] [4] B. Asadi, A. Vahidi, "Predictive Cruise Control: Utilizing Upcoming Traffic Signal Information for Improving Fuel Economy and Reducing Trip Time". IEEE Transactions on Control System Technology, 2010.

[32] S. Mandava, K. Boriboonsomsin, M. Barth, "Arterial velocity planning based on traffic signal information under light traffic conditions," *12th International IEEE Conference on Intelligent Transportation Systems*, St. Louis, October 2009, 160-165pp.

[33] H. Xia, K. Boriboonsomsin, F. Schweizer, A. Winckler, K. Zhou, WB. Zhang, M. Barth, "Field Operational Testing of ECO-Approach Technology at a Fixed-Time Signalized Intersection", *Proceedings of the IEEE 2012 Intelligent Transportation Systems Conference*, Anchorage, AK, September 2012, 6 pp.

[34] Xia, H., Boriboonsomsin, K., Barth, M., "Dynamic Eco-Driving for Signalized Arterial Corridors and Its Indirect Network-Wide Energy/Emissions Benefits", Journal of Intelligent Transportation System: Technology, Planning, and Operations, Vol 17, Issue 1, 2013.

[35] Xia, H., Boriboonsomsin, K., Barth, M., "Development and Evaluation of an Enhanced Eco-Approach Traffic Signal Application for Connected Vehicles", Intelligent Transportation Systems (ITSC), 16th International IEEE Annual Conference, 2013.

[36] http://www.its.dot.gov/connected_vehicle/connected_vehicle.htm

[37] Labuhn, I. & Chundrlik, W. (1995). Adaptive cruise control. US Patent 5,454,442.

[38] Servin, O., Boriboonsomsin, K., Barth, M., "A Preliminary Design of Speed Control Strategies in Dynamic Intelligent Speed Adaptation System for Freeways", Transportation Research Board 87th Annual Meeting, 2008.

[39] S. Shladover, "Review of the state of development of advanced vehicle control systems (AVCS)," Vehicle Syst. Dyn., vol. 24, pp. 551–595, July 1995.

[40] Vahidi, A., Eskandarian, A., "Research Advances in Intelligent Collision Avoidance and Adaptive Cruise Control", IEEE Transaction on Intelligent Transportation Systems, 2003.

[41] P. Ioannou and H. Raza, "Vehicle following control design for automated highway systems," in Proc. 1997 IEEE Vehicular Technology Conf., Phoenix, AZ, 1997, pp. 904–908.

[42] P. Ioannou and H. Raza, "Vehicle following control design for automated highway systems," IEEE Control Syst. Mag., vol. 6, pp. 43–60, Dec. 1996.

[43] D. Swaroop and R. Huandra, "Intelligent cruise control design based on a traffic flow specification," Vehicle Syst. Dyn., vol. 30, pp. 319–344, Nov. 1998.

[44] D. Swaropp and K. Rajagopal, "Intelligent cruise control systems and traffic flow stability," Transport. Res., pt. C, vol. 7, pp. 329–352, Dec. 1999.

[45] D. Swaroop, K. Hedrick, C. Chien, and P. Ioannou, "Comparison of spacing and headway control laws for automatically controlled vehicles," Vehicle Syst. Dyn., vol. 23, pp. 597–625, Nov. 1994.

[46] S. Shladover, "Review of the state of development of advanced vehicle control systems (AVCS)," Vehicle Syst. Dyn., vol. 24, pp. 551–595, July 1995.

[47] D. Swaropp and K. Rajagopal, "Intelligent cruise control systems and traffic flow stability," Transport. Res., pt. C, vol. 7, pp. 329–352, Dec. 1999.

[48] D. Swaroop, K. Hedrick, C. Chien, and P. Ioannou, "Comparison of spacing and headway control laws for automatically controlled vehicles," Vehicle Syst. Dyn., vol. 23, pp. 597–625, Nov. 1994.

[49] Y. Zhang, E. Kosmatopoulos, P. Ioannou, and C. Chien, "Autonomous intelligent cruise control using front and back information for tight vehicle following maneuvers," IEEE Trans. Veh. Technol., vol. 48, pp. 319–328, Jan. 1999.

[50] S. Germann and R. Isermann, “Nonlinear distance and cruise control for passenger cars,” in Proc. American Control Conf., Seattle, WA, 1995, pp. 3081–3085.

[51] H. Holzmann, C. Halfmann, S. Germann, M. Würtenberger, and R. Isermann, “Longitudinal and lateral control and supervision of autonomous intelligent vehicles,” Contr. Eng. Practice, vol. 5, pp. 1599–1605, Nov. 1997.

[52] P. Chakroborty and S. Kikuchi, “Evaluation of the general motors based car-following models and a proposed fuzzy inference model,” Trans- port. Res.: Emerging Technologies, pt. C, vol. 7, pp. 209–235, Aug. 1999.

[53] J. Gerdes and K. Hedrick, “Vehicle speed and spacing control via co- ordinated throttle and brake actuation,” Control Engineering Practice, vol. 5, pp. 1607–1614, Nov. 1997.

[54] X. Lu, H. Tan, S. Shladover, and K. Hedrick, “Nonlinear longitudinal controller implementation and comparison for automated cars,” ASME J. Dyn. Syst., Meas., Contr., vol. 123, pp. 161–167, June 2001.

[55] Barth M. and Boriboonsomsin, K. “The Potential Role of Vehicle Automation in Reducing Traffic-Related Energy and Emissions”, International Conference on Connected Vehicles and Expo, 2013.

[56] U.S. Environmental Protection Agency. Technical Guidance on the Use of MOVES2010 for Emission Inventory Preparation in State Implementation Plans and Transportation Conformity. Report No. EPA-420-B-10-023, Ann Arbor, MI, April 2010.

[57] Dresser, C., (2011). “Generating Operating Mode Distributions and Link Drive Schedules in MOVES.” Presented at the 90th Annual Meeting of the Transportation Research Board, Washington, DC, January 23-27.

[58] Wang, X., Lee, H., Salles, M. V., Gao, O. H., Gerhke, J., Amber, W., Mohseni, A., Chiao, K.-A. (2011). “Development of Post-Processing Software for the Integration of MOVES and NYMTC’s Activity-based Travel Demand Model.” Presented at the 90th Annual Meeting of the Transportation Research Board, Washington, DC, January 23-27.

[59] Chamberlin, R., Swanson, B., Talbot, E., Dumont, J., and Pesci, S. (2011). “Analysis of MOVES and CMEM for Evaluating the Emission Impacts of an Intersection Control Change.” Proceedings of the 90th Annual Meeting of the Transportation Research Board, Washington, DC, January 23-27.

[60] Lin, J., Chiu, Y.-C., Bai, S., and Vallamsundar, S. (2011). "Integration of MOVES and Dynamic Traffic Assignment Models for Fine-Grained Transportation and Air Quality Analyses." Presented at the 90th Annual Meeting of the Transportation Research Board, Washington, DC, January 23-27.

[61] Claggett, M. (2011). "OpMode Look-Up Tables for Linking Traffic Simulation Models and MOVES Emissions." Presented at the 90th Annual Meeting of the Transportation Research Board, Washington, DC, January 23-27.

[62] William L. Eisele and William E. Frawley. Estimating the Safety and Operational Impact of Raised Medians and Driveway Density: Experiences from Texas and Oklahoma Case Studies. In Transportation Research Record, No. 1931, TRB, National Research Council, Washington, DC, 2005, pp. 108-116.

[63] El Esawey, M. and Sayed, T. A. Comparison of Two Unconventional Intersection Schemes: Crossover Displaced Left-Turn and Upstream Signalized Crossover Intersections. In Transportation Research Record, No. 2023, TRB, National Research Council, Washington, DC, 2007, pp. 10-19.

[64] Boriboonsomsin, K. and Barth, M. "Impacts of Freeway High-Occupancy Vehicle Lane Configuration on Vehicle Emissions". Transportation Research Part D, Vol. 13, No. 2, 2008, pp. 112-125.

[65] Wu, G., K. Boriboonsomsin, W.-B. Zhang, M. Li, and M. Barth. Energy and Emission Benefit Comparison between Stationary and In-Vehicle Advanced Driving Alert Systems." In Transportation Research Record, No. 2189, TRB, National Research Council, Washington, DC, 2010, pp. 98-106.

[66] "Freeway System Operational Assessment," Paramics Calibration and Validation Guidelines (Draft), Technical Report I-33, Wisconsin DOT, District 2, June 2002.

[67] Ma, T., and Abdulhai, B., "Genetic Algorithm-Based Optimization Approach and Generic Tool for Calibrating Traffic Microscopic Simulation Parameters", Transportation Research Record: Journal of Transportation Research Board, No. 1800, 2002, pp.6-15.

[68] Toledo, T., Ben-Akiva, M. E., Darda, D., Jha, M., and Koutsopoulos, H. N., "Calibration of Microscopic Traffic Simulation Models with Aggregate Data", Transportation Research Record: Journal of Transportation Research Board, No. 1876, 2004, pp.10-19.

[69] Jha, M., Gopalan, G., Garms, A., Mahanti, B.P., Toledo, T., and Ben-Akiva, M.E., "Development and Calibration of a Large-Scale Microscopic Traffic Simulation Model", Transportation Research Record: Journal of Transportation Research Board, No. 1876, 2004, pp.121-131.

[70] NGSIM. http://ngsim-community.org/, accessed July 15, 2011.

[71] Punzo, V., M. T. Borzacchiello, and B. Ciuffo. Estimation of Vehicle Trajectories from Observed Discrete Positions and Next-Generation Simulation Program (NGSIM) Data. In Proceedings of the 88th TRB Annual Meeting CD-ROM, 2009.

[72] Jun, J., S. Yoon, and R. Guensler. Impacts of Acceleration Calculation Methods on Onroad Vehicle Engine Power Estimation. Air and Waste Management Association, 99th Annual Meeting Proceedings (CD-ROM); Pittsburgh, PA; June 2006.

[73] PARAMICS. http://www.paramics-online.com/ accessed on July 15, 2011.

[74] Cambridge Systematics. NGSIM Lankershim Data Analysis --- Summary Report prepared for Federal Highway Administration. March, 2006.

[75] Kamalanathsharma, R., Rakha, H. "Agent-Based Simulation of Eco-Speed Controlled Vehicles at Signalized Intersections". Transportation Research Board Annual Meeting. 2014.

[76] Bayless, S., Guan, A., Son P., Murphy, S., Shaw, A., "Connected Vehicle Insights: Trends in Roadway Domain Active Sensing: Developments in Radar, LIDAR, and other Sensing Technologies, and Impact on Vehicle Crash Avoidance/Automation and Active Traffic Management". The Intelligent Transportation Society of America. 2014

[77] Li, J., Zhou, K., Shladover, S., Skabardonis, A., "Estimating Queue Length Under Connected Vehicle Technology: Using Probe Vehicle, Loop Detector, and Fused Data". Transportation Research Record: Journal of the Transportation Research Board. 2013.

[78] Goodall, N. J., Smith, B. L., and Park, B. "Microscopic Estimation of Freeway Vehicle Positions from the Behavior of Connected Vehicles." Journal of Intelligent Transportation Systems. 2014.

[79] Talebpour, A., Mahmassani, H. S., Mete, F., Hamdar, S. H., Dala Chiara, B., "Near-Crash Identification in a Connected Vehicle Environment", Transportation Research Board 93rd Annual Meeting. 2014.

[80] Lee, J., Park, B., Yun, I., "Cumulative Travel-Time Responsive Real-Time Intersection Control Algorithm in the Connected Vehicle Environment". Journal of Transportation Research. 2013.

[81] Brookhuis, K. and D. Dewaard, Limiting speed, towards an intelligent speed adapter (ISA). Transportation Research Part F: Traffic Psychology and Behaviour, 1999. 2: p. 81-90.

[82] Asadi, B. and A. Vahidi, Predictive Cruise Control: Utilizing Upcoming Traffic Signal Information for Improving Fuel Economy and Reducing Trip Time. Control Systems Technology, IEEE Transactions, 2010: p. 1-9.

[83] 2070 Controller. California Department of Transportation. Oregon.gov.

[84] FHWA Type 170 Traffic Controller System. Washington State Department of Transportation.

[85] "Dedicated Short Range Communications (DSRC) Message Set Dictionary", SAE Standards. SAE International. 2009.